COMPARATIVE MORPHOMETRIC ANALYSIS OF LONG BONE ONTOGENY IN HOMINOID PRIMATES

Dissertation

zur

Erlangung der naturwissenschaftlichen Doktorwürde

(Dr. sc. nat.)

vorgelegt der

Mathematisch-naturwissenschaftlichen Fakultät

der

Universität Zürich

von

Naoki Morimoto

aus

Japan

Promotionskomitee

Prof. Dr. Christoph P.E. Zollikofer (Vorsitz, Leiter der Dissertation)
Dr. Marcia S. Ponce de León
Prof. Dr. Hugo Bucher

Zürich, 2012

Contents

Abstract

Acquisition of bipedality is a hallmark of human evolution. Long bones are the key elements for locomotion, and thus it is generally assumed that long bone morphology reflects taxon-specific locomotor behaviors of primates. Form-function relationships of long bones are complex, however, since long bone morphology results from evolutionary adaptation, taxon-specific developmental programs and *in-vivo* loading patterns during an individual's lifetime. The central question addressed in my thesis is whether long bone diaphyseal (shaft) morphology and corresponding musculature reflect taxon-specific locomotor adaptations or phylogenetic relationships of hominoids.

Long bone diaphyses serve as load-bearing structures during locomotion, implying a close relationship between diaphyseal form and its locomotor function through bone remodeling during an individual's lifetime. The effects of the latter process ("Wolff's Law") are best assessed by comparing diaphyseal morphologies of conspecific individuals under different locomotor regimes. Here I use morphometric mapping to analyze the morphology of entire femoral diaphyses in an ontogenetic series of wild and captive common chimpanzees (*Pan troglodytes troglodytes*). Morphometric mapping reveals patterns of variation of diaphyseal structural and functional properties, which cannot be recognized with conventional cross-sectional analysis and/or geometric morphometric methods. The data show that diaphyseal shape, cortical bone distribution and inferred cross-sectional biomechanical properties vary both along ontogenetic trajectories and independent of ontogeny. Mean ontogenetic trajectories of wild and captive chimpanzees, however, were found to be statistically identical. This indicates that the basic developmental program of the diaphysis is not altered by different loading conditions. Overall, thus, the hypothesis that Wolff's Law predominantly governs long bone diaphyseal morphology is rejected.

The relationship between femoral morphology and femoropelvic musculature is of special relevance for locomotion. The proximal femoral morphology of fossil hominins is routinely interpreted in terms of muscular topography and associated locomotor modes. However, the detailed correspondence between hard and soft tissue structures in the proximal femoral region of extant great apes is relatively unknown, because dissection protocols typically do not comprise in-depth osteological descriptions. Here I use computed tomography and virtopsy (virtual dissection) for non-invasive examination of the femoropelvic musculoskeletal anatomy in *Pan troglodytes*, *P. paniscus*, *Gorilla gorilla*, *Pongo pygmaeus*, and *Homo sapiens*. Specifically, I analyze the topographic relationship between muscle attachment sites and surface structures of the proximal femoral shaft such as the lateral spiral pilaster. The results show that the origin of the *vastus lateralis* muscle is anterior to the insertion of *gluteus maximus* in all examined great ape specimens and humans. In gorillas and orangutans, the insertion of *gluteus maximus* is on the inferior (anterolateral) side of the lateral spiral pilaster. In chimpanzees, however, the *maximus* insertion is on its superior (posteromedial) side, similar to the situation in modern humans. These findings support the hypothesis that chimpanzees and humans exhibit a shared-derived musculoskeletal topography of the proximal femoral region, irrespective of their different locomotor modes, while gorillas and orangutans represent the primitive condition. Caution is thus warranted when inferring locomotor behavior from the surface topography of the proximal femur of fossil hominins, as the morphology of this region may contain a strong phyletic signal that tends to blur locomotor adaptation.

How bipedality evolved from great ape-like locomotor behaviors is still highly debated. This is mainly because it is difficult to infer locomotor function, and even more so locomotor kinematics, from fossil hominin long bones. Long bone morphology reflects processes of evolutionary adaptation

and in-vivo modification during individual's lifetime. Here I discriminate between these factors by investigating the morphology of long bones in fetal and neonate great apes and humans, before the onset of locomotion. Comparative morphometric analysis of the femoral diaphysis indicates that its morphology reflects phyletic relationships between hominoid taxa to a greater extent than taxon-specific locomotor adaptations. Diaphyseal morphology in humans and chimpanzees exhibits several shared-derived features, despite substantial differences in locomotor adaptations. Orangutan and gorilla morphologies are largely similar, and likely represent the primitive hominoid state. These findings are compatible with two possible evolutionary scenarios. Diaphyseal morphology may reflect retained adaptive traits of ancestral taxa, hence human-chimpanzee shared-derived features may be indicative of the locomotor behavior of our last common ancestor. Alternatively, diaphyseal morphology might reflect evolution by genetic drift (neutral evolution) rather than selection, and might thus be more informative about phyletic relationships between taxa than about locomotor adaptations. Both scenarios are consistent with the hypothesis that knuckle-walking in chimpanzees and gorillas resulted from convergent evolution, and that the evolution of human bipedality is unrelated to extant great ape locomotor specializations.

Overall, the results of these studies converge in the conclusion that, in hominoids, femoral diaphyseal morphology and corresponding topography of major locomotor muscles reflect phylogenetic relationships and taxon-specific developmental programs to a greater extent than taxon-specific locomotor adaptations. The results of this thesis thus indicate that an extended, form-function-phylogeny, approach could complement the classical form-function approach to the evolution of long bone morphology and of locomotor behaviours of humans and great apes.

Keywords: human bipedality, development, human, great ape, femur, geometric morphometrics, morphometric mapping

Zusammenfassung

Die zweibeinige Fortbewegung ist ein zentrales Element der menschlichen Evolution. Langknochen sind wichtige Strukturen der Fortbewegung und es wird deshalb allgemein angenommen, dass ihre Morphologie die artspezifische Fortbewegungsweise wiedergibt. Form-Funktions-Zusammenhänge sind allerdings komplex, da die Form der Langknochen durch ein Zusammenspiel von evolutionärer Adaptation, artspezifischen Entwicklungsprogrammen und in-vivo-Belastungsmustern entsteht. Die zentrale Frage, die in dieser Dissertation untersucht wird, ist in welchem Ausmass die Morphologie der Langknochen von Menschenaffen und Menschen durch diese Faktoren bestimmt wird.

Der Einfluss von *in-vivo*-Prozessen der Knochenmodifikation (bone remodeling) wird am besten durch die Analyse von Individuen derselben Art, aber unter verschiedenen Belastungsbedingungen untersucht. Das Gesetz von Wolff besagt, dass in-vivo Modifikationen funktionsspezifisch sind und aus der Knochenmorphologie auf das Fortbewegungsverhalten eines Individuums geschlossen werden kann. Um diese Hypothese zu testen, kommt ein neu entwickeltes Verfahren der "morphometrischen Kartierung" (morphometric mapping) zur Anwendung, das es erlaubt, die Morphologie des Schafts von Langknochen im Detail zu untersuchen. Dies war mit konventionellen geometrisch-morphometrischen Methoden bisher nicht möglich. Ein Vergleich von Wild- und Zootieren am Beispiel des Schimpansen (*Pan troglodytes troglodytes*) zeigt, dass sich die grundlegenden Entwicklungsmuster des Femurs in diesen Gruppen statistisch nicht unterscheiden, obwohl sie stark unterschiedliche Bewegungsmuster aufweisen. Diese empirischen Daten zeigen, dass der Zusammenhang zwischen individueller Langknochenform und Bewegungsmustern relativ lose ist, und dass artspezifische Entwicklungsprogramme der dominierende Faktor sind.

Die Beziehung zwischen der Morphologie des Femurs und der umliegenden Muskulatur des Beckengebiets ist speziell relevant für die Unterscheidung zwischen quadrupeder und bipeder Fortbewegung. Allerdings ist die topographische Beziehung zwischen Knochen- und Muskel/Sehnenstrukturen in dieser Region nur wenig bekannt. Der zweite Teil dieser Dissertation präsentiert eine vergleichende Studie mittels Virtopsie (virtuelle Autopsie), die diese Strukturen non-invasiv untersucht. Ein wichtiges Ergebnis des Vergleichs von Mensch, Schimpanse, Gorilla und Orangutan ist, dass sich die ersten beiden Arten in vielen Details von Muskelansatzstellen gleichen, während sie sich stark von der Topographie bei Gorilla und Orangutan unterscheiden. Dies betrifft vor allem die Ansatzstelle des gluteus maximus an Femur, die oft als Unterscheidungsmerkmal zwischen quadrupeder und bipeder Fortbewegung gebraucht wird. Bei der Interpretation der Femur-Morphologie von fossilen Homininen ist somit Vorsicht geboten, da diese Merkmale die gemeinsame Phylogenie von Mensch und Schimpanse wiederspiegeln und funktionell weniger wichtig sind als bisher angenommen.

Im dritten Teil der Dissertation wird die Rolle von evolutionären und *in-vivo*-Faktoren bei der Entwicklung der Femur-Morphologie untersucht. Um zwischen diesen Faktoren zu unterscheiden, wurde die Femur-Morphologie in Föten und Neonaten von Menschenaffen und Menschen verglichen. Bei diesen jungen Entwicklungsstadien kann die Morphologie der Knochen untersucht werden, bevor sie unter dem Einfluss von Fortbewegungsmustern stehen. Die Studie zeigt, dass Menschen und Schimpansen einige gemeinsame abgeleitete Merkmale des Femurs aufweisen, während Gorillas und Orangutans sehr ähnliche, ursprüngliche Morphologien haben. Es bleibt abzuklären, ob die Mensch-Schimpanse-Gemeinsamkeiten Rückschlüsse auf die Fortbewegungsweise unseres letzten gemeinsamen Vorfahren erlauben. Zusammenfassend lässt sich festhalten, dass die Morphologie des

Femurs bei Menschen und Menschenaffen stärker von artspezifischen Entwicklungsprogrammen bestimmt ist, als dies bisher angenommen wurde.

Schlüsselwörter: Zweibeinigkeit, Zweibeinigkeit, Mensch, Menschenaffen, Femur, Geometrische Morphometrie, Morphometric Mapping

Abstract for non-academic audience

In my thesis I investigated the relationship between the morphology of the locomotor system of great apes and humans and their actual locomotor behavior. The results show that form does not follow function. The morphology of limb muscles and bones reflects evolutionary relationships between humans and great ape species rather than locomotor similarity.

Entspricht die Morphologie des Bewegungsapparats von Mensch und Menschenaffen ihren Fortbewegungsmustern? Die Resultate meiner Doktorarbeit zeigen, dass die Evolution von Form und Funktion des relativ unabhängig voneinander verlaufen ist. Die Muskel- und Skelettmorphologie der Extremitäten zeigt eher die evolutionären Verwandtschaftsbeziehunen zwischen Mensch und Menschenaffenarten, als Ähnlichkeiten in der Fortbewegung.

Introduction

Hominoid locomotion and its evolution

The acquisition of bipedality is a hallmark of human evolution. The oldest direct evidence of human bipedality consists in the fossilized footprints from Laetoli (Tanzania, Africa), which date back to about 3.7 mya (Leakey and Hay, 1979). Recently, another series of footprints have been found near Ileret (Kenya), dated to about 1.5 mya (Bennett et al., 2009). Compared to the Laetoli footprints, the Ileret footprints bear evidence of a more modern human-like foot morphology, with a more adducted hallux and triangular midfoot shape broadening towards the toes, indicating significant modification of the mode of bipedality during the course of hominin evolution.

Skeletal fossil evidence indicates an early origin of bipedality in the hominid lineage (species that stem from the common ancestors of [gibbons, [orangutans, gorillas, chimpanzees, [humans]]] are denoted as [hominoids, [hominids, [hominins]]], respectively (Wood and Richmond, 2000)), and possibly independent emergence in several lines. *Ardipithecus*, dated to about 4.4 mya, is suggested to be a facultative biped primarily based on the morphologies of pelvic, femoral and foot bones (Lovejoy et al., 2009a; Lovejoy et al., 2009d). *Orrorin*, (~6mya), is thought to be a biped due to its proximal femoral morphology (Senut et al., 2001; Pickford et al., 2002; Galik et al., 2004; Richmond and Jungers, 2008). The earliest known hominin, *Sahelanthropus*, indicates an origin of bipedality dating back to about 7 mya based on its cranial morphology (Brunet et al., 2002; Zollikofer et al., 2005). The late Miocene ape *Oreopithecus*, which dates to about 7-9 mya, is suggested to be a biped based on the skeletal structure of the pelvis (Rook et al., 1999). The phylogenetic affiliation of these key hominids remains controversial (Wood and Harrison, 2011), but these lines of fossil skeletal evidence for bipedality could indicate that bipedality did not evolve only once, and only in the hominin lineage, but independently in various hominid lineages (Rook et al., 1999).

The question of "how" the evolutionary transition from quadrupedal to bipedal locomotor modes occurred is as difficult to answer as the question of "when" the transition occurred. Various hypotheses have been proposed regarding the question as to which ancestral locomotor mode gave rise to human bipedality. One of the major hypotheses is the *knuckle-walking hypothesis*. Since chimpanzees, the sister taxon of humans, and the more distantly related gorillas show knuckle-walking in terrestrial locomotion, this hypothesis postulates that the human-chimpanzee last common ancestor also exhibited knuckle-walking (Richmond and Strait, 2000). The *climbing hypothesis* postulates that human bipedality evolved from arboreal climbing behaviors. This hypothesis argues that musculoskeletal and corresponding biomechanical features for hindlimb-dominated arboreal locomotion serve as a preadaptation for terrestrial bipedality (Stern and Susman, 1981). The *orangutan hypothesis* postulates that human bipedality evolved from orangutan-like bipedal/quadrupedal arboreal locomotion (Thorpe et al., 2007). This hypothesis suggests that chimpanzee and gorilla modes of knuckle-walking are derived rather than primitive, and evolved in convergence. The climbing and orangutan hypotheses differ from the knuckle-walking hypothesis in that they do not consider great ape terrestrial locomotion as a significant component for the evolution of human bipedality.

While the current major hypotheses listed above link the origin of human bipedality with locomotor repertoires of extant hominoid species, functional analyses of the morphologies of the fossil skeleton of *Ardipithecus* suggest that human bipedality evolved from locomotor behaviors no longer present in extant hominoid species (Lovejoy et al., 2009a; Lovejoy et al., 2009d; White et al.,

2009). This view, in a way, puts chimpanzees (and gorillas) aside as specialized hominids in terms of locomotion.

Regardless of whether the locomotor behaviors of extant hominoid species serve as a model of locomotor behavior of the human-chimpanzee common ancestor, locomotor behaviors of extant hominoid species are undoubtedly of special relevance as a reference for the evolution of human bipedality. Humans and other living hominoid primates have evolved a wide range of locomotor modes: e.g., habitual/short bouts of bipedal locomotion, hand-supported bipedalism, terrestrial/arboreal quadrupedalism, suspensory behavior (brachiation), and quadrumanous climbing. In association with the great diversity of the locomotor behaviors of extant hominoids, structure-function and structure-phylogeny inferences drawn from their skeletal morphologies are central for the phyletic and functional interpretation of fossil hominin specimens.

Among postcranial bones, long bones are of special relevance for locomotion because they serve as beam structures to bear mechanical loads. Among the long bones, the femur is especially important because great ape locomotion is hindlimb dominated (Schmitt, 2003), and because various locomotor muscles attach to the femur. Along with functional locomotor diversity, hominoid long bones exhibit conspicuous morphological diversity. Femora of humans and great apes show differences in length, proportion, and proximal and distal joint morphology (Aiello and Dean, 1990; Ruff and Runestad, 1992; Ruff, 2002; Harmon, 2007; Holliday et al., 2010) (Fig. 1). For example, the human femur, which is long and robust relative to the humerus, is typically associated with bipedality (Ruff, 2009), and the relatively large femoral head of orangutans is associated with greater mobility of the hip joint for arboreal locomotion (Ruff, 1988).

The conspicuous variation of long bone morphology and the diverse locomotor behaviors in hominoid primates raise a question: to what extent do long bone morphologies reflect taxon-specific locomotor behaviors, and to what extent do they reflect phyletic relationships among hominoid taxa? It is typically held that phenotypic traits reflect adaptation to a relatively greater extent than phylogeny, whereas (neutral) molecular markers reflect phylogeny. One principal problem with the interpretation of phenotypic traits is the well-known „spandrel effect“ (Gould and Lewontin, 1979): it is often the case that the interpretation of a trait is “adaptationist”, while the trait itself is not necessarily adaptive.

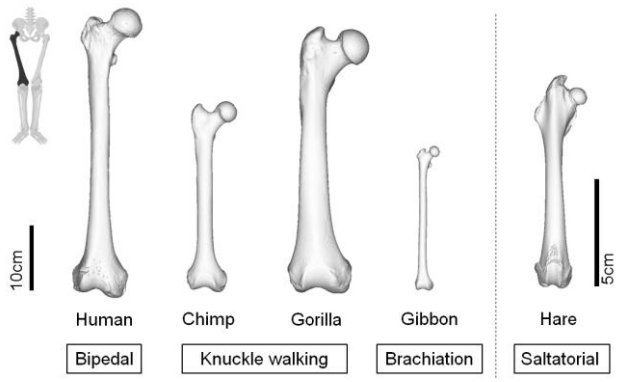

Fig. 1 Variation of femoral morphology and locomotor modes. Is long bone morphology correlated with taxon-specific locomotor modes?

Hominoid locomotion and its ontogeny

As indicated by *Oreopithecus*, bipedality is not unique to humans. However, human bipedality has various unique features that are not found in the bipedality of other animals. Human bipedality is more economical in walking but more costly in running in terms of required energy per unit mass and per unit distance of travel compared to bipedal and quadrupedal locomotion of other mammals, indicating that locomotor energetics is an important factor for the evolution of hominin bipedality (Rodman and McHenry, 1980; Alexander, 2004; Sockol et al., 2007; Pontzer et al., 2009). However, a recent experimental study showed that the human musculoskeletal system is optimized neither specifically for walking nor for running as previously suggested (Bramble and Lieberman, 2004), but functions suboptimally and multi-purposely for various locomotor behaviors (Carrier et al., 2011).

Characteristic features of human bipedal walking are the extended knee- and hip-joints with erect trunk while non-human primates (and other mammals) typically exhibit more bent joint postures and a more horizontally inclined trunk during their bipedal or quadrupedal locomotor behaviors (Schmitt, 2003; Alexander, 2004). Extended knee- and hip-joints are thought to be energetically advantageous. A straightened knee joint during the stance phase permits the hind-limb to work as a stiff pole to carry the center of gravity in a way which is similar to an inverted pendulum. The inverted pendulum-like motion allows effective conversion of kinetic and potential energies resulting in reduction of locomotor costs (Cavagna et al., 1977). This energy-saving mechanism is, however, not unique to humans, but widespread in terrestrial quadrupedal animals (Minetti et al., 1999; Griffin et al., 2004).

Humans change locomotor modes during ontogeny from neonatal limited mobility, (quadrupedal) crawling (about 9 months after birth), supported bipedal walking (about 12 months) and independent walking (about 18 months), and these changes are associated with neurological maturation (Sutherland et al., 1980; Standring, 2004). In terms of skeletal morphology, it has been reported that the onset of bipedal locomotion, which is associated with increased mechanical loadings, occurs in parallel with an increase in rigidity of the hindlimb long bones (Ruff et al., 1994; Sumner and Andriacchi, 1996; Ruff, 2003b, 2003a).

Not only humans but also great apes show remarkable ontogenetic changes of locomotor behavior and substrate use. Chimpanzees and gorillas exhibit similar modes of terrestrial locomotion (knuckle-walking) during adulthood, and follow similar transition pattern of locomotor behaviors during ontogeny: both species exhibit arboreal behaviors and short bouts of hand-assisted and/or supported bipedal locomotion more frequently in infant stages, and exhibit terrestrial locomotion more frequently toward adulthood (Doran, 1992, 1993, 1997). Gorillas, on the other hand, show an accelerated ontogenetic pattern of transition of locomotor behaviors compared to chimpanzees (Doran, 1997).

Regardless of whether the locomotor behavior is precocial or altricial, there are shared patterns of long bone development in primates, mammals in general, and even birds. Long bones of immature individuals are stouter relative to the length compared to mature individuals (Schultz, 1969; Heinrich et al., 1999; Lammers and German, 2002; Main and Biewener, 2007; Young et al., 2009). It has been suggested that the stouter shape serves to mitigate the risk of injury during locomotion when musculoskeletal structures are still immature (Carrier, 1996; Young et al., 2009). While behavioral and theoretical aspects of primate locomotion are relatively well documented, our knowledge about

detailed structural changes of long bones during ontogeny is still relatively scarce. Specifically, it remains to be explored when and how taxon-specific features of long bones appear during ontogeny.

Long bone morphology: ontogenetic programs vs. *in-vivo* factors

Discrimination between genetic and environmental factors determining long bone structures is of special relevance for the interpretation of fossil skeletal morphology (Pearson and Lieberman, 2004). It is typically hypothesized that long bone morphology is optimally adapted *in-vivo* for its function according to "Wolff's Law" (Wolff, 1892), or "bone functional adaptation" (Ruff et al., 2006)[1]. A familiar example of environmental influence on bone structure is the hypertrophy of the playing arm compared to the non-playing arm of athletes (Jones et al., 1977; Bass et al., 2002). In an analysis of the cross-sectional geometry of human long bone shafts it has been shown that the mechanical loading pattern during early ontogeny is a decisive factor for the robustness of long bone diaphyses at adulthood (Ruff et al., 1994; Ruff, 2003a). Various experimental studies have provided data that support Wolff's Law (e.g., Lanyon and Baggott, 1976; Goodship et al., 1979; Lanyon and Bourn, 1979; Lanyon, 1987; Robling et al., 2002; Warden et al., 2005). It has been reported that the rate (amplitude) and frequency of the strain (local deformation of the bone by mechanical loading) are more important factors than strain magnitude (Turner et al., 1994; Turner et al., 1995; Mosley and Lanyon, 1998). Experimental studies have shown that skeletal tissues have a receptor and reaction system (so-called mechano-transduction system) to sense mechanical loading via strain-induced fluid flow in bone tissues, and to remodel bone tissue accordingly (Turner et al., 1994; Turner et al., 1995).

Wolff's Law has also been applied to infer the activity patterns of humans and Neanderthals from humeral and femoral morphologies (e.g., Trinkaus et al., 1994; Holt, 2003; Rhodes and Knüsel, 2005; Sparacello and Marchi, 2008). However, it has been gradually acknowledged that modeling and remodeling of the postcranial bones are related to various factors such as temperature of the external environment (Serrat et al., 2008), growth hormones, *in-vivo* loading patterns, age, and – last but not least – evolutionary adaptation, such that clarifying structure-function relationships in postcranial bones is a complex task (Pearson, 2000; Pearson and Lieberman, 2004). For example, various strain gauge studies showed that *in-vivo* bone strain patterns change dynamically during locomotion, and that long bone shape may be better correlated with peak loads (e.g. during galloping) rather than average loading patterns (Szivek et al., 1992; Demes et al., 2001; Lieberman et al., 2004).

While Wolff's Law serves as a useful basic hypothesis of how bone structure is related to function especially in controlled settings, a growing body of empirical evidence challenges the extension or application of Wolff's Law at an evolutionary scale. As a direct counter-argument, it was suggested that bone modification could be explained by factors other than mechanical loading such as bone inflammation and regeneration or bone fracture and repair processes (Bertram and Swartz, 1991). Various recent developmental studies (reviewed in Lovejoy et al., 2003) indicate that long bone shape largely reflects developmental programs rather than *in-vivo* mechanical loading patterns. Further, a recent evolutionary experimental study showed that the robustness of long bones found in a given generation is not determined by *in-vivo* mechanical loadings in this generation, but by inheritance from the ancestral generations (Wallace et al., 2010b).

[1] Since the notion of "functional adaptation" is ambiguous (it is typically used in an evolutionary context), I will use "bone modification" to denote *in-vivo* processes.

Overall, it appears that long bone morphology reflects the outcome of three main processes: taxon-specific evolutionary adaptation, *in-vivo* modification, and taxon-specific developmental programs. To discriminate between these factors, an evolutionary developmental approach is required. Specifically, patterns of change in long bone morphology during the entire course of ontogeny, and patterns of ontogenetic variability among humans and great apes remain to be explored.

Long bone morphology: structure-function and structure-phylogeny

According to Darwinian theory, the combination of mutation and selection drives evolution, although the proportion of advantageous mutation is small compared to deleterious mutations. In contrast, neutral theory postulates that there is a considerable proportion of mutations which is neutral to selection (Kimura, 1968). It is generally assumed that phenotypic traits reflect adaptive evolution to a great extent. This is expressed, for example, in the term "functional morphology". Reconstruction of the phylogenetic relationships of fossil hominins is often debated (Harrison, 2010) because various morphological characters are prone to homoplasy such that it remains unclear whether a given phenotypic trait found in two taxa represents functional or phylogenetic similarity (Lockwood, 1999; Lockwood and Fleagle, 2007; Wood and Harrison, 2011).

On the other hand, several studies have shown that phylogenetic signals are contained not only in neutral molecular markers but also in various hard and soft tissue structures, for example in temporal bone morphology of hominoids (Lockwood et al., 2004), in size-controlled data of craniodental characters of papionins (Gilbert and Rossie, 2007) and various soft tissue structures of hominoids (Gibbs et al., 2000, 2002; Diogo and Wood, 2011).

Long bones are thought to reflect adaptive evolutionary processes because of their importance in locomotion. For example, various features of long bones such as the cross-sectional geometry of diaphyses (e.g., Ruff and Runestad, 1992; Carlson, 2005; Ruff, 2009), proximal femoral morphologies (e.g., Harmon, 2007; Richmond and Jungers, 2008; Harmon, 2009) and limb proportions (Schultz, 1937; Aiello and Dean, 1990; Young et al., 2010) have been shown to be indicative of locomotor behaviors of great apes, humans and fossil hominins. On the other hand, it has been shown that long bones convey different phylogenetic signals, depending on the traits considered (e.g., overall length, articular surface areas), and on scaling factors for general quadrupedal primates (O'Neill and Dobson, 2008). This indicates that long bone morphologies reflect phylogenetic relationships, at least to some extent. – Overall, structure-phylogeny relationships of long bones need to be explored in greater depth, by controlling effects of *in-vivo* functional adaptation and ontogeny.

Long bone morphology: musculoskeletal relationships

Musculoskeletal anatomy and its variation is well documented in humans (Netter, 2003; Standring, 2004) and great apes (Beddard, 1893; Primrose, 1898; Boyer, 1935; Raven, 1950; Uhlmann, 1968; Sigmon, 1974; Swindler and Wood, 1982). Various studies have shown that there are human-specific musculoskeletal features characteristic of obligate terrestrial bipedalism. For example, compared to great apes, humans have large hip and knee extensors (*gluteus maximus*, and *vastus* muscles) relative to body mass (Stern, 1972; Lovejoy et al., 2002; Lieberman et al., 2006). On the other hand, given the evidence that soft tissue structures exhibit „phyletic inertia" (Gibbs et al., 2000, 2002; Diogo and

Wood, 2011), it is sensible to assume that the evolutionary modification of soft tissue structures is governed by strong phylogenetic and developmental constraints.

While inferences on muscle function are important to understand the evolution of hominin locomotion, still relatively little is known about the exact topographic relationships between muscular and bony elements of the locomotor system in the great apes (Lovejoy et al., 2002). Most importantly, the morphology of the entire femoral diaphysis and the correspondence between diaphyseal morphology and muscular attachment sites and topography remain to be explored in detail. Analyzing both hard and soft tissues in one and the same animal is expected to yield precise insights into the structure-function relationships of musculoskeletal features.

Long bone ontogeny and modularity

To date, studies on the evolution of human bipedality from the perspective of long bones have focused mainly on the proximal and distal epiphyseal morphologies of the femur in living hominoids, in modern humans and in fossil hominins (e.g., Lovejoy et al., 2002; Harmon, 2007; Richmond and Jungers, 2008; Harmon, 2009; Holliday et al., 2010). Diaphyseal morphology has received less detailed attention, and this may be in part because it is difficult to define phenotypic traits, or obtain three-dimensional morphometric measurements [most studies use length, diameter, and cross-sectional properties (e.g., O'Neill and Dobson, 2008; Ruff, 2009; Young et al., 2010)]. However, diaphyses are as relevant to understand long bone evolution as are the epiphyses. Diaphyses are especially important to investigate the development of long bones, because they ossify earlier during ontogeny than epiphyses (Fig. 2). Also, they have special functional importance as the principal load-bearing structures. And finally, long bone diaphyses are well represented in the fossil hominin record, and typically well preserved, thus constituting an important yet relatively unexplored source of information for hominin development, evolution, and adaptation.

Epiphyses and diaphyses represent relatively independent developmental components deriving from distinct ossification centers (Schwartz, 1995; Scheuer et al., 2000; Standring, 2005) (although epiphyseal and diaphyseal developmental processes are coordinated with each other at the growth plates (Serrat et al., 2007)). Long bone diaphyses have two distinct growth directions; longitudinal and radial growth. Longitudinal and radial growth are mediated by two different ossification mechanisms. Longitudinal growth is brought about by endochondral ossification, i.e., replacement of the precursor cartilages, while radial growth is due to direct ossification at the subperiosteal surface (Schwartz, 1995). Differences of longitudinal and radial growth result in differences of length and circumferential morphologies, respectively.

Limb development has been investigated intesively, especially for the early embryonic period. Interestingly, however, still relatively little is known about the development of three-dimensional limb form. Typically, limb patterning and pattern formation are analyzed along principal anatomical axes (anteroposterior, transverse, and dorsoventral) (Benazet and Zeller, 2009; Butterfield et al., 2010), and limb morphogenesis is explored with two-dimensional morphogenetic models (e.g., Dillon and Othmer, 1999; Morishita and Iwasa, 2008). However, it has recently been shown that limb morphogenetic processes are better understood by exploring three-dimensional spatiotemporal patterns, without the use of pre-defined axes (Boehm et al., 2010). Overall, thus, theoretical aspects of three-dimensional limb development are only beginning to be explored, and new morphometric methods need to be devised to quantify diaphyseal shape independent of predefined axes. These novel

Fig. 2 Ontogenetic series of human femora from fetus to adult. Long bone diaphysis ossifies earlier than epiphysis.

methods are required to explore how the morphology of the entire femoral diaphysis develops throughout ontogeny, and how it is modified throughout phylogeny.

Morphometric approaches to long bone diaphyses

Several methods have been proposed to analyze long bone diaphyseal morphologies. One approach is to define discrete scoring schemes according to which the degree of hypertrophy of musculoskeletal stress-markers can be assessed. This semi-quantitative method has typically been used to infer mechanical loading patterns and behavioral histories during the lifetime of human individuals (e.g., Molnar, 2006; Cardoso and Henderson, 2010; Villotte et al., 2010). However, this approach is difficult to apply in comparative analyses of humans and great apes where relationships between the skeletal morphologies and patterns of *in-vivo* mechanical loading history are relatively unknown.

Another approach consists in measuring cross-sectional geometric properties of long bone diaphyses, which serve as a proxy for their biomechanical properties. Cross-sectional properties such as diaphyseal diameter, cortical area, second moments of area and section modulus are widely and routinely used in human evolutionary studies, (Ruff and Hayes, 1983; Sumner and Andriacchi, 1996; Ruff et al., 1999; Ruff, 2009). These measurements are typically taken at the level of the mid-shaft, and/or at additional pre-defined standard locations along the long bone diaphysis (e.g., Carlson, 2005; Carlson et al., 2006; Ruff, 2009), assuming that these standard locations represent functionally and developmentally equivalent regions in different individuals and in different taxa, and assuming that they represent key locations characteristic of the morphology and biomechanics of the entire diaphysis. Specifically, the mid-shaft has been assumed to most closely reflect diaphyseal biomechanical function, because the diaphysis is assumed to undergo the greatest strain during locomotion-induced bending (Ward, 2002 and references therein). However, this assumption is based on the „standard beam model“ used in engineering. Clearly, diaphyses deviate considerably from a standard beam (Lieberman et al., 2004) so it remains as an untested hypothesis whether cross-sections selected according to predefined criteria best represent functional properties of long bone diaphyses.

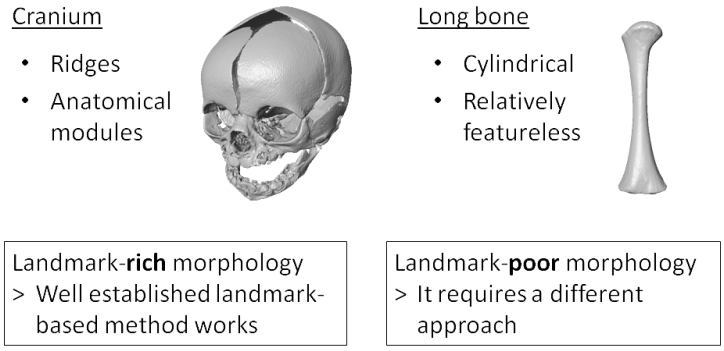

Fig. 3 Comparison of cranial and long bone morphologies. Cranium consists of relatively many anatomical modules and is landmark-rich compared to long bones.

Furthermore, cross-sectional data are typically sampled for a set of standard orientations around the diaphysis (e.g., in antero-posterior and medio-lateral directions). However, data sampled along predefined orientations can be difficult to evaluate, because anatomical axes are typically defined without testing homology (both in the sense of phyletic/developmental homology, and biomechanical equivalence) around the diaphysis. In essence, similar arguments may apply here, as are now applied in molecular studies on morphogen gradients in embryos along predefined standard anatomical axes.

The third approach is Geometric Morphometrics (GM) (Bookstein, 1991). GM methods provide a powerful means to investigate morphological variability, and they have been applied mainly to the cranium to document similarities and differences between taxon-specific ontogenetic patterns (e.g., O'Higgins and Jones, 1998; Ponce de León and Zollikofer, 2001; Penin et al., 2002; Mitteroecker et al., 2005; Cobb and O'Higgins, 2007). However, since the long bone diaphysis is relatively featureless, and has relatively few well-defined anatomical points of reference (so-called landmarks) compared to the cranium, application of landmark-based geometric morphometrics has been limited to epiphyseal morphology (Harmon, 2007, 2009; Holliday et al., 2010; Turley et al., 2011). Overall, thus, the morphology (shape) of long bone diaphyses is difficult to quantify comprehensively and reliably (Fig. 3). New methods are thus required, which not only permit full quantification of the external and internal diaphyseal morphology, but also permit visualization of patterns of diaphyseal shape change during ontogeny, and of patterns of intra- and inter-taxon variability in shape.

Questions and aims of the dissertation

The principal aim of this dissertation is to understand the association between long bone morphologies and taxon-specific locomotor modes in hominoid primates from the aspect of development, evolution, and function. To achieve this aim, a novel set of landmark-free geometric morphometric methods is developed, which permits in-depth analyses of the three-dimensional (external and internal) shape of long bone diaphyses.

These methods are used to quantify, analyze and visualize the morphological variability of the femoral diaphysis in modern humans and great apes (chimpanzees [*Pan troglodytes*], bonobos [*P. paniscus*], gorillas [*Gorilla gorilla*], orangutans [*Pongo pygmaues*]), from fetal stages to adulthood.

In the three studies comprised in this PhD thesis, I ask the following specific questions:

- *In-vivo* loading history: does Wolff's Law apply during the ontogeny of the femoral diaphyses? This question is addressed with a quantitative comparison of femoral diaphyseal ontogeny in captive and wild chimpanzees, *P. troglodytes troglodytes*. These groups differ widely in locomotor behavior, such that tracking femoral diaphyseal ontogeny reveals the effects of *in-vivo* modification against the effects of a common (gene-mediated) developmental program.

- Phylogeny versus locomotor adaptation: to which extent does femoropelvic musculoskeletal topography reflect taxon-specific locomotor adaptation in the hominoids, and to which extent does it reflect their phyletic history? This question is investigated with methods of virtopsy (virtual autopsy, typically used in forensics) extended to the great apes, permitting simultaneous analysis of hard and soft tissues of one and the same specimen.

- Taxon-specific developmental programs: how, when and why do taxon-specific femoral diaphyseal features of hominoids appear during ontogeny? This question is addressed by investigating fetal specimens in humans, chimpanzees, gorillas and orangutans where the inter-specific variation is undisturbed by the taxon-specific postnatal mechanical loading schemes. These data provide insights into the role of early (prenatal) ontogenetic processes in shaping taxon-specific diaphyseal morphologies.

References

Aiello L, Dean C. 1990. An Introduction to Human Evolutionary Anatomy. London: Academic Press.

Alexander RM. 2004. Bipedal animals, and their differences from humans. J Anat 204:321-330.

Bass S, Saxon L, Daly R, Turner C, Robling A, Seeman E, Stuckey S. 2002. Effect of mechanical loading on the size and shape of bone in pre-, peri-, and postpubertal girls: a study in tennis players. J Bone Miner Res 17:2274-2280.

Beddard F. 1893. Contributions to the anatomy of the anthropoid apes. Trans Zool Soc London 13:177-218.

Benazet JD, Zeller R. 2009. Vertebrate limb development: moving from classical morphogen gradients to an integrated 4-dimensional patterning system. Cold Spring Harbor Perspectives in Biology 1.

Bennett MR, Harris JWK, Richmond BG, Braun DR, Mbua E, Kiura P, Olago D, Kibunjia M, Omuombo C, Behrensmeyer AK, Huddart D, Gonzalez S. 2009. Early hominin foot morphology based on 1.5-million-year-old footprints from Ileret, Kenya. Science 323:1197-1201.

Bertram JEA, Swartz SM. 1991. The law of bone transformation - a case of crying Wolff. Biol Rev Camb Philos Soc 66:245-273.

Boehm B, Westerberg H, Lesnicar-Pucko G, Raja S, Rautschka M, Cotterell J, Swoger J, Sharpe J. 2010. The role of spatially controlled cell proliferation in limb bud morphogenesis. PLoS Biol 8:e1000420.

Bookstein F. 1991. Morphometric Tools for Landmark Data: Geometry and Biology. Cambridge: Camnridge University Press.

Boyer E. 1935. The musculature of the inferior extremity of the orang-utan *Simia satyrus*. Am J Anat 56:192-256.

Bramble DM, Lieberman DE. 2004. Endurance running and the evolution of *Homo*. Nature 432:345-352.

Brunet M, Guy F, Pilbeam D, Mackaye HT, Likius A, Ahounta D, Beauvilain A, Blondel C, Bocherens H, Boisserie JR, De Bonis L, Coppens Y, Dejax J, Denys C, Duringer P, Eisenmann VR, Fanone G, Fronty P, Geraads D, Lehmann T, Lihoreau F, Louchart A, Mahamat A, Merceron G, Mouchelin G, Otero O, Campomanes PP, De Leon MP, Rage JC, Sapanet M, Schuster M, Sudre J, Tassy P, Valentin X, Vignaud P, Viriot L, Zazzo A, Zollikofer C. 2002. A new hominid from the Upper Miocene of Chad, central Africa. Nature 418:145-151.

Butterfield NC, McGlinn E, Wicking C. 2010. The molecular regulation of vertebrate limb patterning. In: Organogenesis in Development: Elsevier. p 319-341.

Cardoso FA, Henderson CY. 2010. Enthesopathy Formation in the Humerus: Data from Known Age-at-Death and Known Occupation Skeletal Collections. Am J Phys Anthropol 141:550-560.

Carlson KJ. 2005. Investigating the form-function interface in African apes: Relationships between principal moments of area and positional behaviors in femoral and humeral diaphyses. Am J Phys Anthropol 127:312-334.

Carlson KJ, Doran-Sheehy DM, Hunt KD, Nishida T, Yamanaka A, Boesch C. 2006. Locomotor behavior and long bone morphology in individual free-ranging chimpanzees. J Hum Evol 50:394-404.

Carrier DR. 1996. Ontogenetic limits on locomotor performance. Physiol Zool 69:467-488.

Carrier DR, Anders C, Schilling N. 2011. The musculoskeletal system of humans is not tuned to maximize the economy of locomotion. Proc Natl Acad Sci U S A 108:18631-18636.

Cavagna GA, Heglund NC, Taylor CR. 1977. Mechanical work in terrestrial locomotion: two basic mechanisms for minimizing energy expenditure. Am J Physiol 233:R243-261.

Cobb SN, O'Higgins P. 2007. The ontogeny of sexual dimorphism in the facial skeleton of the African apes. J Hum Evol 53:176-190.

Demes B, Qin YX, Stern JT, Jr., Larson SG, Rubin CT. 2001. Patterns of strain in the macaque tibia during functional activity. Am J Phys Anthropol 116:257-265.

Dillon R, Othmer HG. 1999. A mathematical model for outgrowth and spatial patterning of the vertebrate limb bud. J Theor Biol 197:295-330.

Diogo R, Wood B. 2011. Soft-tissue anatomy of the primates: phylogenetic analyses based on the muscles of the head, neck, pectoral region and upper limb, with notes on the evolution of these muscles. J Anat 219:273-359.

Doran DM. 1992. The ontogeny of chimpanzee and pygmy chimpanzee locomotor behavior - a case-study of paedomorphism and its behavioral-correlates. J Hum Evol 23:139-157.

Doran DM. 1993. Comparative locomotor behavior of chimpanzees and bonobos - the influence of morphology on locomotion. Am J Phys Anthropol 91:83-98.

Doran DM. 1997. Ontogeny of locomotion in mountain gorillas and chimpanzees. J Hum Evol 32:323-344.

Galik K, Senut B, Pickford M, Gommery D, Treil J, Kuperavage AJ, Eckhardt RB. 2004. External and internal morphology of the BAR 1002 ' 00 *Orrorin tugenensis* femur. Science 305:1450-1453.

Gibbs S, Collard M, Wood B. 2000. Soft-tissue characters in higher primate phylogenetics. Proc Natl Acad Sci USA 97:11130-11132.

Gibbs S, Collard M, Wood B. 2002. Soft-tissue anatomy of the extant hominoids: a review and phylogenetic analysis. J Anat 200:3-49.

Gilbert CC, Rossie JB. 2007. Congruence of molecules and morphology using a narrow allometric approach. Proc Natl Acad Sci USA 104:11910-11914.

Goodship AE, Lanyon LE, McFie H. 1979. Functional adaptation of bone to increased stress - experimental-study. Journal of Bone and Joint Surgery-American Volume 61:539-546.

Gould SJ, Lewontin RC. 1979. The spandrels of San Marco and the Panglossian paradigm: a critique of the adaptationist programme. Proc R Soc Lond, Ser B: Biol Sci 205:581-598.
Griffin TM, Main RP, Farley CT. 2004. Biomechanics of quadrupedal walking: how do four-legged animals achieve inverted pendulum-like movements? J Exp Biol 207:3545-3558.
Harmon EH. 2007. The shape of the hominoid proximal femur: a geometric morphometric analysis. J Anat 210:170-185.
Harmon EH. 2009. The shape of the early hominin proximal femur. Am J Phys Anthropol 139:154-171.
Harrison T. 2010. Apes among the tangled branches of human origins. Science 327:532-534.
Heinrich RE, Ruff CB, Adamczewski JZ. 1999. Ontogenetic changes in mineralization and bone geometry in the femur of muskoxen (Ovibos moschatus). J Zool 247:215-223.
Holliday TW, Hutchinson VT, Morrow MMB, Livesay GA. 2010. Geometric morphometric analyses of hominid proximal femora: Taxonomic and phylogenetic considerations. Homo-Journal of Comparative Human Biology 61:3-15.
Holt BM. 2003. Mobility in Upper Paleolithic and Mesolithic Europe: Evidence from the lower limb. Am J Phys Anthropol 122:200-215.
Jones HH, Priest JD, Hayes WC, Tichenor CC, Nagel DA. 1977. Humeral hypertrophy in response to exercise. J Bone Joint Surg Am 59:204-208.
Kimura M. 1968. Evolutionary rate at the molecular level. Nature 217:624-626.
Lammers AR, German RZ. 2002. Ontogenetic allometry in the locomotor skeleton of specialized half-bounding mammals. J Zool 258:485-495.
Lanyon LE. 1987. Functional strain in bone tissue as an objective, and controlling stimulus for adaptive bone remodeling. J Biomech 20:1083-1093.
Lanyon LE, Baggott DG. 1976. Mechanical function as an influence on structure and form of bone. J Bone Joint Surg-Br Vol 58:436-443.
Lanyon LE, Bourn S. 1979. Influence of mechanical function on the development and remodeling of the tibia - experimental-study in sheep. Journal of Bone and Joint Surgery-American Volume 61:263-273.
Leakey MD, Hay RL. 1979. Pliocene footprints in the Laetolil beds at Laetoli, northern Tanzania. Nature 278:317-323.
Lieberman DE, Polk JD, Demes B. 2004. Predicting long bone loading from cross-sectional geometry. Am J Phys Anthropol 123:156-171.
Lieberman DE, Raichlen DA, Pontzer H, Bramble DM, Cutright-Smith E. 2006. The human gluteus maximus and its role in running. J Exp Biol 209:2143-2155.
Lockwood CA. 1999. Homoplasy and adaptation in the atelid postcranium. Am J Phys Anthropol 108:459-482.
Lockwood CA, Fleagle JG. 2007. Homoplasy in primate and human evolution. J Hum Evol 52:471-472.
Lockwood CA, Kimbel WH, Lynch JM. 2004. Morphometrics and hominoid phylogeny: Support for a chimpanzee-human clade and differentiation among great ape subspecies. Proc Natl Acad Sci USA 101:4356-4360.
Lovejoy CO, Latimer B, Suwa G, Asfaw B, White TD. 2009a. Combining prehension and propulsion: The foot of *Ardipithecus ramidus*. Science 326:72.
Lovejoy CO, McCollum MA, Reno PL, Rosenman BA. 2003. Developmental biology and human evolution. Annu Rev Anthropol 32:85-109.
Lovejoy CO, Meindl RS, Ohman JC, Heiple KG, White TD. 2002. The Maka femur and its bearing on the antiquity of human walking: Applying contemporary concepts of morphogenesis to the human fossil record. Am J Phys Anthropol 119:97-133.
Lovejoy CO, Suwa G, Spurlock L, Asfaw B, White TD. 2009b. The pelvis and femur of *Ardipithecus ramidus*: The emergence of upright walking. Science 326:71.
Main RP, Biewener AA. 2007. Skeletal strain patterns and growth in the emu hindlimb during ontogeny. J Exp Biol 210:2676-2690.
Minetti AE, Ardig OL, Reinach E, Saibene F, Prabhakar S, Visel A, Akiyama JA, Shoukry M, Lewis KD, Holt A, Plajzer-Frick I, Morrison H, Fitzpatrick DR, Afzal V, Pennacchio LA, Rubin EM,

Noonan JP, Reno PL, McCollum MA, Cohn MJ, Meindl RS, Hamrick M, Lovejoy CO. 1999. The relationship between mechanical work and energy expenditure of locomotion in horses. J Exp Biol 202:2329-2338.

Mitteroecker P, Gunz P, Bookstein FL. 2005. Heterochrony and geometric morphometrics: a comparison of cranial growth in *Pan paniscus* versus *Pan troglodytes*. Evol Dev 7:244-258.

Molnar P. 2006. Tracing prehistoric activities: Musculoskeletal stress marker analysis of a stone-age population on the island of Gotland in the Baltic Sea. Am J Phys Anthropol 129:12-23.

Morishita Y, Iwasa Y. 2008. Growth based morphogenesis of vertebrate limb bud. Bull Math Biol 70:1957-1978.

Mosley JR, Lanyon LE. 1998. Strain rate as a controlling influence on adaptive modeling in response to dynamic loading of the ulna in growing male rats. Bone 23:313-318.

Netter F. 2003. Atlas of Human Anatomy, 3 ed. Philadelphia: Saunders.

O'Higgins P, Jones N. 1998. Facial growth in Cercocebus torquatus: an application of three-dimensional geometric morphometric techniques to the study of morphological variation. J Anat 193:251-272.

O'Neill MC, Dobson SD. 2008. The degree and pattern of phylogenetic signal in primate long-bone structure. J Hum Evol 54:309-322.

Pearson OM. 2000. Postcranial remains and the origin of modern humans. Evol Anthropol 9:229-247.

Pearson OM, Lieberman DE. 2004. The aging of Wolff's "Law": Ontogeny and responses to mechanical loading in cortical bone. Yearb Phys Anthropol 47:63-99.

Penin X, Berge C, Baylac M. 2002. Ontogenetic study of the skull in modern humans and the common chimpanzees: neotenic hypothesis reconsidered with a tridimensional Procrustes analysis. Am J Phys Anthropol 118:50-62.

Pickford M, Senut B, Gommery D, Treil J. 2002. Bipedalism in *Orrorin tugenensis* revealed by its femora. C R Palevol 1:191-203.

Ponce de León MS, Zollikofer CPE. 2001. Neanderthal cranial ontogeny and its implications for late hominid diversity. Nature 412:534-538.

Pontzer H, Raichlen DA, Sockol MD. 2009. The metabolic cost of walking in humans, chimpanzees, and early hominins. J Hum Evol 56:43-54.

Primrose A. 1898. The anatomy of the Orang utang (*Simia satyrus*). Trans Canad Inst 6:507-598.

Raven H. 1950. Regional anatomy of the gorilla. In: Gregory W, editor. The Anatomy of the Gorilla. New York: Columbia University Press.

Rhodes JA, Knüsel CJ. 2005. Activity-related skeletal change in medieval humeri: Cross-sectional and architectural alterations. Am J Phys Anthropol 128:536-546.

Richmond BG, Jungers WL. 2008. *Orrorin tugenensis* femoral morphology and the evolution of hominin bipedalism. Science 319:1662-1665.

Richmond BG, Strait DS. 2000. Evidence that humans evolved from a knuckle-walking ancestor. Nature 404:382-385.

Robling AG, Hinant FM, Burr DB, Turner CH. 2002. Improved bone structure and strength after long-term mechanical loading is greatest if loading is separated into short bouts. J Bone Miner Res 17:1545-1554.

Rodman PS, McHenry HM. 1980. Bioenergetics and the origin of hominid bipedalism. Am J Phys Anthropol 52:103-106.

Rook L, Bondioli L, Kohler M, Moya-Sola S, Macchiarelli R. 1999. *Oreopithecus* was a bipedal ape after all: Evidence from the iliac cancellous architecture. Proc Natl Acad Sci USA 96:8795-8799.

Ruff CB. 1988. Hindlimb articular surface allometry in hominoidea and *Macaca*, with comparisons to diaphyseal scaling. J Hum Evol 17:687-714.

Ruff CB. 2002. Long bone articular and diaphyseal structure in old world monkeys and apes. I: Locomotor effects. Am J Phys Anthropol 119:305-342.

Ruff CB. 2003a. Growth in bone strength, body size, and muscle size in a juvenile longitudinal sample. Bone 33:317-329.

Ruff CB. 2003b. Ontogenetic adaptation to bipedalism: age changes in femoral to humeral length and strength proportions in humans, with a comparison to baboons. J Hum Evol 45:317-349.

Ruff CB. 2009. Relative limb strength and locomotion in *Homo habilis*. Am J Phys Anthropol 138:90-100.
Ruff CB, Hayes WC. 1983. Cross-sectional geometry of Pecos Pueblo femora and tibiae--a biomechanical investigation: I. Method and general patterns of variation. Am J Phys Anthropol 60:359-381.
Ruff CB, Holt B, Trinkaus E. 2006. Who's afraid of the big bad wolff? "Wolff is law" and bone functional adaptation. Am J Phys Anthropol 129:484-498.
Ruff CB, McHenry HM, Thackeray JF. 1999. Cross-sectional morphology of the SK 82 and 97 proximal femora. Am J Phys Anthropol 109:509-521.
Ruff CB, Runestad JA. 1992. Primate limb bone structural adaptations. Annu Rev Anthropol 21:407-433.
Ruff CB, Walker A, Trinkaus E. 1994. Postcranial robusticity in *Homo*. III: ontogeny. Am J Phys Anthropol 93:35-54.
Scheuer L, Black S, Christie A. 2000. Developmental Juvenile Osteology. San Diego, San Francisco, New York, Boston, London, Sydney, Tokyo: Academic Press.
Schmitt D. 2003. Insights into the evolution of human bipedalism from experimental studies of humans and other primates. J Exp Biol 206:1437-1448.
Schultz AH. 1937. Proportions, variability and asymmetries of the long bones of the limbs and the clavicles in man and apes. Hum Biol 9:281-328.
Schultz AH. 1969. The skeleton of the chimpanzee. In: Bourne GH, editor. The Chimpanzee, Vol. 1. Basel: Karger. p 50-103.
Schwartz JH. 1995. Skeleton Keys: An Introduction to Human Skeletal Morphology, Development, and Analysis. Oxford: Oxford University Press.
Senut B, Pickford M, Gommery D, Mein P, Cheboi K, Coppens Y. 2001. First hominid from the Miocene (Lukeino Formation, Kenya). C R Acad Sci Paris Ser II a 332:137-144.
Serrat MA, King D, Lovejoy CO. 2008. Temperature regulates limb length in homeotherms by directly modulating cartilage growth. Proc Natl Acad Sci USA 105:19348-19353.
Serrat MA, Lovejoy CO, King D. 2007. Age- and site-specific decline in insulin-like growth factor-I receptor expression is correlated with differential growth plate activity in the mouse hindlimb. The Anatomical Record: Advances in Integrative Anatomy and Evolutionary Biology 290:375-381.
Sigmon BA. 1974. A functional analysis of pongid hip and thigh musculature. J Hum Evol 3:161-185.
Sockol MD, Raichlen DA, Pontzer H. 2007. Chimpanzee locomotor energetics and the origin of human bipedalism. Proc Natl Acad Sci USA 104:12265-12269.
Sparacello V, Marchi D. 2008. Mobility and subsistence economy: A diachronic comparison between two groups settled in the same geographical area (Liguria, Italy). Am J Phys Anthropol 136:485-495.
Standring S, editor. 2004. Gray's Anatomy, 39 ed. Edinburgh/London/New York: Churchill Livingstone.
Standring S, editor. 2005. Gray's anatomy: Churchill Livingstone.
Stern JT. 1972. Anatomical and functional specializations of human gluteus maximus. Am J Phys Anthropol 36:315-338.
Stern JT, Susman RL. 1981. Electromyography of the gluteal muscles in *Hylobates*, *Pongo*, and *Pan* - implications for the evolution of hominid bipedality. Am J Phys Anthropol 55:153-166.
Sumner DR, Andriacchi TP. 1996. Adaptation to differential loading: Comparison of growth-related changes in cross-sectional properties of the human femur and humerus. Bone 19:121-126.
Sutherland DH, Olshen R, Cooper L, Woo SL. 1980. The development of mature gait. J Bone Joint Surg Am 62:336-353.
Swindler D, Wood C. 1982. An Atlas of Primate Gross Anatomy. Malabar: Robert E. Krieger Publishing Company.
Szivek JA, Johnson EM, Magee FP. 1992. *In vivo* strain analysis of the greyhound femoral diaphysis. Journal of Investigative Surgery 5:91-108.
Thorpe SKS, Holder RL, Crompton RH. 2007. Origin of human bipedalism as an adaptation for locomotion on flexible branches. Science 316:1328-1331.

Trinkaus E, Churchill SE, Ruff CB. 1994. Postcranial robusticity in *Homo*. II: Humeral bilateral asymmetry and bone plasticity. Am J Phys Anthropol 93:1-34.

Turley K, Guthrie EH, Frost SR. 2011. Geometric Morphometric Analysis of Tibial Shape and Presentation Among Catarrhine Taxa. The Anatomical Record: Advances in Integrative Anatomy and Evolutionary Biology 294:217-230.

Turner CH, Forwood MR, Otter MW. 1994. Mechanotransduction in bone - do bone-cells act as sensors of fluid-flow. FASEB J 8:875-878.

Turner CH, Owan I, Takano Y. 1995. Mechanotransduction in bone - role of strain-rate. American Journal of Physiology-Endocrinology and Metabolism 269:E438-E442.

Uhlmann K. 1968. Hüft- und Oberschenkelmuskulatur: Systematische und vergleichende Anatomie. In: Hofer H, Schultz AH, Starck D, editors. Primatologia: Handbuch der Primatenkunde. Basel: Karger.

Villotte S, Castex D, Couallier V, Dutour O, Knusel CJ, Henry-Gambier D. 2010. Enthesopathies as occupational stress markers: evidence from the upper limb. Am J Phys Anthropol 142:224-234.

Wallace IJ, Middleton KM, Svetlana L, Kelly SA, Stefan J, Theodore G, Jr., Brigitte D. 2010. Functional significance of genetic variation underlying limb bone diaphyseal structure. In.

Ward CV. 2002. Interpreting the posture and locomotion of *Australopithecus afarensis*: where do we stand? Am J Phys Anthropol Suppl 35:185-215.

Warden SJ, Hurst JA, Sanders MS, Turner CH, Burr DB, Li J. 2005. Bone adaptation to a mechanical loading program significantly increases skeletal fatigue resistance. J Bone Miner Res 20:809-816.

White TD, Asfaw B, Beyene Y, Haile-Selassie Y, Lovejoy CO, Suwa G, WoldeGabriel G. 2009. *Ardipithecus ramidus* and the paleobiology of early hominids. Science 326:75-86.

Wolff J. 1892. Das Gesetz der Transformation der Knochen. Berlin: A. Hirschwald.

Wood B, Harrison T. 2011. The evolutionary context of the first hominins. Nature 470:347-352.

Wood B, Richmond BG. 2000. Human evolution: taxonomy and paleobiology. J Anat 197 (Pt 1):19-60.

Young JW, Fernandez D, Fleagle JG. 2009. Ontogeny of long bone geometry in capuchin monkeys (Cebus albifrons and Cebus apella): implications for locomotor development and life history. Biol Lett 6:197-200.

Young NM, Wagner GP, Hallgrímsson B. 2010. Development and the evolvability of human limbs. Proc Natl Acad Sci USA 107:3400-3405.

Zollikofer CPE, de Leon MSP, Lieberman DE, Guy F, Pilbeam D, Likius A, Mackaye HT, Vignaud P, Brunet M. 2005. Virtual cranial reconstruction of *Sahelanthropus tchadensis*. Nature 434:755-759.

Chapter 1 Exploring femoral diaphyseal shape variation in wild and captive chimpanzees by means of morphometric mapping: a test of Wolff's Law

Reference: *Anatomical Record* 294:589-609.

Abstract

Long bone shafts (diaphyses) serve as load-bearing structures during locomotion, implying a close relationship between diaphyseal form and its locomotor function. Diaphyseal form-function relationships, however, are complex, as they are mediated by various factors such as developmental programs, evolutionary adaptation, and functional adaptation through bone remodeling during an individual's lifetime. The effects of the latter process ("Wolff's Law") are best assessed by comparing diaphyseal morphologies of conspecific individuals under different locomotor regimes. Here we use morphometric mapping to analyze the morphology of entire femoral diaphyses in an ontogenetic series of wild and captive common chimpanzees (*Pan troglodytes troglodytes*). Morphometric mapping reveals patterns of variation of diaphyseal structural and functional properties, which cannot be recognized with conventional cross-sectional analysis and/or geometric morphometric methods. Our data show that diaphyseal shape, cortical bone distribution and inferred cross-sectional biomechanical properties vary both along ontogenetic trajectories and independent of ontogeny. Mean ontogenetic trajectories of wild and captive chimpanzees, however, were found to be statistically identical. This indicates that the basic developmental program of the diaphysis is not altered by different loading conditions. Significant differences in diaphyseal shape between groups could only be identified in the distal diaphysis, where wild chimpanzees exhibit higher mediolateral relative to anteroposterior cortical bone thickness. Overall, thus, the hypothesis that Wolff's Law predominantly governs long bone diaphyseal morphology is rejected.

Key words: ontogeny, long bone, femur, functional bone adaptation, cross-sectional geometry, geometric morphometrics, cylindrical parameterization

Introduction

Primate long bone diaphyses show considerable morphological variation, reflecting a wide diversity of inter- and intraspecific modes of locomotion. Diaphyses serve as beams that must withstand the mechanical loads generated during locomotion, but how exactly diaphyseal form is related to locomotor function depends on a variety of factors. Relevant factors are gene-mediated developmental programs, long-term (evolutionary) adaptation as a response to selective pressures, and short-term (*in-vivo*) modification as a response to mechanical loading patterns experienced during an individual's life. The relationship between these factors is complex, and the relative impact of each of them on long bone morphology is often difficult to assess (Pearson and Lieberman, 2004).

It is typically hypothesized that diaphyseal shape reflects locomotor behavior[1] according to Wolff's Law (WL; Wolff, 1892; Wolff, 1986), which posits that bones are remodeled *in vivo* to optimally resist mechanical loading patterns. WL has recently be restated in a more general form as "bone functional adaptation"[2] (Ruff et al., 2006). WL is supported by various experimental studies that investigate the effects of mechanical loading in controlled settings (e.g., Lanyon and Baggott, 1976; Lanyon and Bourn, 1979; Lanyon, 1987; Turner et al., 1995; Robling et al., 2002; Warden et al., 2005). Another example is hypertrophy of the playing arm relative to the non-playing arm in professional athletes (e.g., Jones et al., 1977; Bass et al., 2002). While WL still serves as a useful basic hypothesis of how diaphyseal form is related to function, it was challenged on several grounds. Due to difficulties in identifying direct effects of mechanical *in-vivo* loading on diaphyseal shape, it was suggested that bone modification could be explained by factors other than mechanical loading such as bone inflammation and regeneration or bone fracture repair processes (Bertram and Swartz, 1991). Furthermore, various recent developmental studies (reviewed in Lovejoy et al., 2003) indicate that long bone shape largely reflects developmental programs. An additional level of complexity in diaphyseal form-function relationships was revealed by *in-vivo* strain analyses, which showed that inferred biomechanical properties of long bones (e.g., inferred bending strength relative to the neutral axis) do not always coincide with biomechanical properties measured with strain gauges during locomotion (e.g., actual bending direction) (Demes et al., 2001; Lieberman et al., 2004).

Various research strategies are currently followed to gain new insights into form-function relationships in long bones. The first is to perform more detailed *in-vivo* bone strain measurements to establish direct links between locomotor modes, spatiotemporal loading patterns, biomechanical properties, and diaphyseal morphology. Several studies showed, for example, that *in-vivo* bone strain patterns change dynamically during locomotion, and that bone shape may be better correlated with peak loads than with average loading patterns (Szivek et al., 1992; Demes et al., 2001; Lieberman et al., 2004). The second strategy is an approach, which simulates the evolutionary process experimentally (Garland and Rose, 2009). A recent study showed that more robust diaphyses reflect the evolutionary history rather than *in-vivo* activity levels of an individual, indicating a strong genetic influence on long bone diaphyseal development and morphology (Wallace et al., 2010b).

[1] In this study, *locomotor behavior* is defined as the relative frequencies of *locomotor modes* (e.g. climbing, terrestrial bipedal walking, etc.) displayed by an individual over a given time span (e.g. as an infant or adult).

[2] In this study, *modification* is used as a more general term in place of *functional adaptation* (Ruff et al. 2006) to discern between adaptation as a long-term evolutionary process and modification as a process occurring during an individual's lifetime.

The third strategy, which is adopted here, consists in analyzing patterns of variation of diaphyseal morphology. Data from different species, from ontogenetic series, and from individuals with known differences in *in-vivo* loading histories help assess the respective roles of phylogenetic processes, developmental programs, and specific loading patterns on bone shape. Two approaches may be used to quantify diaphyseal morphology. The first evaluates biomechanical (*i.e.*, functional) properties according to standard models of beam theory (Lovejoy et al., 1976; Ruff and Hayes, 1983; Ruff and Runestad, 1992). The second quantifies biologically homologous features and is known as Geometric Morphometrics (GM) (Bookstein, 1991). During the analysis of long bone diaphyseal morphologies, each approach has its specific potential and limitations.

Biomechanical properties of long bones such as resistance against axial loading or bending are typically quantified by cross-sectional properties, such as cortical bone area, second moments of area, and section modulus. Often, such data are acquired at the mid-shaft assuming that the mid-shaft represents a functionally equivalent region in different taxa. Various studies demonstrated a clear relationship between locomotor modes and cross-sectional properties of long bone diaphyses (Burr et al., 1989; Kimura, 1991; Ruff and Runestad, 1992; Demes and Jungers, 1993; Kimura, 1995; Ruff, 2002). For example, primates show greater cross-sectional strength than terrestrial mammals at similar body mass, which was interpreted as an adaptation to arboreal environments (Kimura, 1991, 1995). However, within primates and within rodents the relationship between cross-sectional strength and arboreality/terrestriality does not hold, indicating that other factors are relevant in determining diaphyseal shape (Polk et al., 2000). Also, it has been shown that specific locomotor modes are correlated with specific cross-sectional properties; for example, prosimian species specialized in leaping exhibit anteroposteriorly expanded femoral cross sections compared to non-leaping species of similar body mass (Demes and Jungers, 1993). Further, a comparative analysis of three *Macaca* species (Burr et al., 1989) demonstrated that humeral and femoral cross-sectional rigidity is higher in more terrestrial species than arboreal ones, and that relative strengths of fore- and hind limbs distinguish suspensory and leaping species in primates (Ruff, 2002).

Several studies compared cross-sectional properties of long bone diaphyses within species, be it between wild and captive individuals, or between individuals with known locomotor histories in the wild or in experimental setups. A comparative analysis of wild and captive *Lemur catta* did not find significant differences between groups in length, cross-sectional area and section modulus of the humerus and femur (Demes and Jungers, 1993). On the other hand, captive individuals of *Macaca nemestrina* showed greater second moments of area in humerus and femur relative to body mass than wild individuals in absolute value, but profiles of relative magnitude of second moments of area along femoral/humeral diaphyses did not differ between the two groups (Burr et al., 1989). Comparison of chimpanzees with known individual locomotor behaviors showed that femoral/humeral diaphyseal cross-sectional properties are only loosely correlated with the frequency of arboreal/quadrupedal locomotion (Carlson, 2005; Carlson et al., 2006), but well correlated with age (Carlson et al., 2008a). Differences were found between female chimpanzees from Taï versus Mahale/Gombe in the ratio of maximum to minimum bending rigidity (I_{max}/I_{min}) at the mid-proximal diaphysis of the humerus, and the mid-distal diaphysis of femur (Carlson et al., 2008a), but the question remains open whether such contrasts reflect differences between population-specific locomotor behavior, or between population-specific developmental programs. Comparison of diaphyseal morphology between two groups of mice with different locomotor regimes (straight and curved-course running) showed that different activity patterns do not result in significant differences in various cross-sectional properties of cortical bone (cortical area, second moments of area in mediolateral and anteroposterior direction) nor in trabecular

bone structure (Carlson and Judex, 2007; Carlson et al., 2008b). The ratio of mediolateral to anteroposterior bending rigidity was, however, found to be significantly different between groups (Carlson and Judex, 2007).

Some analyses thus show that cross-sectional properties convey functionally relevant information, but others do not provide clear links between form and function. This might be due to limitations in the data rather than to actual absence of correlation. Cross-sectional data typically come from selected regions of the diaphysis (e.g. the midshaft), and biomechanical properties such as second moments of area are evaluated for a set of standard orientations around the diaphysis. Using such data, various studies showed that the midshaft is an adequate region to compare diaphyseal cross-sectional properties (e.g., Ruff et al., 1994; Ruff, 2002, 2009). Actual long bone loading patterns, however, may exhibit high spatial heterogeneity, as they result from a combination of bone geometry and the topography and activation patterns of the locomotor muscles acting on the bone. It was demonstrated that long bones experience dynamically changing patterns of strain during locomotion (Demes et al., 2001; Lieberman et al., 2004), and that they exhibit different remodeling patterns at different locations (Bass et al., 2002). Also, various muscles that are biomechanically relevant for quadrupedal versus bipedal locomotion attach to the proximal femoral diaphysis (Crass, 1952; Stern, 1972; Swindler and Wood, 1982; Lovejoy et al., 2002), such that one might expect different form-function relationships in proximal compared to middle and distal areas of the diaphysis. Accordingly, if we take into account that the second moment of area is a directional integral, tracking changes in its magnitude around and along the diaphysis may provide relevant additional data on bending resistance under complex *in-vivo* loading conditions.

In studies analyzing form-function relationships, the femur has received special attention, because primate locomotion is typically hindlimb-dominated (Kimura et al., 1979; Reynolds, 1985; Demes et al., 1994; Schmitt and Lemelin, 2002), and because the transition from quadrupedal modes of locomotion (Lovejoy et al., 2009a; Lovejoy et al., 2009b; Lovejoy et al., 2009c) to obligate bipedalism in the hominins involved key changes in femoral biomechanics. How can structurally and functionally relevant quantitative information be gathered from the diaphysis as a whole, and in a comprehensive form? One possibility is to use landmark (or semilandmark)-based geometric morphometric (GM) methods, which permit quantitative analyses of entire organismic forms in two or three spatial dimensions. GM methods use anatomical points of reference (so-called landmarks) to establish point-to-point homology between specimens of a sample. GM methods are thus optimized for the analysis of landmark-rich, modular biological structures such as the cranium of hominins and non-human primates (e.g., O'Higgins and Jones, 1998; Ponce de León and Zollikofer, 2001). Recently, GM has also been used to study long bone morphology, but while this set of methods is well applicable to epiphyses (Harmon, 2007, 2009; Holliday et al., 2010), it is less suited for diaphyses. Diaphyses consist of a single developmental module and exhibit only few clearly defined landmarks. In principle, ridge structures on the diaphyseal surface can be used to define semilandmarks, which quantify geometric (rather than biological) homology between specimens (Gunz et al., 2005), but most diaphyses exhibit relatively few such structures, which themselves tend to be highly variable.

Application of GM to long bone diaphyses also has technical and graphical limitations. In GM, size is normalized by centroid size (Bookstein, 1991) prior to analysis of shape variation. While this approach works well for landmark configurations with an approximately isotropic distribution in space, it is not suited for the cylindrical geometry of diaphyses, where most of size variation is due to differences in diaphyseal length. A straightforward workaround is to apply some form of affine normalization with different scaling factors along and across the diaphyseal geometry. However, the results of a semilandmark-based GM analysis of diaphyseal shape variation are difficult to visualize

comprehensively, because our visual system is relatively inefficient in recognizing patterns of variation in a cylindrical geometry.

Measuring long bone structural and functional properties along the entire diaphysis, and visualizing and analyzing these data comprehensively thus represents a double challenge. GM methods must be expanded to permit shape analysis of the essentially landmark-free diaphysis, and the analysis of cross-sectional properties must be extended to comprise the entire diaphysis. Here we use morphometric mapping techniques to meet these challenges. The concept of morphometric mapping (MM) was introduced by Amtmann and Schmitt (1968) to analyze patterns of cortical bone distribution and biomechanical properties along the femoral diaphysis (Amtmann and Schmitt, 1968). Later, MM was formalized and combined with 3D imaging to compare geometric and cross-sectional properties of human and great ape femora (Jungers and Minns, 1979) (Zollikofer and Ponce de León, 2001). Recently, MM was re-applied to visualize femoral cortical bone thickness and canine dentine distribution (Bondioli et al., 2010). While MM has mainly been used as a visualization tool, we embed it here into the generalized framework of morphometric surface parameterization. Surface parameterization denotes the process of mapping the surfaces of biological structures onto Euclidean bodies. The latter can then be used as a frame of reference to compare the specimens of a sample. One example is spherical surface parameterization, which was introduced to map endocranial surfaces onto a sphere, and to analyze endocranial shape variation in terms of deformation of the sphere (Specht et al., 2007). In this paper, we use cylindrical parameterization as a means to represent the distribution of data sampled on long bone diaphyses. These data represent geometric features of the diaphysis such as cross-sectional shape, surface curvature and cortical bone thickness, as well as biomechanical properties such as cross-sectional cortical bone area and second moments of area.

Aims and hypotheses

This paper has two aims. The first is to introduce MM as a new analytical tool kit for long bone diaphyseal analysis and to compare its performance with traditional cross-sectional analysis and with GM methods. The second aim is to apply these methods to investigate patterns of femoral diaphyseal shape variation in an ontogenetic series of wild and captive common chimpanzees (*Pan troglodytes troglodytes*). This sample is used to address the question how developmental programs versus *in-vivo* loading patterns influence femoral geometric and biomechanical properties. The captive chimpanzees used in this study were all held in traditional zoos (specimens were collected by A.H. Schultz between 1930 and 1950). This implies that these chimpanzees lived in spatially more confined and structurally less complex environments than their wild conspecifics, resulting in less overall locomotor activity and restricted/modified diversity of species-specific locomotor patterns (Jensvold et al., 2001).

Direct information about the locomotor behavior of the zoo individuals in our sample is not available, but clear differences between zoo and wild animals in locomotor behavior have been reported: Captive chimpanzees do not have the opportunity of long-distance traveling, as is typically observed in natural environments (Goodall, 1986; Jensvold et al., 2001). Chimpanzees held in traditional zoos exhibit a higher proportion of suspensory and climbing behaviors compared to wild chimpanzees, but no leaping behavior (Jensvold et al., 2001). When transferred from traditional to modern zoos offering large living areas and improved climbing structures, captive chimpanzees showed higher frequencies of bipedal, climbing, and leaping behaviors. Compared to wild-living individuals, they spent more time for standing bipedally/quadrupedally and lying (Jensvold et al.,

2001), such that even in modern zoos locomotor behavior is constrained relative to free-range behavior. In summary, locomotor behavior of chimpanzees in captivity is constrained/modified compared with free-ranging chimpanzees in three respects: (a) in the diversity of the locomotor repertoire, (b) in the frequency of each locomotor mode, and (c) in activity levels. Comparing femoral morphology in wild and captive chimpanzees (all belonging to the same subspecies) thus provides an ideal test case to investigate the effects of locomotor differences in a sample with a common genetic and developmental background.

First, we ask whether differences in locomotor behavior between subsamples manifest themselves as differences in morphological and biomechanical properties of the femoral diaphysis. We hypothesize that ontogenetic trajectories between wild and captive chimpanzees diverge as an effect of *in-vivo* bone modification [WL, or functional bone adaptation *sensu* Ruff et al. (2006)]. Accordingly, we expect femoral diaphyseal shape variation in the pooled sample to be larger in adult than in immature specimens. Second, we ask whether cross-sectional measurements taken at the femoral midshaft optimally capture differences between subsamples. To test this hypothesis, we perform separate MM analyses of the proximal, middle, and distal thirds of the femoral diaphysis, and analyze which region, and which morphometric and biomechanical features, discriminate best between wild and captive chimpanzees. Third, we compare the outcomes of MM, GM, and midshaft cross-sectional analyses to assess the potential and limitations of each method.

Materials and methods

Sample

Wild (*N*=22) and captive (*N*=26) chimpanzees (*Pan troglodytes troglodytes*) from infant to adult stages (pooled sex; femoral diaphyseal length: 79 to 212mm) were obtained from the collection of the Anthropological Institute and Museum of the University of Zurich. To facilitate visualization of age-related trends, the sample is divided into three developmental categories according to femoral diaphyseal length (I: ≤120mm; II: 121-180mm; III: >180mm). These categories largely correspond to the following dental eruption stages: I: second deciduous molar erupted (infant); II: M1-M2 erupted (juvenile); III: M2-M3 erupted (adult) (see Fig. S1 for details). As mentioned, all captive individuals are from „traditional“ zoos, *i.e.*, where chimpanzees were held in small living areas and could not engage in long-range locomotion.

Volumetric and cross-sectional data acquisition

Femora of all specimens were scanned using a Siemens 64-detector-array CT device with the following data acquisition and image reconstruction parameters: beam collimation: 1.0mm; pitch: 0.5-0.75; image reconstruction kernel: standard/sharp (B30s/B70s); slice increment: 0.3 to 0.5mm. This resulted in volume data sets with isotropic spatial resolution in the range of 0.3 to 0.5mm. Small specimens (femoral length <150mm) were scanned using a micro-CT scanner (µCT80, Scanco Medical, Switzerland), and volume data were reconstructed at an isotropic voxel resolution of 75 µm.

Using the software package Amira 4.1 (Mercury Systems), each original CT data set was resampled along the principal axis of the femoral diaphysis in order to obtain *K*=300 equally-spaced cross-sectional images along the entire diaphysis (Fig. 1A). These standardized data sets served as a

basis for all further calculations. Biomechanical properties (such as second moments of area, see below) were calculated directly from the cross-sectional image data. Endosteal (internal, L_{int}) and subperiosteal (external, L_{ext}) outlines were extracted from each cross section (Fig. 1B), and each outline was submitted to Elliptic Fourier analysis (EFA; Kuhl and Giardina (1982); see Appendix A for details). EFA was used to represent each outline by a parametric function, which represents the position of consecutive points on the outline as a function of the distance traveled along the outline. EFœA provides a convenient means to control the level of detail of an outline representation (which is useful for noise reduction), to calculate standard geometric descriptors such as normal/tangent vectors, and to evaluate various morphometric variables (see below).

Morphometric data acquisition

Fig. 1 (A-C) provides a scheme of morphometric data acquisition. Various structural and functional variables can be defined on diaphyseal cross sections, such as external/internal radius, external/internal curvature, cortical bone thickness, and second moments of area. These variables depend on each other to some extent. For example, cortical bone thickness is derived from external and internal radius; curvature is a function of the first and second derivatives of the outline; second moments of area are area integrals related to radius and thickness. According to the question asked [structural (geometric) and/or functional (biomechanical)] it is convenient to visualize, explore and analyze various combinations of variables. In this study, we focus on external radius, external surface curvature, cortical bone thickness and second moments of area to investigate overall shape, surface topography, cortical bone distribution patterns, and biomechanical properties of the femoral diaphysis.

Radii r_{ext} and r_{int} were calculated as the distance from the center of mass to the periosteal and endosteal outlines respectively (Fig. 1B). Surface curvature k_{ext} was calculated analytically using the parametric function of the external outline (Fig. 1B; see Appendix A for details). Cortical bone thickness h was measured as the distance from a point P_{int} on the endosteal outline to the periosteal outline, measured along the surface normal vector at P_{int} (Fig. 1B). This definition of cortical bone thickness provides locally unbiased measurements even when cross-sectional shape deviates significantly from circularity.

To estimate resistance against bending, second moments of area, I_θ, were evaluated (Fig. 1C). I_θ represents the variance (spatial distribution) of cortical bone distribution orthogonal to the bending plane with normal vector θ (see Appendix B for details). I_θ is typically calculated at a single location of the diaphysis (midshaft) and along selected directions θ (e.g. anteroposteriorly/mediolaterally, and along directions of maximum/minimum rigidity). Here, we evaluate the spatial distribution of I_θ along and around the entire diaphysis. Section modulus Z was calculated using I_θ and local maxima of r_{ext} (Fig. 1C). Since the *in-vivo* neutral axis may deviate significantly from the centroid axis (Demes et al., 2001; Lieberman et al., 2004; Demes, 2007), these variables should be considered as proxies of bending resistance.

Longitudinal features such as diaphyseal bending (which is a measure of longitudinal curvature) (Yamanaka et al., 2005; Groote et al., 2010), or general spatial features such as 3D-surface curvature can, in principle, also be analyzed with morphometric mapping methods. One longitudinal feature that is considered here is diaphyseal torsion. Long bone torsion is typically measured as the difference in orientation of proximal and distal joint axes (e.g., Elftman, 1945; Aiello and Dean, 1990;

Cowgill, 2007). Here diaphyseal torsion is measured by changes in the orientation of the cross-sectional principal axis along the diaphysis (Fig. 1B).

Morphometric mapping

Fig. 1 (D-F) shows the principle of cylindrical projection and morphometric mapping. For each specimen, measurements of r, k, h and I_θ were sampled in each cross section, and along the entire diaphysis. These data were normalized to their respective median values, and mapped onto a cylindrical coordinate system (ρ, θ, z), where ρ=1=const. denotes the radius of the cylinder, angle θ denotes the anatomical direction (θ=0º→360º: lateral → anterior → medial → posterior → lateral; note the periodicity around θ), and z denotes the normalized position along the diaphysis (z=0 → 1: distal → proximal) (Zollikofer and Ponce de León, 2001) (Fig. 1 E, F). The orientation of the diaphysis in anatomical space was determined by calculating its three principal axes of cortical bone distribution: While the first axis represents the anteroposterior direction, the second and third axes were used to define the mediolateral and anteroposterior directions, respectively (as will be described below, further fine-adjustment was performed for quantitative comparative analyses). Since the radius ρ=1=const., data can be visualized as two-dimensional morphometric maps $\mathbf{M}(\theta, z)$, and distributions of $r(\theta, z)$, $k(\theta, z)$, $h(\theta, z)$ and $I(\theta, z)$ can be represented as $K\times L$ matrices where K and L denote the number of elements along θ and z respectively (K=L=300) (Fig. 1B, C, Fig. 2). In formal terms, these procedures carry out a cylindrical surface parameterization (Fig. 1E). In practical terms, MMs are similar to topographic maps: the „longitude“(θ) of these maps corresponds to the anatomical orientation around the diaphysis, the „latitude“ (z) to the position along the diaphysis („north“=proximal; „south“=distal), and the „altitude“ represents local values of morphometric variables (r, k, h, I).

MMs are visualized using false-color mapping schemes, which render relative values of morphometric variables according to a pre-defined color scale (Fig. 1G). The resulting „topographies“ provide a comprehensive overview over the spatial distribution of variables r, k, h, and I around and along the diaphysis. As an additional feature, the orientations of cross-sectional major and minor axes (which indicate directions of maximum/minimum diameter) along the diaphysis are visualized as lines (Fig. 1E, F)

To go beyond visual comparisons of MMs (Fig. 2), methods for quantitative comparative analysis of entire morphometric maps of multiple specimens are required. Here we propose a combination of standard methods of image analysis and multivariate analysis. MMs have the same structure as images ($K\times L$ matrices), whose spatial properties are conveniently quantified by the 2D-Fourier transform (FT, see Appendix C for details). The FT is especially appropriate here for the following reasons: (a) MMs have a natural periodicity in θ (*i.e.*, around the shaft), which is optimally represented by the periodic basis functions used in FT; (b) the FT provides a quantitative method to compare non-landmark structures; (c) the FT can be extended to the third dimension ($K\times L\times J$), where J morphometric maps representing different aspects of long bone morphology and/or biomechanics (variables r, k, h, I) are analyzed together, as described below.

MM-based shape analysis

In analogy to standard GM procedures, MM-based analyses require that specimens be superimposed according to a best-fit criterion prior to shape analysis. While GM superposition involves size normalization, translation and rotation via Generalized Procrustes Analysis (GPA) (Rohlf, 1990), MM superposition is performed by rotation around θ, which represents the only degree of freedom remaining after cylindrical projection. The method described above to evaluate mediolateral and anteroposterior directions of the diaphysis was used as a first step to orient all specimens in a similar direction. In a second step, optimal alignment was achieved by iteratively minimizing inter-specimen distances in Fourier space through appropriate rotation of each specimen around θ. This procedure performs small rotations around θ until differences between specimens are minimized. Together, the superposition procedures yield a set [**M**] of aligned MMs of all specimens (see Appendix C for details).

2D-FTs $F(\mathbf{M})$ are then calculated for each **M**, resulting in $K \times L$ Fourier coefficient sets. To identify principal patterns of shape variability in the sample, Fourier coefficient sets are submitted to Principal Components Analysis (PCA). In analogy to GM, the mean (consensus) map $\langle\mathbf{M}\rangle$ can be used as a reference shape, and specimens can be expressed by their deviation from the consensus map: $\mathbf{M'}=\mathbf{M}-\langle\mathbf{M}\rangle$. Nevertheless, PCA of $F(\mathbf{M}-\langle\mathbf{M}\rangle)$ is mathematically equivalent to PCA of $F(\mathbf{M})$, such that both methods produce identical results. Here we use the latter method to reduce computing time. The Fourier Transform represents MMs as a set of spatial frequencies with associated amplitudes. Accordingly, a basic property of the FT is that the low-frequency domain captures global features (i.e., large-scale variation), while the high frequency domain captures local features (i.e., small-scale variation). Low-pass filtering in Fourier space (i.e., removal of the high-frequency domain) thus allows to capture variation in global features. As will be shown below, the statistically most relevant information about shape variation in the sample is typically contained in the low frequency domain.

To facilitate visual inspection of the results of PCA, MMs are reconstructed by transforming a given point **P*** in PC space into its corresponding set of Fourier coefficients $F(\mathbf{M}^*)$, and applying an inverse Fourier transform to obtain a morphometric map **M***.

The principal goal of PCA is to reduce the high dimensionality ($K \times L$ or $K \times L \times J$ [analysis of J features]) of MM-based shape analyses. Graphing the first few PCs is a convenient means to explore statistically relevant patterns of shape variability in the sample; however, variation along a given PC does not typically represent variation caused by a single biological factor. It is thus more adequate to visualize patterns of shape variation and shape difference as a function of specific factors, such as body size, age, sex, and zoo/wild condition. Overall, it should be reiterated that, unlike GM, the proposed method of MM-based shape analysis does not presume point-to-point homology between specimens; rather, it analyzes variation of morphometric patterns along and around the entire long bone diaphysis.

Comparison of ontogenetic trajectories

When group-specific ontogenetic trajectories through PC space (shape space) are approximately linear, they can be characterized by their position and direction in shape space. Accordingly, they can be compared by measuring between-trajectory distance and divergence. Trajectory position was measured by the group mean position in shape space. Trajectory direction was quantified with two

methods: (a) the principal direction of the group-specific distribution in shape space (first principal axis), and (b) the ontogenetic allometric vector (multivariate regression of shape against diaphyseal length) (Penin et al., 2002; Zollikofer and Ponce de León, 2006). As an additional method to compare group-specific distribution patterns in shape space, the distance between group-specific variance-covariance matrices was calculated following a method proposed by Mitteroecker and Bookstein (2009) (see Appendix D for details). Statistical tests on differences between groups were performed with bootstrapping (1000 resamplings). All calculations were performed in MATLAB 7.7 (MathWorks).

Results

MMs as a tool for visualizing patterns of diaphyseal shape variation

Fig. 2 provides an MM-based visual comparison of femoral diaphyseal morphology in two adult captive chimpanzees, who represent extremes of the shape variation contained in the sample (these specimens are represented by vertical and horizontal rectangles in graphs of Figs. 3, 4, 8, 9). The MM of the external radius (Fig. 2B) visualizes diaphyseal surface morphology in terms of how cross-sectional shape deviates from a circle, thus permitting identification of regions of platymery. The MM of surface curvature (Fig. 2C) permits identification of ridges (crests) and grooves (fossae), and of their relative location and orientation along the diaphysis. Surface curvature reveals anatomically well-defined but often highly variable features, such as the linea aspera (*la*), the lateral spiral pilaster (*lsp*) (Lovejoy et al., 2002), the lateral supracondylar line (*lsl*), medial ridge (*mr*), and the pectineal line (*pl*). The MM of cortical bone thickness (Fig. 2D) gives a comprehensive view of cortical bone distribution along and around the diaphysis. The MMs of second moments of area (Fig. 2E) and section modulus (Fig. 2F) visualize the distribution of diaphyseal rigidity against bending, revealing changes in the direction and magnitude of bending rigidity along and around the diaphysis.

The MMs of Fig. 2 reveal considerable inter-individual variation in diaphyseal morphology and biomechanical properties. Basic anatomical features can be identified in MMs of both individuals, but these features differ in location, orientation and prominence. Overall, the diaphysis of individual 1 is rounder than that of individual 2 (Fig. 2B). At the same time, it exhibits a more prominent linea aspera (Fig. 2C). Diaphyseal torsion (lines in Fig. 2D) is more expressed, and cortical bone thickness is increased in the posterior diaphysis (Fig. 2D-1). Comparison of Figs. 2D and E shows that areas of increased cortical bone thickness coincide with the orientation of the principal cross-sectional axes (Fig. 2D) and with some, but not all, features on the external surface (Fig. 2B). MMs of biomechanical properties (Figs. 2E, F) indicate differences between individuals in absolute and relative values of bending rigidity. Individual 1 shows higher second moments of area in anteroposterior direction than in mediolateral direction (Fig. 2E-1), while the situation is reverse in individual 2 (Fig. 2E-2). MMs of section modulus (Fig. 2F) are largely similar to those of second moments of area (Fig. 2E). Overall, compared with direct inspection of femoral diaphyseal anatomy (Fig. 2A), MMs provide a comprehensive visualization of the spatial distribution of morphological and biomechanical features, which facilitates explorative studies of diaphyseal shape variation.

MM-based shape analysis

MM-based shape analyses of the entire sample (pooled wild and captive specimens) were performed for external diaphyseal radius (Fig. 3A), external surface curvature (Fig. 3B), and cortical bone thickness (Fig. 3C), respectively, as well as for these variables together (Fig. 3D). Results are presented as PC plots (Figs. 3, 6) and MM visualizations (Figs. 4-7). Statistical tests for differences between captive and wild animals were performed for the following measurements:

(a) group-specific means (H0: zero distance between group centroids in PC space)

(b) group-specific principal directions in PC space (H0: directions are identical)

(c) group-specific ontogenetic allometric trajectories (H0: trajectories are parallel)

(d) group-specific modes of variation (H0: zero distance between variance-covariance matrices).

None of these tests yielded significant results that would permit rejection of the respective null hypotheses (Table 1). Also, both groups show similar common ontogenetic allometric shapes at a given femoral diaphyseal length and cross-sectional area (Fig. 3D-3; slope: p=0.66 and 0.73, intercept: p=0.25 and 0.17, respectively).

Wild and captive chimpanzees thus exhibit statistically indistinguishable femoral diaphyseal shapes and patterns of diaphyseal ontogeny. Variation along and across the ontogenetic trajectory was calculated as the variance of the data scatter along the ontogenetic trajectory vector, and as the maximum variance perpendicular to it, respectively. Diaphyseal shape variation across the trajectory is similar in magnitude to the variation along the ontogenetic trajectory (Table 1), and already present at early developmental stages.

Since ontogenetic trajectories do not differ statistically between the two groups, common ontogenetic patterns are visualized as MMs (Fig. 4). Fig. 4A shows that proximal and distal ends of the diaphysis are mediolaterally more extended (relative to the mid-shaft) in immature individuals. Fig. 4B (surface curvature) shows development of the pectineal line, lateral spiral pilaster, linea aspera and medial ridge. The linea aspera is more laterally located in early ontogenetic stages and shifts to a more posterior location during ontogeny. Fig. 4C (cortical bone thickness) shows that cortical bone is more evenly distributed in young individuals, and becomes proximally concentrated in adult individuals.

Fig. 5 visualizes femoral diaphyseal shape variation independent of the ontogenetic stage (*i.e.*, across the ontogenetic trajectory) with two MMs corresponding to the positions of the two diamonds in Fig. 3D-1. While overall diaphyseal topography is similar in both instances, differences can be observed in prominence and orientation of the linea aspera, in the degree of platymery (mediolateral relative to anteroposterior expansion) of the diaphysis (Fig. 5A), in prominence and position of the lateral spiral pilaster and pectineal line (Fig. 5B), and in the proximodistal distribution of cortical bone (Fig. 5C).

Fig. 6 visualizes patterns of variation in biomechanical properties (second moments of cross-sectional cortical area). No statistical differences could be found between wild and captive chimpanzees (Fig. 6A, Table 1), such that patterns of variation are visualized along and across a common ontogenetic trajectory. In infant chimpanzees, diaphyseal bending rigidity exhibits strong

mediolateral to anteroposterior polarity especially toward the distal end of the shaft. During ontogeny, this pattern becomes more homogeneous along the shaft. Intraspecific variation independent of ontogeny (i.e., across the ontogenetic trajectory; Fig. 6C) is largely similar to the pattern visualized for the two examples in Fig. 2F, exhibiting a continuum between diaphyses exhibiting mediolaterally versus anteroposteriorly increased bending rigidity.

Femoral length, median external radius and median cortical bone thickness are plotted against each other in Fig. 7. None of these graphs shows statistical differences between wild and captive groups (length-radius, slope: p=0.08, intercept: p=0.16; length-thickness, slope: p=0.46, intercept: p=0.79; radius-thickness, slope: p=0.12, intercept: p=0.45). Independent of ontogenetic stage, some captive individuals exhibit slightly thicker cortical bone (Fig. 7B). However, captive and wild subsamples do not differ significantly in adult mean values (p=0.41, t-test). External radius and thickness shows negative and positive allometry against femoral diaphyseal length (exponents: 0.94 and 1.37, respectively), and thickness shows positive allometry against external radius (exponent: 1.38).

MM-based analysis of diaphyseal subregions

MM analyses were also performed for the proximal, middle and distal thirds of the diaphysis separately (Fig. 8A, B, C-1). Analyzing surface curvature and cortical bone distribution in each of these subregions separately permits comparisons with earlier studies, which typically focus on the midshaft, and can be expected to reveal localized differences between captive and wild subsamples. Results are represented as PC plots (Fig. 8) and MMs (Fig. 9), and statistics are summarized in Table 1.

Significant differences between wild and captive chimpanzees could be identified in only one region: Cortical bone distribution in the distal diaphysis exhibits distinct patterns (Fig. 8C-2, Table 1), while the surface topography is indistinguishable between the two groups (Fig. 8C-3). Also, the captive group shows significantly greater variance in cortical bone distribution (Fig. 8C) (p<0.01, F-test). Corresponding MMs and cross-sectional representations of cortical bone distribution are visualized in Fig. 9A and B. While wild individuals show increased cortical bone thickness on medial and lateral sides of the distal femoral diaphysis, captive individuals show thicker anterior and posterior sides.

Comparison of MM methods with geometric morphometric and cross-sectional methods

To compare the new MM methods proposed here with earlier methods, long bone diaphyseal morphology was also analyzed using geometric morphometric (GM) methods, and traditional cross-sectional analysis. A semilandmark-based GM approach was used to represent internal and external diaphyseal surfaces (internal surface: 60×25 3D coordinates; external surface: 60×50 3D coordinates). To control for the predominant effects of variation in diaphyseal length, specimens were normalized to unit diaphyseal length and unit median radius respectively, then submitted to standard semilandmark-based PCA of shape (Gunz et al., 2005). GM analyses were performed for the entire diaphysis (Fig. 10) and for the three subregions (Fig. S2). Similar statistical analyses were performed to permit comparison with MM methods (Table 1). PC scores of MM and GM analyses were compared using least-squares fitting, and the results showed that PCs of GM and MM analyses are

largely similar (Table 2). MM and GM methods thus capture similar patterns of diaphyseal shape variation, and GM-based visualization (Fig. 10B) shows patterns of ontogenetic shape change, which largely correspond to the MMs in Fig. 4. However, characteristic features observed in MMs (Fig. 4, 5, 6, 8) such as changes in cortical bone distribution and in prominence of surface features cannot be visualized with GM methods, despite the large number of semilandmarks (Fig. 10).

For comparison, standard cross-sectional analyses were performed for the proximal, middle and distal shaft (Fig. S3). None of these analyses reveals statistically significant differences between femoral diaphyseal biomechanical properties of wild and captive chimpanzees.

Discussion

Summary of results and comparison with earlier studies

The main results of this study can be summarized as follows:

a) The MM methods proposed here provide an efficient tool kit to analyze cross-sectional geometric and biomechanical properties of entire long bone diaphyses, to visualize the results comprehensively, and to identify group-specific features and modes of variation.
b) Average modes of femoral diaphyseal ontogeny and shape variation are largely similar in wild and zoo chimpanzees. During ontogeny, the relative diameter of the proximal and distal ends of the diaphysis decreases, and the linea aspera, lateral spiral pilaster and medial ridge become more prominent. Cortical bone is more evenly distributed along the shaft in early stages of ontogeny and becomes more concentrated proximally in adults. A large proportion of variation in femoral diaphyseal shape is not related to ontogenetic change.
c) MM reveals subtle differences between wild and zoo chimpanzees in femoral diaphyseal ontogeny and patterns of shape variation. Overall, femoral shape variation in the zoo sample is larger than in the wild sample, especially with regard to variability in patterns of cortical bone distribution. Differences between groups have been identified in the distal third of the shaft. In captive animals, cortical bone deposition on the anterior and posterior endosteal surfaces is more intense. Midshaft morphology, which is the subject of many studies, does not exhibit significant differences between groups.
d) Traditional GM-based analyses yield largely similar analytical results, but visualization and interpretation of patterns of shape change and shape variation is less effective than with MM methods. Cross-section-based analysis cannot detect the differences found with MM methods between wild and zoo animals.

The result that average femoral morphology does not differ between wild and captive chimpanzees (*P. t. troglodytes*) is consistent with earlier studies: Wild and captive *Lemur catta* do not differ significantly in diaphyseal biomechanical properties (Demes and Jungers, 1993), nor do wild and captive *Macaca nemestrina* in relative magnitudes of second moments of area (Burr et al., 1989). The present study further showed that wild and captive groups did not differ in femoral morphology along the course of ontogeny. Convergent results from three different primate species with different locomotor modes indicate that captivity does not have a major impact on *average* diaphyseal morphology. The results of our study are also in congruence with earlier studies of chimpanzee long bone cross-sectional properties (Carlson, 2005; Carlson et al., 2006; Carlson et al., 2008a), which showed that differences between individuals in locomotor behavior are not paralleled by significant differences in cross-sectional biomechanical properties of the femoral diaphysis.

The MM-based comparative analyses performed in this study revealed subtle differences between wild and captive chimpanzees in the internal morphology of the distal femoral diaphysis. Such differences have not been found in earlier studies analyzing cross-sectional properties at pre-defined locations along the diaphysis. This demonstrates that MM methods, which use comprehensive diaphyseal cross-sectional data, are highly sensitive tools to detect inter-group differences in diaphyseal morphology and biomechanical properties. The results described here are best compared with those of a study reporting differences between two chimpanzee communities (8 Mahale vs. 4 Taï female chimpanzees) in biomechanical properties (I_{max}/I_{min}) of the mid-distal femoral diaphysis (Carlson et al., 2008a). Such differences between wild-living groups may indeed reflect population-specific differences in locomotor behavior. However, Mahale and Taï populations represent evolutionary divergence at the subspecies level (*P. t. troglodytes*, and *P. t. verus*), such that it remains to be clarified whether the reported differences reflect taxon-specific diaphyseal morphologies unrelated to *in-vivo* locomotor loading history.

Overall, the findings of this study, and of the studies of Carlson and colleagues (Carlson, 2005; Carlson et al., 2006; Carlson et al., 2008a) imply that differences in locomotor behavior have comparatively little impact on femoral diaphyseal morphology and development. One possible explanation for this lack of correlation is that long bone diaphyseal shape is mainly controlled by genes and the developmental program. Another possible explanation is that even notable differences in locomotor behaviors may result in only minor differences in actual diaphyseal loading patterns. This second possibility would imply that the musculoskeletal system tends to maintain biomechanical homeostasis: different locomotor modes elicit different force patterns, but these differences are buffered through differential muscular activity, resulting in largely similar loading patterns on long bone diaphyses.

In any case, our findings have several implications for the interpretation of the femoral diaphyseal morphology of fossil hominins. Reconstruction of the locomotor behavior of fossil hominins has often been based on Wolff's Law, *i.e.*, the assumption that diaphyseal cross-sectional properties reflect the mechanical loading history and the locomotor behavior of the specimen under study. For example, long bone diaphyses of early *Homo* typically exhibit higher degrees of robusticity (i.e., larger cortical cross-sectional area and different shapes) than those of modern humans, and this condition is thought to be associated with higher levels of mechanical loading during lifetime (Ruff et al., 1993; Ruff et al., 1994). Actualistic support for this hypothesis comes from various studies analyzing changes in long bone cross-sectional geometry during human ontogeny. It has been reported that increased rigidity of long bones reflects increased mechanical loading during lifetime (Ruff et al., 1994; Sumner and Andriacchi, 1996), specifically at the onset of bipedal locomotion (Ruff, 2003b, 2003a). Likewise, increased diaphyseal cross-sectional robusticity of the humerus relative to femur of early hominins is thought to be indicative of higher proportions of arboreal locomotion in early *Homo* compared to *H. erectus* and modern humans (Ruff, 2009).

Our data, however, indicate that differences between locomotor behaviors do not necessarily result in distinct morphologies or different degrees of robusticity of the femoral diaphysis. Caution is thus warranted when interpreting fossil diaphyseal cross-sectional data in terms of individual locomotor behavior, and the following range of possible alternative explanations must be considered:

- differences between diaphyseal morphologies in fact reflect *in-vivo* functional adaptation to different locomotor behaviors

- differences between diaphyseal morphologies reflect evolutionary adaptation to taxon-specific locomotor behaviors, i.e. taxon-specific developmental programs (Wallace et al., 2010b)

- differences between diaphyseal morphologies reflect differences in taxon-specific developmental programs not related to actual locomotor adaptations (Wallace et al., 2010b)

This leads to the question as to which mechanisms – if not *in-vivo* functional adaptation *sensu* Ruff et al. (2006) – govern ontogenetic changes of the chimpanzee femoral diaphysis (Fig. 4). As stated in the above list, one hypothesis is that the underlying developmental program reflects evolutionary adaptation, such that changes in femoral diaphyseal morphology are in concert with changes in locomotor modes during a typical chimpanzee's ontogeny: During early stages of ontogeny, chimpanzees exhibit hand-assisted or short bouts of free bipedalism, as well as climbing and suspensory behavior more frequently than during later stages, while knuckle-walking frequency increases toward adulthood (Doran, 1992, 1997). These changes are paralleled by ontogenetic changes of diaphyseal features: Cortical bone thickness and second moments of area exhibit a more homogeneous distribution around and along the femoral diaphysis in infants than in juveniles and adults (Fig. 4B, 6B). A homogeneous distribution might represent an optimum biomechanical design for the wide variability of loading patterns occurring in mixed terrestrial/arboreal activities of young chimpanzees (Demes and Carlson, 2009). Cortical bone becomes concentrated proximally, and the distal diaphysis becomes relatively smaller in diameter during later development toward adulthood. Concentration of mass toward the proximal femur might contribute to reduce the energy needed to swing the hind-limb during locomotion. A higher degree of platymery (Fig. 4A, Fig. 6B) and a more slender shape (Fig. 7B) of the femoral diaphysis might be favorable during terrestrial locomotion, because increased platymery could be consistent with a more stable loading pattern in terrestrial locomotion (Demes and Carlson, 2009), and longer limbs permit energetically more efficient locomotion (Pontzer et al., 2009).

While this set of hypotheses postulates direct links between developmental programs and stage-specific locomotor repertoires, it remains to be tested whether the developmental pattern of the femoral diaphysis of chimpanzees (Fig. 4) in fact closely reflects chimpanzee-specific locomotor behavior. An alternative hypothesis is that it reflects general developmental processes and associated biomechanical constraints experienced by any developing hominoid primate, such as increase in body size, neurological maturation, and changes in social behavior (Doran, 1992, 1997). Also, evolutionary developmental inertia needs to be considered, implying that the diaphyseal development in extant chimpanzees reflects adaptation to an ancestral form of locomotion. Clearly, additional empirical evidence from a wider range of hominoid species, and from other long bones (especially the humerus) is required to resolve these issues, and to investigate how long bone development is related to the development of locomotor behavior.

Chimpanzee femoral ontogeny and Wolff's Law

WL predicts that wild and captive groups of chimpanzees show different ontogenetic patterns in femoral diaphyseal morphology reflecting their different locomotor modes. However, *average* developmental patterns of femoral diaphysis of wild and captive chimpanzees are indistinguishable with regard to both morphology and biomechanical properties (Figs. 3, 6, 7, 10). Moreover, the range of variation across ontogenetic trajectories does not increase during ontogeny but is already high at early stages. A constant amount of variation throughout ontogeny could indicate that morphological

variation is not primarily due to *in-vivo* differences in mechanical loading but has a strong genetic component. Alternatively, one could argue that variation in fact reflects *in-vivo* differences between individuals, but that the factors causing these differences are largely unknown.

While wild and zoo animals are similar in *average* femoral diaphyseal morphology and ontogeny, it appears that femoral diaphyseal shape *variation* is constrained to a narrower range in wild compared to captive chimpanzees (Fig. 8C-2). Apparently, the large inter-individual variation in zoo animals is canceled out, and the average ontogenetic trajectory tends to reflect „WL-free“ developmental programs. Overall, the fact that wild and captive chimps exhibit the same *average* trajectory of diaphyseal ontogeny is relevant, because it indicates that there is no systematic "bias" due to WL. We may thus infer that the basic developmental program of the diaphysis is not affected by differences in locomotor modes, but that *in-vivo* modification (WL) acts as a powerful modulator of femoral morphological *variation*: natural locomotor modes and loading patterns clearly constrain variation, while locomotion in a zoo environment permits a wide range of morphological variation.

This finding seems paradoxical at first sight, because a natural environment permits a more diverse locomotor repertoire than a zoo environment. However, locomotion under natural conditions is biomechanically and metabolically more demanding, such that actual loading patterns are expected to exert a stronger influence on diaphyseal shape than under the less constrained conditions of a zoo environment. These findings may explain why comparative studies of wild individuals did not reveal significant correlations between locomotor habits and diaphyseal morphology (Carlson et al., 2006): even if differences between individual locomotor behaviors are significant, overall constraints (probably due to high levels of physical activity) are predominant in shaping diaphyseal morphology. This finding is relevant for practical work too, as it demonstrates that MM methods permit to retrieve basic ontogenetic patterns despite large interindividual variation. Also, our data indicate that wild and captive samples can be pooled in studies focusing on average modes of morphological change. This might be especially valuable in developmental studies, where sample sizes of wild immature specimens are typically small. Applying MM methods to compare diaphyseal developmental modes in various hominoid taxa can thus be expected to yield new insights into the evolution of long bone development and of locomotor behaviors (Shea, 1981; Ruff, 2003b, 2003a)

Collectively, the hypothesis that WL predominantly governs long bone morphology (i.e., that long bone morphology reflects *in-vivo* mechanical loading of locomotion) can be rejected. As shown in the analyses of diaphyseal subregions (Figs. 8, 9), bone functional modification tends to occur locally, on specific features in a specific region of the diaphysis, and probably of a specific individual, rather than on the average morphology and developmental pattern. We conclude that femoral diaphyseal morphology is largely determined by genetically defined developmental modes, while *in-vivo* modification only partly reflects *in-vivo* mechanical loading conditions.

Diaphyseal ontogeny proceeds via external (subperiosteal) bone deposition and internal (endosteal) bone resorption (modeling), while *in-vivo* modification (remodeling) is achieved via internal deposition/resorption in adults (Carter, 1990; Standring, 2004). Accordingly, ontogenetic changes in the external surface (MMs of external radius and curvature) indicate differential external (re-)modeling processes, while ontogenetic changes in cortical bone distribution (MMs of bone thickness) indicate differential internal (re-)modeling. Our data provide evidence for both processes (Fig. 4): endosteal remodeling yields a thickness gradient in proximodistal direction, while subperiosteal surface remodeling yields more prominent ridge structures. The first process might reflect changes in diaphyseal loading patters with increasing body mass (Moro et al., 1996; van der Meulen et al., 1996), while the second process might reflect changes in muscle strength (Benjamin et al., 2002 and references therein; Weiss, 2004; Drapeau, 2008).

While MMs represent relative values of morphometric variables, absolute values of external radius, cortical bone thickness and femoral diaphyseal length are informative regarding actual rates of external versus internal bone deposition/resorption: If thickness remains constant, this indicates equal rates of external deposition and internal resorption. If thickness grows faster than external radius, this indicates higher deposition than resorption rates, and if external radius grows faster than thickness, this indicates higher internal resorption rate than external deposition rate. Our results (Fig. 7) show that, relative to its length, the chimpanzee femoral diaphysis becomes thin in diameter and strong in cortical bone thickness during ontogeny. Rates of endosteal bone resorption are thus smaller than rates of subperiosteal bone apposition, and the latter are smaller than rates of diaphyseal proximodistal extension.

Some, but not all, captive chimpanzees exhibit thicker cortical bone than wild chimpanzees (Fig. 7). Because external morphology showed smaller variation than cortical bone thickness, and external morphology was indistinguishable between wild and captive groups, this likely reflects differences in endosteal bone deposition (Ruff et al., 1994; Pearson and Lieberman, 2004). This is also supported by the analyses of diaphyseal subregions in which wild and captive groups exhibited indistinguishable external morphology but different distribution patterns of cortical bone. Different bone deposition patterns could reflect different loading conditions, but also result from dietary differences relative to activity levels (Bass et al., 2005). In any case, increasing cortical bone thickness alone (without increasing the external diaphyseal radius) does not substantially increase biomechanical rigidity (Sparacello and Pearson, 2010), because biomechanical rigidity is primarily defined by the external radius (note that second moments of area is proportional to fourth power of radius).

Locomotor modes and femoral diaphyseal morphology

MM analyses of subregions of femoral diaphysis showed that it is not the mid-shaft but the distal diaphysis that exhibits significant differences between zoo and wild chimpanzees. The second hypothesis that the femoral mid-shaft optimally reflects differences in locomotor modes is not supported by this study. The “captive” pattern is characterized by anteroposteriorly increased cortical bone thickness whereas the “wild” pattern is characterized by mediolaterally increased cortical bone thickness (Fig. 9). Because the external morphology of the distal diaphysis is similar in the two groups (Fig. 8A-3,B-3,C-3), differences in cortical bone distribution most likely are due to differences in endosteal bone deposition/resorption. These might reflect different mechanical loading conditions. Currently we cannot associate these patterns with specific inter-individual differences in locomotor modes. However, our data indicate that differences in activity patterns/locomotor modes could be best revealed in the distal femur, while the mid-shaft might be sub-optimal for such comparisons.

Comparison of MM methods with landmark-based GM methods

A comparison of semilandmark-based and MM-based PCAs shows that these methods yield largely convergent results (Figs. 3, 10; Table 2). Both methods are thus equally efficient in detecting patterns of variation of long bone diaphyseal morphology. However, MM methods are advantageous in various respects. MM methods are especially suitable for the analysis of the „featureless“ morphologies of long bone diaphyses, since these methods do not require a-priori definition of landmarks and/or semilandmarks (e.g. on ridge lines). MM methods clearly facilitate visual inspection and exploration of morphometric data. MM-guided feature detection may ultimately lead to a-posteriori definition of features such as „ridge lines“ along the diaphyseal surface, which can

be used as biologically and/or geometrically homologous structures in subsequent landmark-based analyses. An additional benefit of MM methods is that they permit to investigate external and internal morphologies, as well as biomechanical properties. Accordingly, while GM is restricted to the analysis of 3D point coordinates on surfaces, MM also permits analysis of higher-order geometric and biomechanical properties of the 3D data volume representing the diaphysis. MM methods provide a means to effectively visualize such higher-order anatomical/biomechanical features (Figs. 2, 4, 5, 6) which are hardly recognizable in GM-based visualizations (Fig. 11). However, MMs also have several limitations. Since MM methods do not assume point-to-point or line-to-line homologies, feature similarity (e.g. ridges at corresponding locations in MMs) does not imply functional or developmental homology between individuals or groups. While MM analysis is a powerful tool to reveal previously „unseen" morphological features and modes of diaphyseal shape variation, direct inspection of the original morphologies is indispensable to check the results of MM analyses and to obtain developmentally and functionally significant insights into diaphyseal shape variation.

Conclusions

In this study, we used new methods of Morphometric Mapping (MM) for a comprehensive analysis of the spatial distribution of geometric and biomechanical features around and along the femoral diaphysis. We demonstrated that MM methods provide new insights into diaphyseal form variability that cannot be gained with traditional cross-sectional analyses, nor with geometric-morphometric analyses. We used these methods to compare femoral diaphyseal ontogeny in captive and wild common chimpanzees (*Pan troglodytes troglodytes*), and to test Wolff's Law, which predicts that differences in locomotor behavior between these groups result in different diaphyseal ontogenies and morphologies. Our data indicate that the hypothesis underlying WL must be rejected: *in-vivo* functional bone modification only accounts for a minor part of the observed morphological variability, and it appears that femoral diaphyseal shape is mainly mediated by taxon-specific developmental programs. While these results put a caveat on inferring locomotor behavior from fossil hominin long bone morphology, the visual and analytical methods proposed here should encourage further exploration and morphometric mapping of the *terra incognita* of long bone diaphyses in terms of evolution, development and function.

References

Aiello L, Dean C. 1990. An Introduction to Human Evolutionary Anatomy. London: Academic Press.

Alexander RM. 2004. Bipedal animals, and their differences from humans. J Anat 204:321-330.

Amtmann E, Schmitt H. 1968. Über die Verteilung der Corticalisdichte im menschlichen Femurschaft und ihre Bedeutung für die Bestimmung der Knochenfestigkeit. Zeit Anat Entwick 127:25–41.

Bass S, Saxon L, Daly R, Turner C, Robling A, Seeman E, Stuckey S. 2002. Effect of mechanical loading on the size and shape of bone in pre-, peri-, and postpubertal girls: a study in tennis players. J Bone Miner Res 17:2274-2280.

Bass SL, Eser P, Daly R. 2005. The effect of exercise and nutrition on the mechanostat. J Musculoskelet Neuronal Interact 5:239-254.

Beddard F. 1893. Contributions to the anatomy of the anthropoid apes. Trans Zool Soc London 13:177-218.

Benazet JD, Zeller R. 2009. Vertebrate limb development: moving from classical morphogen gradients to an integrated 4-dimensional patterning system. Cold Spring Harbor Perspectives in Biology 1.

Benjamin M, Kumai T, Milz S, Boszczyk BM, Boszczyk AA, Ralphs JR. 2002. The skeletal attachment of tendons - tendon 'entheses'. Comparative Biochemistry and Physiology a-Molecular and Integrative Physiology 133:931-945.

Bennett MR, Harris JWK, Richmond BG, Braun DR, Mbua E, Kiura P, Olago D, Kibunjia M, Omuombo C, Behrensmeyer AK, Huddart D, Gonzalez S. 2009. Early hominin foot morphology based on 1.5-million-year-old footprints from Ileret, Kenya. Science 323:1197-1201.

Bertram JEA, Swartz SM. 1991. The law of bone transformation - a case of crying Wolff. Biol Rev Camb Philos Soc 66:245-273.

Boehm B, Westerberg H, Lesnicar-Pucko G, Raja S, Rautschka M, Cotterell J, Swoger J, Sharpe J. 2010. The role of spatially controlled cell proliferation in limb bud morphogenesis. PLoS Biol 8:e1000420.

Bondioli L, Bayle P, Dean C, Mazurier A, Puymerail L, Ruff C, Stock J, T. , Volpato V, Zanolli C, Macchiarelli R. 2010. Technical note: Morphometric maps of long bone shafts and dental roots for imaging topographic thickness variation. Am J Phys Anthropol 142:328-334.

Bookstein F. 1991. Morphometric Tools for Landmark Data: Geometry and Biology. Cambridge: Camnridge University Press.

Boyer E. 1935. The musculature of the inferior extremity of the orang-utan *Simia satyrus*. Am J Anat 56:192-256.

Bramble DM, Lieberman DE. 2004. Endurance running and the evolution of *Homo*. Nature 432:345-352.

Brunet M, Guy F, Pilbeam D, Mackaye HT, Likius A, Ahounta D, Beauvilain A, Blondel C, Bocherens H, Boisserie JR, De Bonis L, Coppens Y, Dejax J, Denys C, Duringer P, Eisenmann VR, Fanone G, Fronty P, Geraads D, Lehmann T, Lihoreau F, Louchart A, Mahamat A, Merceron G, Mouchelin G, Otero O, Campomanes PP, De Leon MP, Rage JC, Sapanet M, Schuster M, Sudre J, Tassy P, Valentin X, Vignaud P, Viriot L, Zazzo A, Zollikofer C. 2002. A new hominid from the Upper Miocene of Chad, central Africa. Nature 418:145-151.

Burr DB, Ruff CB, Johnson C. 1989. Structural adaptations of the femur and humerus to arboreal and terrestrial environments in 3 species of macaque. Am J Phys Anthropol 79:357-367.

Butterfield NC, McGlinn E, Wicking C. 2010. The molecular regulation of vertebrate limb patterning. In: Organogenesis in Development: Elsevier. p 319-341.

Cardoso FA, Henderson CY. 2010. Enthesopathy Formation in the Humerus: Data from Known Age-at-Death and Known Occupation Skeletal Collections. Am J Phys Anthropol 141:550-560.

Carlson K, Sumner D, Morbeck M, Nishida T, Yamanaka A, Boesch C. 2008a. Role of nonbehavioral factors in adjusting long bone siaphyseal atructure in free-ranging *Pan troglodytes*. Int J Primatol 29:1401-1420.

Carlson KJ. 2005. Investigating the form-function interface in African apes: Relationships between principal moments of area and positional behaviors in femoral and humeral diaphyses. Am J Phys Anthropol 127:312-334.

Carlson KJ, Doran-Sheehy DM, Hunt KD, Nishida T, Yamanaka A, Boesch C. 2006. Locomotor behavior and long bone morphology in individual free-ranging chimpanzees. J Hum Evol 50:394-404.

Carlson KJ, Judex S. 2007. Increased non-linear locomotion alters diaphyseal bone shape. J Exp Biol 210:3117-3125.

Carlson KJ, Lublinsky S, Judex S. 2008b. Do different locomotor modes during growth modulate trabecular architecture in the murine hind limb? Integr Comp Biol 48:385-393.

Carrier DR. 1996. Ontogenetic limits on locomotor performance. Physiol Zool 69:467-488.

Carrier DR, Anders C, Schilling N. 2011. The musculoskeletal system of humans is not tuned to maximize the economy of locomotion. Proc Natl Acad Sci U S A 108:18631-18636.

Carter GJ, editor. 1990. Skeletal biomineralization: patterns, processes, and evolutionary trends. New York: Van Nostrand Reinhold.

Cavagna GA, Heglund NC, Taylor CR. 1977. Mechanical work in terrestrial locomotion: two basic mechanisms for minimizing energy expenditure. Am J Physiol 233:R243-261.

Cobb SN, O'Higgins P. 2007. The ontogeny of sexual dimorphism in the facial skeleton of the African apes. J Hum Evol 53:176-190.
Cowgill LW. 2007. Humeral torsion revisited: A functional and ontogenetic model for populational variation. Am J Phys Anthropol 134:472-480.
Crass E. 1952. Musculature of the hip and thigh of the chimpanzee : a comparison to man and other primates. PhD thesis, Univ Wisconsin.
Demes B. 2007. In vivo bone strain and bone functional adaptation. Am J Phys Anthropol 133:717-722.
Demes B, Carlson KJ. 2009. Locomotor variation and bending regimes of capuchin limb bones. Am J Phys Anthropol 139:558-571.
Demes B, Jungers WL. 1993. Long-bone cross-sectional dimensions, locomotor adaptations and body-size in prosimian primates. J Hum Evol 25:57-74.
Demes B, Larson SG, Stern JT, Jr, , Jungers WL, Biknevicius AR, Schmitt D. 1994. The kinetics of primate quadrupedalism: hindlimb drive reconsidered. J Hum Evol 26:353-374.
Demes B, Qin YX, Stern JT, Jr., Larson SG, Rubin CT. 2001. Patterns of strain in the macaque tibia during functional activity. Am J Phys Anthropol 116:257-265.
Dillon R, Othmer HG. 1999. A mathematical model for outgrowth and spatial patterning of the vertebrate limb bud. J Theor Biol 197:295-330.
Diogo R, Wood B. 2011. Soft-tissue anatomy of the primates: phylogenetic analyses based on the muscles of the head, neck, pectoral region and upper limb, with notes on the evolution of these muscles. J Anat 219:273-359.
Doran DM. 1992. The ontogeny of chimpanzee and pygmy chimpanzee locomotor behavior - a case-study of paedomorphism and its behavioral-correlates. J Hum Evol 23:139-157.
Doran DM. 1993. Comparative locomotor behavior of chimpanzees and bonobos - the influence of morphology on locomotion. Am J Phys Anthropol 91:83-98.
Doran DM. 1997. Ontogeny of locomotion in mountain gorillas and chimpanzees. J Hum Evol 32:323-344.
Drapeau MSM. 2008. Enthesis bilateral asymmetry in humans and African apes. Homo-Journal of Comparative Human Biology 59:93-109.
Elftman H. 1945. Torsion of the lower extremity. Am J Phys Anthropol-New Ser 3:255-265.
Galik K, Senut B, Pickford M, Gommery D, Treil J, Kuperavage AJ, Eckhardt RB. 2004. External and internal morphology of the BAR 1002 ' 00 *Orrorin tugenensis* femur. Science 305:1450-1453.
Garland TJ, Rose MR. 2009. Experimental evolution: concepts, methods, and applications of selection experiments. Berkeley: University of California Press.
Gibbs S, Collard M, Wood B. 2000. Soft-tissue characters in higher primate phylogenetics. Proc Natl Acad Sci USA 97:11130-11132.
Gibbs S, Collard M, Wood B. 2002. Soft-tissue anatomy of the extant hominoids: a review and phylogenetic analysis. J Anat 200:3-49.
Gilbert CC, Rossie JB. 2007. Congruence of molecules and morphology using a narrow allometric approach. Proc Natl Acad Sci USA 104:11910-11914.
Goodall J. 1986. The Chimpanzees of Gombe. Cambridge: Harvard University Press.
Goodship AE, Lanyon LE, McFie H. 1979. Functional adaptation of bone to increased stress - experimental-study. Journal of Bone and Joint Surgery-American Volume 61:539-546.
Gould SJ, Lewontin RC. 1979. The spandrels of San Marco and the Panglossian paradigm: a critique of the adaptationist programme. Proc R Soc Lond, Ser B: Biol Sci 205:581-598.
Griffin TM, Main RP, Farley CT. 2004. Biomechanics of quadrupedal walking: how do four-legged animals achieve inverted pendulum-like movements? J Exp Biol 207:3545-3558.
Groote ID, Lockwood AC, Aiello CL. 2010. Technical note: A new method for measuring long bone curvature using 3D landmarks and semi-landmarks. Am J Phys Anthropol 141:658-664.
Gunz P, Mitteroecker P, Bookstein FL. 2005. Semilandmarks in Three Dimensions. In: Slice DE, editor. Developments in Primatology: Progress and Prospects. New York: Springer.
Harmon EH. 2007. The shape of the hominoid proximal femur: a geometric morphometric analysis. J Anat 210:170-185.

Harmon EH. 2009. The shape of the early hominin proximal femur. Am J Phys Anthropol 139:154-171.

Harrison T. 2010. Apes among the tangled branches of human origins. Science 327:532-534.

Heinrich RE, Ruff CB, Adamczewski JZ. 1999. Ontogenetic changes in mineralization and bone geometry in the femur of muskoxen (Ovibos moschatus). J Zool 247:215-223.

Holliday TW, Hutchinson VT, Morrow MMB, Livesay GA. 2010. Geometric morphometric analyses of hominid proximal femora: Taxonomic and phylogenetic considerations. Homo-Journal of Comparative Human Biology 61:3-15.

Holt BM. 2003. Mobility in Upper Paleolithic and Mesolithic Europe: Evidence from the lower limb. Am J Phys Anthropol 122:200-215.

Jensvold MLA, Sanz CM, Fouts RS, Fouts DH. 2001. Effect of enclosure size and complexity on the behaviors of captive chimpanzees (*Pan troglodytes*). J Appl Anim Welf Sci 4:53- 69.

Jones HH, Priest JD, Hayes WC, Tichenor CC, Nagel DA. 1977. Humeral hypertrophy in response to exercise. J Bone Joint Surg Am 59:204-208.

Jungers WL, Minns RJ. 1979. Computed tomography and biomechanical analysis of fossil long bones. Am J Phys Anthropol 50:285-290.

Kimura M. 1968. Evolutionary rate at the molecular level. Nature 217:624-626.

Kimura T. 1991. Long and robust limb bones of primates. In: Ehara A, Kimura T, Takenaka O, Iwamoto M, editors. Primatology Today. New York: Elsevier. p 495-498.

Kimura T. 1995. Long bone characteristics of primates. Z Morphol Anthropol 80:265-280.

Kimura T, Okada M, Ishida H. 1979. Kinesiological characteristics of primate walking: its significance in human walking. In: Morbeck M, Preuschoft H, Gomberg N, editors. Environment, Behavior, and Morphology: Dynamic Interactions in Primates. New York: Gustav Fischer. p 297-312.

Kuhl F, Giardina C. 1982. Elliptic Fourier features of a closed contour. Computer graphics and image processing 18:236-258.

Lammers AR, German RZ. 2002. Ontogenetic allometry in the locomotor skeleton of specialized half-bounding mammals. J Zool 258:485-495.

Lanyon LE. 1987. Functional strain in bone tissue as an objective, and controlling stimulus for adaptive bone remodeling. J Biomech 20:1083-1093.

Lanyon LE, Baggott DG. 1976. Mechanical function as an influence on structure and form of bone. J Bone Joint Surg-Br Vol 58:436-443.

Lanyon LE, Bourn S. 1979. Influence of mechanical function on the development and remodeling of the tibia - experimental-study in sheep. Journal of Bone and Joint Surgery-American Volume 61:263-273.

Leakey MD, Hay RL. 1979. Pliocene footprints in the Laetolil beds at Laetoli, northern Tanzania. Nature 278:317-323.

Lieberman DE, Polk JD, Demes B. 2004. Predicting long bone loading from cross-sectional geometry. Am J Phys Anthropol 123:156-171.

Lieberman DE, Raichlen DA, Pontzer H, Bramble DM, Cutright-Smith E. 2006. The human gluteus maximus and its role in running. J Exp Biol 209:2143-2155.

Lockwood CA. 1999. Homoplasy and adaptation in the atelid postcranium. Am J Phys Anthropol 108:459-482.

Lockwood CA, Fleagle JG. 2007. Homoplasy in primate and human evolution. J Hum Evol 52:471-472.

Lockwood CA, Kimbel WH, Lynch JM. 2004. Morphometrics and hominoid phylogeny: Support for a chimpanzee-human clade and differentiation among great ape subspecies. Proc Natl Acad Sci USA 101:4356-4360.

Lovejoy CO, Burstein AH, Heiple KG. 1976. Biomechanical analysis of bone strength - method and its application to platycnemia. Am J Phys Anthropol 44:489-505.

Lovejoy CO, Latimer B, Suwa G, Asfaw B, White TD. 2009a. Combining prehension and propulsion: The foot of *Ardipithecus ramidus*. Science 326:72.

Lovejoy CO, McCollum MA, Reno PL, Rosenman BA. 2003. Developmental biology and human evolution. Annu Rev Anthropol 32:85-109.

Lovejoy CO, Meindl RS, Ohman JC, Heiple KG, White TD. 2002. The Maka femur and its bearing on the antiquity of human walking: Applying contemporary concepts of morphogenesis to the human fossil record. Am J Phys Anthropol 119:97-133.

Lovejoy CO, Simpson SW, White TD, Asfaw B, Suwa G. 2009b. Careful climbing in the Miocene: The forelimbs of *Ardipithecus ramidus* and humans are primitive. Science 326:70.

Lovejoy CO, Suwa G, Simpson SW, Matternes JH, White TD. 2009c. The great divides: *Ardipithecus ramidus* reveals the postcrania of our last common ancestors with African apes. Science 326:100-106.

Lovejoy CO, Suwa G, Spurlock L, Asfaw B, White TD. 2009d. The pelvis and femur of *Ardipithecus ramidus*: The emergence of upright walking. Science 326:71.

Main RP, Biewener AA. 2007. Skeletal strain patterns and growth in the emu hindlimb during ontogeny. J Exp Biol 210:2676-2690.

Minetti AE, Ardig OL, Reinach E, Saibene F, Prabhakar S, Visel A, Akiyama JA, Shoukry M, Lewis KD, Holt A, Plajzer-Frick I, Morrison H, Fitzpatrick DR, Afzal V, Pennacchio LA, Rubin EM, Noonan JP, Reno PL, McCollum MA, Cohn MJ, Meindl RS, Hamrick M, Lovejoy CO. 1999. The relationship between mechanical work and energy expenditure of locomotion in horses. J Exp Biol 202:2329-2338.

Mitteroecker P, Bookstein F. 2009. The ontogenetic trajectory of the phenotypic covariance matrix, with examples from craniofacial shape in rats and humans. Evolution 63:727-737.

Mitteroecker P, Gunz P, Bookstein FL. 2005. Heterochrony and geometric morphometrics: a comparison of cranial growth in *Pan paniscus* versus *Pan troglodytes*. Evol Dev 7:244-258.

Molnar P. 2006. Tracing prehistoric activities: Musculoskeletal stress marker analysis of a stone-age population on the island of Gotland in the Baltic Sea. Am J Phys Anthropol 129:12-23.

Morishita Y, Iwasa Y. 2008. Growth based morphogenesis of vertebrate limb bud. Bull Math Biol 70:1957-1978.

Moro M, vanderMeulen MCH, Kiratli BJ, Marcus R, Bachrach LK, Carter DR. 1996. Body mass is the primary determinant of midfemoral bone acquisition during adolescent growth. Bone 19:519-526.

Mosley JR, Lanyon LE. 1998. Strain rate as a controlling influence on adaptive modeling in response to dynamic loading of the ulna in growing male rats. Bone 23:313-318.

Netter F. 2003. Atlas of Human Anatomy, 3 ed. Philadelphia: Saunders.

O'Higgins P, Jones N. 1998. Facial growth in Cercocebus torquatus: an application of three-dimensional geometric morphometric techniques to the study of morphological variation. J Anat 193:251-272.

O'Neill MC, Dobson SD. 2008. The degree and pattern of phylogenetic signal in primate long-bone structure. J Hum Evol 54:309-322.

Pearson OM. 2000. Postcranial remains and the origin of modern humans. Evol Anthropol 9:229-247.

Pearson OM, Lieberman DE. 2004. The aging of Wolff's "Law": Ontogeny and responses to mechanical loading in cortical bone. Yearb Phys Anthropol 47:63-99.

Penin X, Berge C, Baylac M. 2002. Ontogenetic study of the skull in modern humans and the common chimpanzees: neotenic hypothesis reconsidered with a tridimensional Procrustes analysis. Am J Phys Anthropol 118:50-62.

Pickford M, Senut B, Gommery D, Treil J. 2002. Bipedalism in *Orrorin tugenensis* revealed by its femora. C R Palevol 1:191-203.

Polk JD, Demes B, Jungers WL, Biknevicius AR, Heinrich RE, Runestad JA. 2000. A comparison of primate, carnivoran and rodent limb bone cross-sectional properties: are primates really unique? J Hum Evol 39:297 - 325.

Ponce de León MS, Zollikofer CPE. 2001. Neanderthal cranial ontogeny and its implications for late hominid diversity. Nature 412:534-538.

Pontzer H, Raichlen DA, Sockol MD. 2009. The metabolic cost of walking in humans, chimpanzees, and early hominins. J Hum Evol 56:43-54.

Primrose A. 1898. The anatomy of the Orang utang (*Simia satyrus*). Trans Canad Inst 6:507-598.

Raven H. 1950. Regional anatomy of the gorilla. In: Gregory W, editor. The Anatomy of the Gorilla. New York: Columbia University Press.

Reynolds TR. 1985. Stresses on the limbs of quadrupedal primates. Am J Phys Anthropol 67:351-362.

Rhodes JA, Knüsel CJ. 2005. Activity-related skeletal change in medieval humeri: Cross-sectional and architectural alterations. Am J Phys Anthropol 128:536-546.

Richmond BG, Jungers WL. 2008. *Orrorin tugenensis* femoral morphology and the evolution of hominin bipedalism. Science 319:1662-1665.

Richmond BG, Strait DS. 2000. Evidence that humans evolved from a knuckle-walking ancestor. Nature 404:382-385.

Robling AG, Hinant FM, Burr DB, Turner CH. 2002. Improved bone structure and strength after long-term mechanical loading is greatest if loading is separated into short bouts. J Bone Miner Res 17:1545-1554.

Rodman PS, McHenry HM. 1980. Bioenergetics and the origin of hominid bipedalism. Am J Phys Anthropol 52:103-106.

Rohlf FJ. 1990. Rotational fit (Procrustes) methods. In: Rohlf F, Bookstein F, editors. Proceedings of the Michigan Morphometrics Workshop: Univ.of Michigan Museum of Zoology (Special Publication no. 2). p 227–236.

Rook L, Bondioli L, Kohler M, Moya-Sola S, Macchiarelli R. 1999. *Oreopithecus* was a bipedal ape after all: Evidence from the iliac cancellous architecture. Proc Natl Acad Sci USA 96:8795-8799.

Ruff CB. 1988. Hindlimb articular surface allometry in hominoidea and *Macaca*, with comparisons to diaphyseal scaling. J Hum Evol 17:687-714.

Ruff CB. 2002. Long bone articular and diaphyseal structure in old world monkeys and apes. I: Locomotor effects. Am J Phys Anthropol 119:305-342.

Ruff CB. 2003a. Growth in bone strength, body size, and muscle size in a juvenile longitudinal sample. Bone 33:317-329.

Ruff CB. 2003b. Ontogenetic adaptation to bipedalism: age changes in femoral to humeral length and strength proportions in humans, with a comparison to baboons. J Hum Evol 45:317-349.

Ruff CB. 2009. Relative limb strength and locomotion in *Homo habilis*. Am J Phys Anthropol 138:90-100.

Ruff CB, Hayes WC. 1983. Cross-sectional geometry of Pecos Pueblo femora and tibiae--a biomechanical investigation: I. Method and general patterns of variation. Am J Phys Anthropol 60:359-381.

Ruff CB, Holt B, Trinkaus E. 2006. Who's afraid of the big bad wolff? "Wolff is law" and bone functional adaptation. Am J Phys Anthropol 129:484-498.

Ruff CB, McHenry HM, Thackeray JF. 1999. Cross-sectional morphology of the SK 82 and 97 proximal femora. Am J Phys Anthropol 109:509-521.

Ruff CB, Runestad JA. 1992. Primate limb bone structural adaptations. Annu Rev Anthropol 21:407-433.

Ruff CB, Trinkaus E, Walker A, Larsen CS. 1993. Postcranial robusticity in *Homo*. I: Temporal trends and mechanical interpretation. Am J Phys Anthropol 91:21-53.

Ruff CB, Walker A, Trinkaus E. 1994. Postcranial robusticity in *Homo*. III: ontogeny. Am J Phys Anthropol 93:35-54.

Scheuer L, Black S, Christie A. 2000. Developmental Juvenile Osteology. San Diego, San Francisco, New York, Boston, London, Sydney, Tokyo: Academic Press.

Schmitt D. 2003. Insights into the evolution of human bipedalism from experimental studies of humans and other primates. J Exp Biol 206:1437-1448.

Schmitt D, Lemelin P. 2002. The origins of primate locomotion: gait mechanics of the woolly opossum. Am J Phys Anthropol 118:231-238.

Schultz AH. 1937. Proportions, variability and asymmetries of the long bones of the limbs and the clavicles in man and apes. Hum Biol 9:281-328.

Schultz AH. 1969. The skeleton of the chimpanzee. In: Bourne GH, editor. The Chimpanzee, Vol. 1. Basel: Karger. p 50-103.

Schwartz JH. 1995. Skeleton Keys: An Introduction to Human Skeletal Morphology, Development, and Analysis. Oxford: Oxford University Press.

Senut B, Pickford M, Gommery D, Mein P, Cheboi K, Coppens Y. 2001. First hominid from the Miocene (Lukeino Formation, Kenya). C R Acad Sci Paris Ser II a 332:137-144.

Serrat MA, King D, Lovejoy CO. 2008. Temperature regulates limb length in homeotherms by directly modulating cartilage growth. Proc Natl Acad Sci USA 105:19348-19353.

Serrat MA, Lovejoy CO, King D. 2007. Age- and site-specific decline in insulin-like growth factor-I receptor expression is correlated with differential growth plate activity in the mouse hindlimb. The Anatomical Record: Advances in Integrative Anatomy and Evolutionary Biology 290:375-381.

Shea BT. 1981. Relative growth of the limbs and trunk in the African apes. Am J Phys Anthropol 56:179-201.

Sigmon BA. 1974. A functional analysis of pongid hip and thigh musculature. J Hum Evol 3:161-185.

Sockol MD, Raichlen DA, Pontzer H. 2007. Chimpanzee locomotor energetics and the origin of human bipedalism. Proc Natl Acad Sci USA 104:12265-12269.

Sparacello V, Marchi D. 2008. Mobility and subsistence economy: A diachronic comparison between two groups settled in the same geographical area (Liguria, Italy). Am J Phys Anthropol 136:485-495.

Sparacello VS, Pearson OM. 2010. The importance of accounting for the area of the medullary cavity in cross-sectional geometry: A test based on the femoral midshaft. Am J Phys Anthropol 143:612–624.

Specht M, Lebrun R, Zollikofer CPE. 2007. Visualizing shape transformation between chimpanzee and human braincases. Visual Computer 23:743-751.

Standring S, editor. 2004. Gray's Anatomy, 39 ed. Edinburgh/London/New York: Churchill Livingstone.

Standring S, editor. 2005. Gray's anatomy: Churchill Livingstone.

Stern JT. 1972. Anatomical and functional specializations of human gluteus maximus. Am J Phys Anthropol 36:315-338.

Stern JT, Susman RL. 1981. Electromyography of the gluteal muscles in *Hylobates*, *Pongo*, and *Pan* - implications for the evolution of hominid bipedality. Am J Phys Anthropol 55:153-166.

Sumner DR, Andriacchi TP. 1996. Adaptation to differential loading: Comparison of growth-related changes in cross-sectional properties of the human femur and humerus. Bone 19:121-126.

Sutherland DH, Olshen R, Cooper L, Woo SL. 1980. The development of mature gait. J Bone Joint Surg Am 62:336-353.

Swindler D, Wood C. 1982. An Atlas of Primate Gross Anatomy. Malabar: Robert E. Krieger Publishing Company.

Szivek JA, Johnson EM, Magee FP. 1992. *In vivo* strain analysis of the greyhound femoral diaphysis. Journal of Investigative Surgery 5:91-108.

Thorpe SKS, Holder RL, Crompton RH. 2007. Origin of human bipedalism as an adaptation for locomotion on flexible branches. Science 316:1328-1331.

Trinkaus E, Churchill SE, Ruff CB. 1994. Postcranial robusticity in *Homo*. II: Humeral bilateral asymmetry and bone plasticity. Am J Phys Anthropol 93:1-34.

Turley K, Guthrie EH, Frost SR. 2011. Geometric Morphometric Analysis of Tibial Shape and Presentation Among Catarrhine Taxa. The Anatomical Record: Advances in Integrative Anatomy and Evolutionary Biology 294:217-230.

Turner CH, Forwood MR, Otter MW. 1994. Mechanotransduction in bone - do bone-cells act as sensors of fluid-flow. FASEB J 8:875-878.

Turner CH, Owan I, Takano Y. 1995. Mechanotransduction in bone - role of strain-rate. American Journal of Physiology-Endocrinology and Metabolism 269:E438-E442.

Uhlmann K. 1968. Hüft- und Oberschenkelmuskulatur: Systematische und vergleichende Anatomie. In: Hofer H, Schultz AH, Starck D, editors. Primatologia: Handbuch der Primatenkunde. Basel: Karger.

van der Meulen MCH, Ashford MW, Kiratli BJ, Bachrach LK, Carter DR. 1996. Determinants of femoral geometry and structure during adolescent growth. J Orth Res 14:22-29.

Villotte S, Castex D, Couallier V, Dutour O, Knusel CJ, Henry-Gambier D. 2010. Enthesopathies as occupational stress markers: evidence from the upper limb. Am J Phys Anthropol 142:224-234.

Wallace IJ, Middleton KM, Svetlana L, Kelly SA, Stefan J, Theodore G, Jr., Brigitte D. 2010. Functional significance of genetic variation underlying limb bone diaphyseal structure. In.

Ward CV. 2002. Interpreting the posture and locomotion of *Australopithecus afarensis*: where do we stand? Am J Phys Anthropol Suppl 35:185-215.

Warden SJ, Hurst JA, Sanders MS, Turner CH, Burr DB, Li J. 2005. Bone adaptation to a mechanical loading program significantly increases skeletal fatigue resistance. J Bone Miner Res 20:809-816.

Weiss E. 2004. Understanding muscle markers: Lower limbs. Am J Phys Anthropol 125:232-238.

White TD, Asfaw B, Beyene Y, Haile-Selassie Y, Lovejoy CO, Suwa G, WoldeGabriel G. 2009. *Ardipithecus ramidus* and the paleobiology of early hominids. Science 326:75-86.

Wolff J. 1892. Das Gesetz der Transformation der Knochen. Berlin: A. Hirschwald.

Wolff J. 1986. The law of bone remodeling. Berlin: Springer-Verlag.

Wood B, Harrison T. 2011. The evolutionary context of the first hominins. Nature 470:347-352.

Wood B, Richmond BG. 2000. Human evolution: taxonomy and paleobiology. J Anat 197 (Pt 1):19-60.

Yamanaka A, Gunji H, Ishida H. 2005. Curvature, length, and cross-sectional geometry of the femur and humerus in anthropoid primates. Am J Phys Anthropol 127:46-57.

Young JW, Fernandez D, Fleagle JG. 2009. Ontogeny of long bone geometry in capuchin monkeys (Cebus albifrons and Cebus apella): implications for locomotor development and life history. Biol Lett 6:197-200.

Young NM, Wagner GP, Hallgrímsson B. 2010. Development and the evolvability of human limbs. Proc Natl Acad Sci USA 107:3400-3405.

Zollikofer CPE, de Leon MSP, Lieberman DE, Guy F, Pilbeam D, Likius A, Mackaye HT, Vignaud P, Brunet M. 2005. Virtual cranial reconstruction of *Sahelanthropus tchadensis*. Nature 434:755-759.

Zollikofer CPE, Ponce de León MS. 2001. Computer-assisted morphometry of hominoid fossils: the role of morphometric maps. In: De Bonis L, Koufos G, Andrews P, editors. Phylogeny of the Neogene Hominoid Primates of Eurasia. Cambridge: Cambridge University Press. p 50-59.

Zollikofer CPE, Ponce de León MS. 2006. Neanderthals and modern humans - chimps and bonobos: similarities and differences in development and evolution. In: Harvati K, Harrison T, editors. Neanderthals Revisited: New Approaches and Perspectives. New York: Springer. p 71-88.

Acknowledgements

We thank P. Jans for help with sample preparation and CT scanning. Research funded by the Swiss National Science Foundation (grant # 31003A-109344 to C.P.E.Z.) We are also grateful to the three anonymous reviewers for valuable comments and suggestions.

Appendix

A. Elliptic Fourier Analysis

Let

$$L = (x(t), y(t)) \tag{A1}$$

be a parametric representation of a closed line L in the xy-plane, where the x and y coordinates of line points are expressed as functions of path length t along L. Elliptic Fourier Analysis (EFA) is based on the respective Fourier decompositions of the independent functions $x(t)$ and $y(t)$:

$$x(t) = A_o + \sum_{n=1}^{N} a_n \cos nt + \sum_{n=1}^{N} b_n \sin nt\,,$$

$$y(t) = C_o + \sum_{n=1}^{N} c_n \cos nt + \sum_{n=1}^{N} d_n \sin nt\,. \tag{A2}$$

Using these parametric functions, surface curvature k is analytically calculated as

$$k(t) = \frac{x'(t)y''(t) - y'(t)x''(t)}{\left[\{x'(t)\}^2 + \{y'(t)\}^2\right]^{3/2}}\,, \tag{A3}$$

where positive/negative values of k represent convex/concave regions of the outline.

B. Second moments of area

Second moments of area I_θ are calculated for each diaphyseal cross section as

$$I_\theta = \sum A_{ij} d_j^{\,2}, \tag{A4}$$

where θ is the direction of the normal vector of the bending plane (**B**-**B**; see Fig. 1C), i and j are coordinates across/perpendicular to the bending plane (coordinate origin is at the center of mass), A_{ij} is the area of cortical bone at pixel location (i,j), and d_j is the distance of that pixel from the bending plane (Fig. 1C).

C. Two-dimensional Fourier transform

A morphometric map with its coordinate system (θ, z) represents a 2-dimensional image, which is periodic in θ. The two-dimensional Fourier Transform (FT) of an image of size of $K \times L$ is defined as

$$F(u,v) = \frac{1}{KL} \sum_{u=0}^{K-1} \sum_{v=0}^{L-1} f(x,y) e^{-i2\pi\left(\frac{ux}{K} + \frac{vy}{L}\right)}. \tag{A5}$$

A $K \times L$ image yields an $K \times L$ set of Fourier coefficients (complex numbers). The inverse FT is defined as

$$f(x,y) = \sum_{u=0}^{K-1} \sum_{v=0}^{L-1} F(u,v) e^{i2\pi\left(\frac{ux}{K}+\frac{vy}{L}\right)}, \quad \text{(A6)}$$

and used here to calculate a $K \times L$ MM from a $K \times L$ set of Fourier coefficients.

D. Optimal superposition (alignment) of Morphometric Maps

MMs are optimally superimposed by rotating diaphyses around their long axes until a predefined morphometric distance metric is minimized. MM superposition is performed by minimizing the distance D_F in Fourier space between each MM's FT $F(\mathbf{M_n})$ (n=1, 2, …, N) and the FT of the consensus map $F(<\mathbf{M}>)$

$$D_F\,(F(\mathbf{M_n}), F(<\mathbf{M}>)) \rightarrow \min. \quad \text{(A7)}$$

Rotating a diaphysis around its longitudinal axis corresponds to a horizontal shift of its MM. According to the Fourier shift theorem, a horizontal shift of MM(θ, z) by A can be expressed as

$$f(\theta - A, z) = e^{-iAu} F(u,v). \quad \text{(A9)}$$

When each MM is aligned to the reference map, the reference should be a biologically relevant consensus. Therefore, when there are several groups for comparison, it is recommended to first calculate a consensus map for each group separately, and align each MM to this group-specific consensus. One can minimize the distance among group-specific consensus maps to avoid a "biased" reference due to different numbers of specimens in each group (i.e., calculating mean of mean).

E. Comparison of ontogenetic trajectories

Trajectory divergence V_{ij} was calculated as

$$V_{ij} = 1 - \left(a_i \cdot a_j\right)^2, \quad \text{(A9)}$$

where $\mathbf{a}_i$ and $\mathbf{a}_j$ are normalized trajectory direction vectors. Larger value of V_{ij} means larger divergence between two vectors. The difference between group-specific modes of variation is measured as the variance-covariance matrix distance

$$C_{ij} = \left\| S_i, S_j \right\|_{\text{cov}} = \sqrt{\sum \left(\log \lambda_k\right)^2}, \quad \text{(A10)}$$

where λ_k are the relative eigenvalues of group-specific covariance matrices S_i and S_j as defined in (Mitteroecker and Bookstein, 2009).

F. Abbreviations

FT: Fourier Transform

GM: geometric morphometrics

MM: Morphometric Map, Morphometric Mapping

WL: Wolff's Law

Table 1. Comparison of ontogenetic trajectories

	distance	principal directions	ontogenetic allometric trajectory	mode of variation	relative magnitude of variation*
Entire diaphysis analyses					
MM (radius ext)	0.951	0.661	0.549	0.868	0.56
MM (curvature)	0.420	0.284	0.221	0.648	0.88
MM (thickness)	0.079	0.725	0.389	0.730	0.86
MM (radius+curvature+thickness)	0.152	0.428	0.234	0.713	0.83
MM (second moments of area)	0.618	0.903	0.900	0.966	0.34
GM (radius ext)	0.947	0.646	0.493	0.854	0.61
Subregion analyses					
MM (curvature)					
prox	0.220	0.660	0.138	0.856	
mid	0.459	0.510	0.456	0.860	
dist	0.802	0.264	0.169	0.578	
MM (thickness)					
prox	0.190	0.384	0.308	0.892	
mid	0.261	0.340	0.545	0.431	
dist	**0.026**	0.379	0.895	0.366	
I_{ML}/I_{AP}	Slope	Intercept			
prox	0.35	0.43			
mid	0.87	0.62			
dist	0.57	0.42			
I_{max}/I_{min}	Slope	Intercept			
prox	0.14	0.78			
mid	0.88	0.62			
dist	0.57	0.42			
Cross-sectional area	Slope	Intercept			
prox	0.42	0.34			
mid	0.60	0.57			
dist	0.78	0.42			

* relative magnitude of variation = (variation across ontogeny) / (variation along ontogeny)

Table 2. Coefficients of least square fitting

r_{ext}	PC1 (GM)	PC2 (GM)	PC3 (GM)
PC1 (MM)	**0.98**	-0.02	-0.01
PC2 (MM)	-0.02	**0.96**	-0.02
PC3 (MM)	-0.01	-0.02	**0.96**

$r_{ext+\ int}$	PC1 (GM)	PC2 (GM)	PC3 (GM)
PC1 (MM)	**0.97**	0.0002	-0.02
PC2 (MM)	0.003	**0.96**	-0.01
PC3 (MM)	-0.02	-0.01	**0.94**

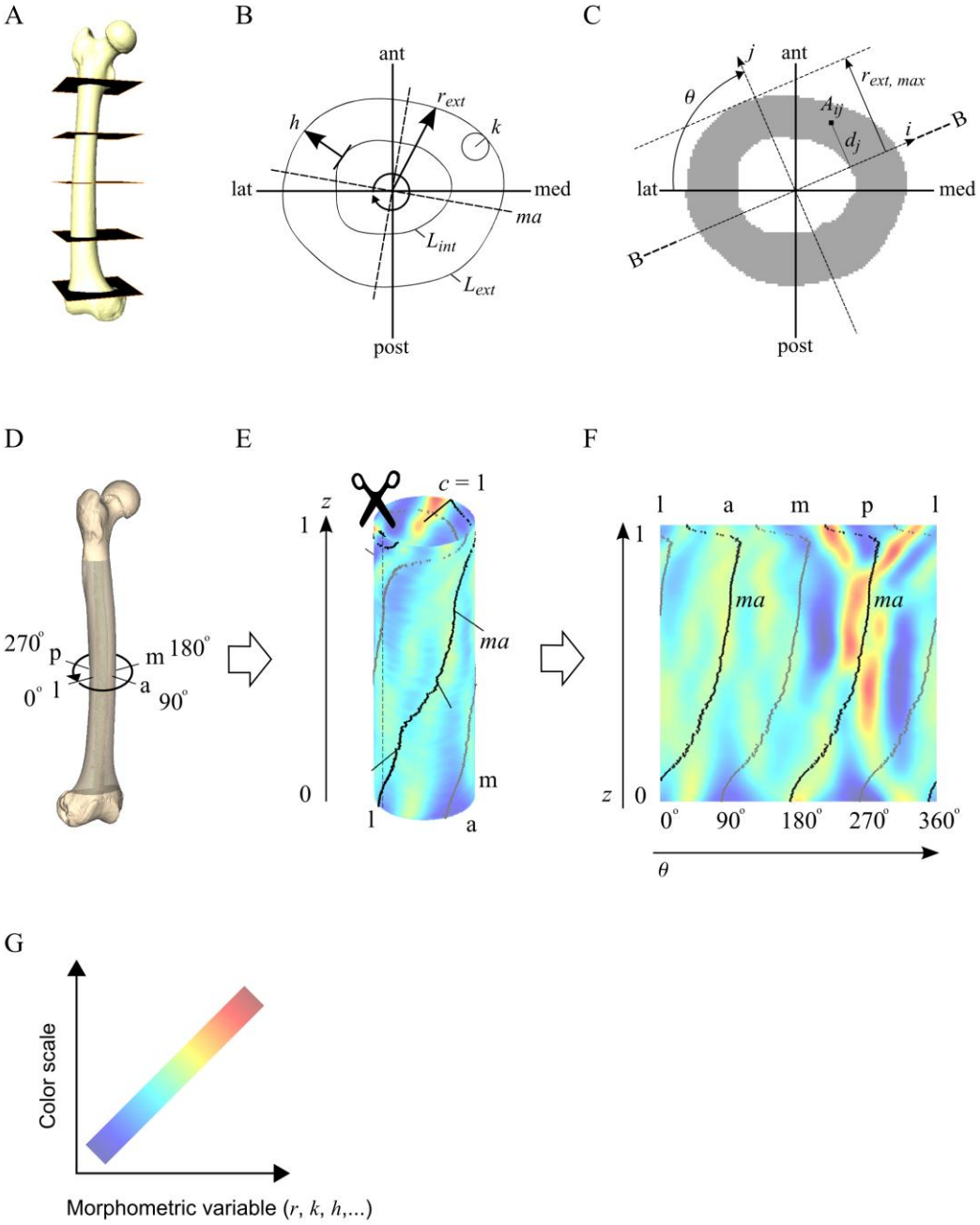

Fig. 1 Scheme of morphometric data sampling and morphometric mapping. A, volumetric data are acquired using medical and/or micro CT. B, explicit representation of external/internal outlines (L_{ext}/L_{int}) and definition of morphometric variables: radius (r), surface curvature (k), cortical bone thickness (h). C, calculation of second moments of area (I_θ). The bending plane (B-B) is assumed to go through center of mass; $r_{ext,max}$ is the maximum radius used to calculate section modulus Z_θ. All data are sampled around and along the entire diaphysis. D, 3D representation of the right femur. Diaphysis is delimited using proximal (distal to lesser trochanter) and distal epiphyseal lines. E, F, principle of cylindrical projection. Morphometric data are projected to the normal cylinder (radius =1; height = 1). The cylinder is cut open laterally and unrolled into a planar image (black/gray lines show the direction of major/minor cross-sectional axes). F, principle of morphometric mapping: lateral [0°] → anterior [90°] → medial [180°] → posterior [270°] → lateral [360°]. *ma*: direction of cross-sectional major axis.

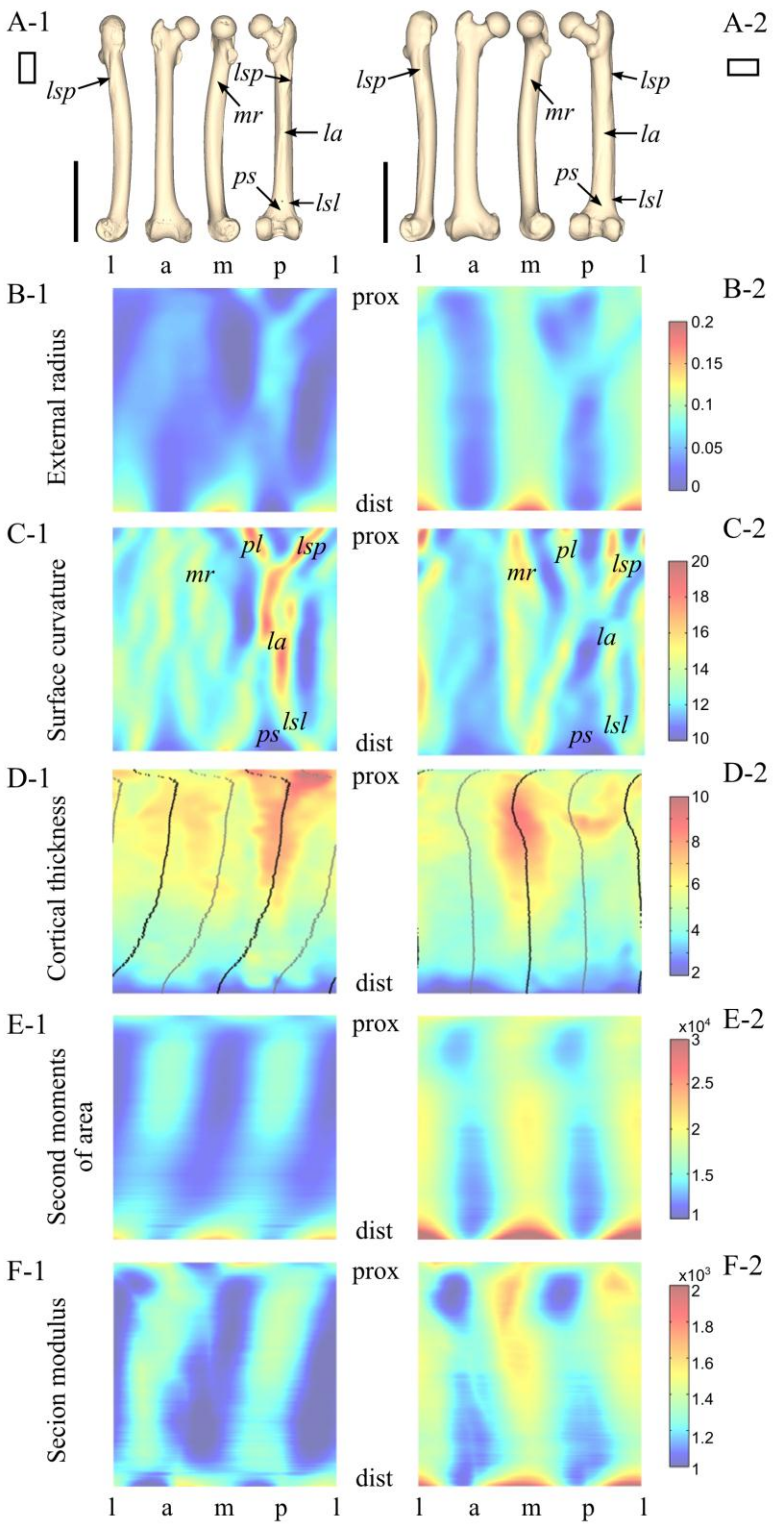

Fig. 2 Interindividual variation of chimpanzee femoral diaphyseal morphology. Femora of two adult captive individuals (left/right panels) are compared. A, 3D representation of the right femur in standard orientations (linea aspera [*la*], lateral spiral pilaster [*lsp*], popliteal surface [*ps*], medial ridge [*mr*]). B-F, morphometric maps of external radius (B), surface curvature (C), cortical bone thickness (D), second moments of area (E) and section modulus (F). Black/gray lines in D indicate orientation of major/minor cross-sectional axes.

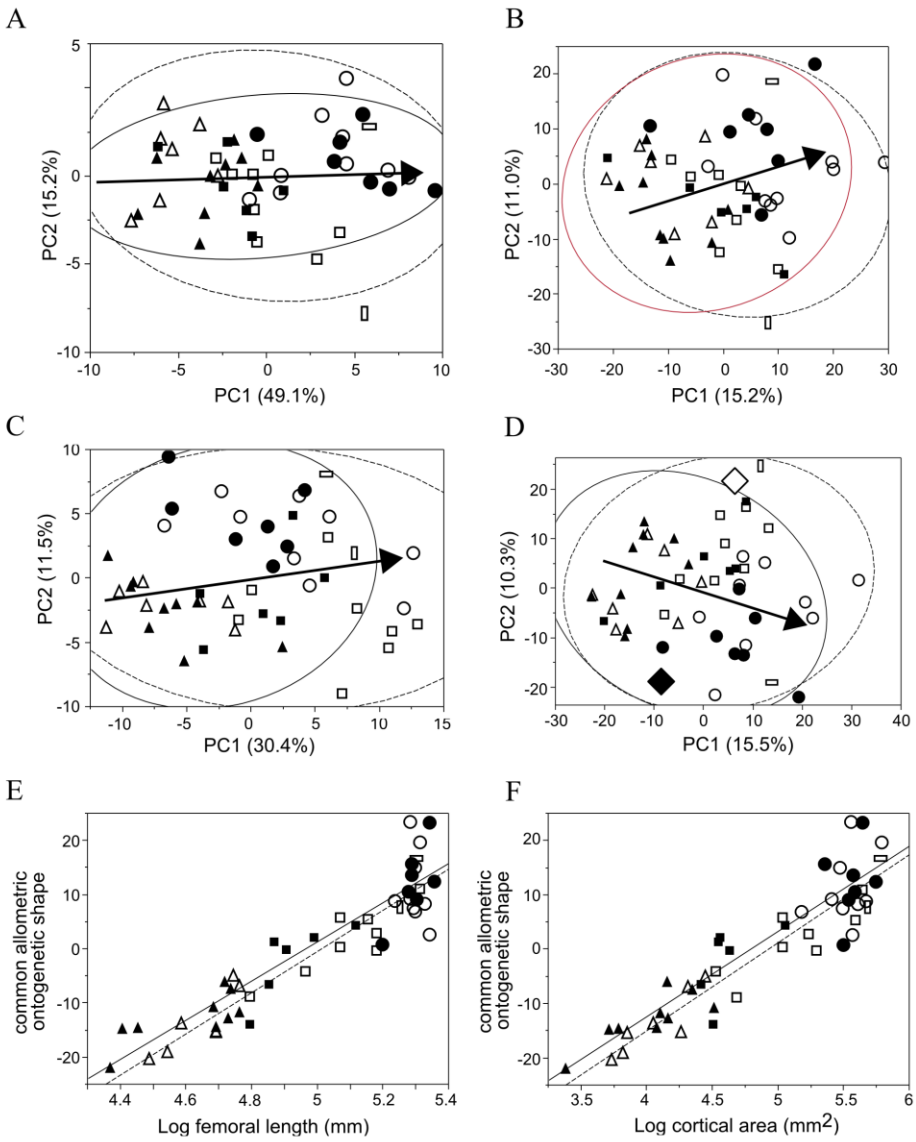

Fig. 3 MM-based PCA of femoral diaphyseal shape variation. PC plots for external radius (A), surface curvature (B), cortical bone thickness (C) and all morphometric features together (D). (filled/open markers: wild/captive individuals; triangles: infant, squares: juvenile, circles: adults). Solid/dashed outlines show 95%-density ellipses for wild/captive groups. Black arrow shows common allometric ontogenetic vector (average ontogenetic vector of wild and captive groups). E, F, graph of common allometric ontogenetic shape against femoral length and median cortical area. In all analyses, wild/captive chimpanzee ontogenetic trajectories are indistinguishable in their position and slope (see Table 1).

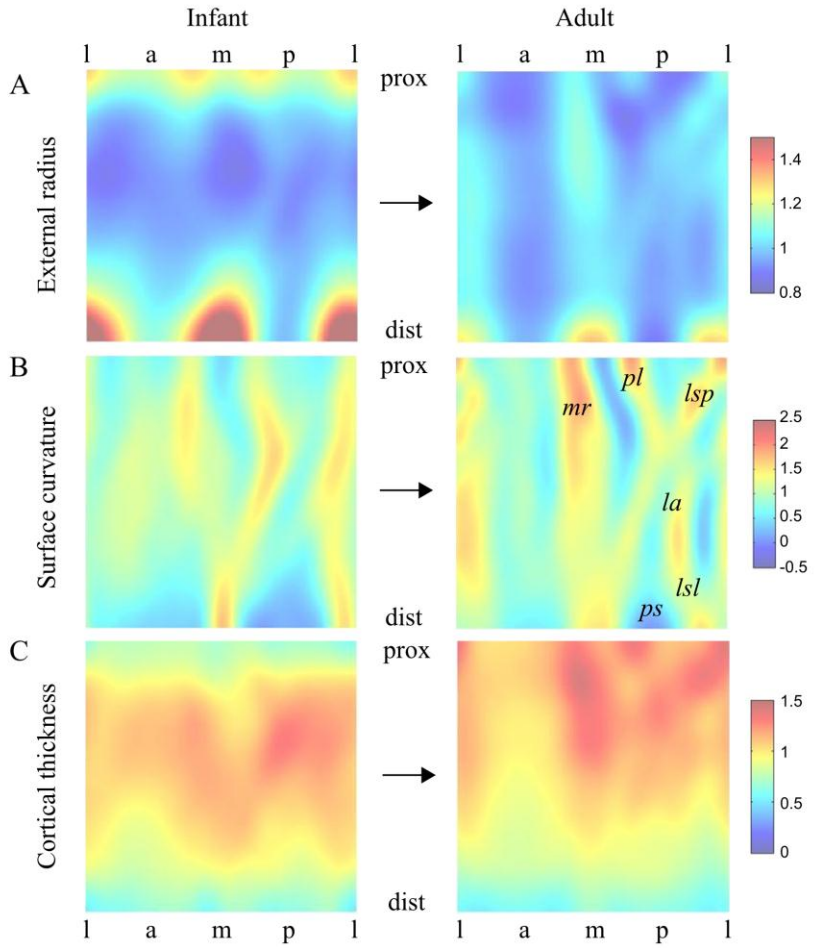

Fig. 4 Ontogeny of femoral diaphyseal morphology. A, external radius; B, external surface curvature; C, cortical bone thickness (MMs for infants [left] and adults [right] corresponding to the base and tip of the ontogenetic vector in Fig. 3, respectively). In young specimens, proximal and distal ends of femoral diaphysis are wider relative to mid-shaft (A). Note development of marked linea aspera (B), and of a proximo-distal gradient of cortical bone thickness (C).

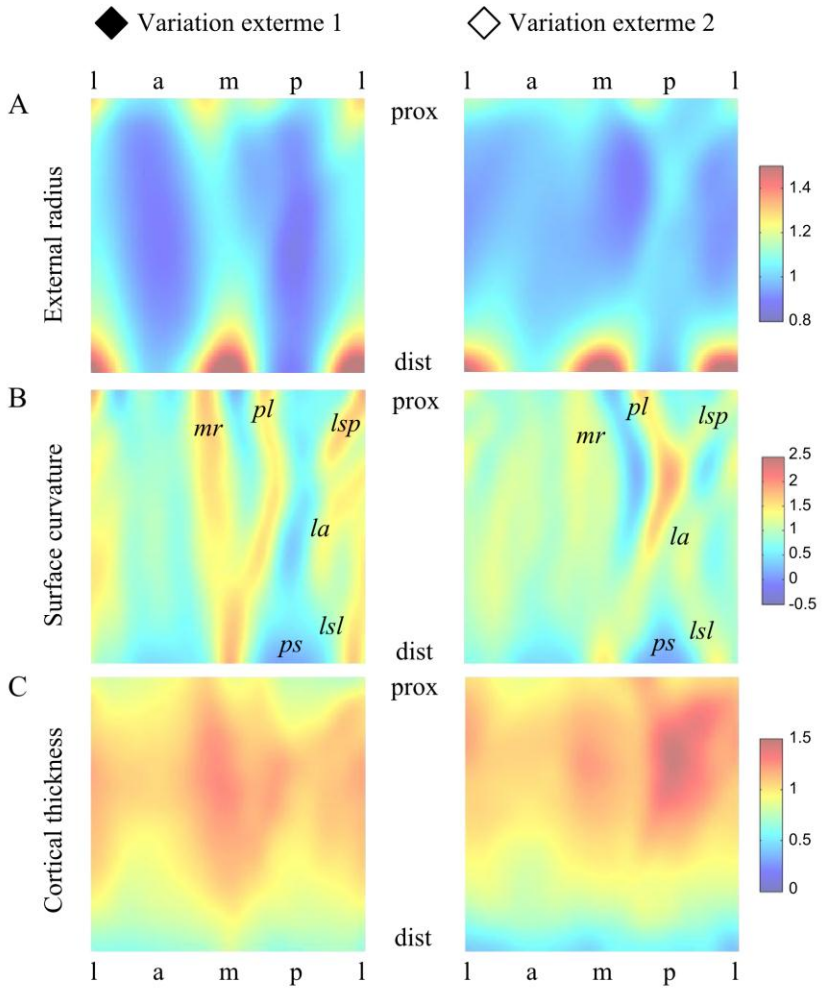

Fig. 5 Principal patterns of intraspecific variation of femoral diaphyseal morphology. Variation is visualized with MMs for extreme shapes (corresponding to the diamonds in Fig. 3D); A, external radius; B, surface curvature; C, cortical bone thickness.

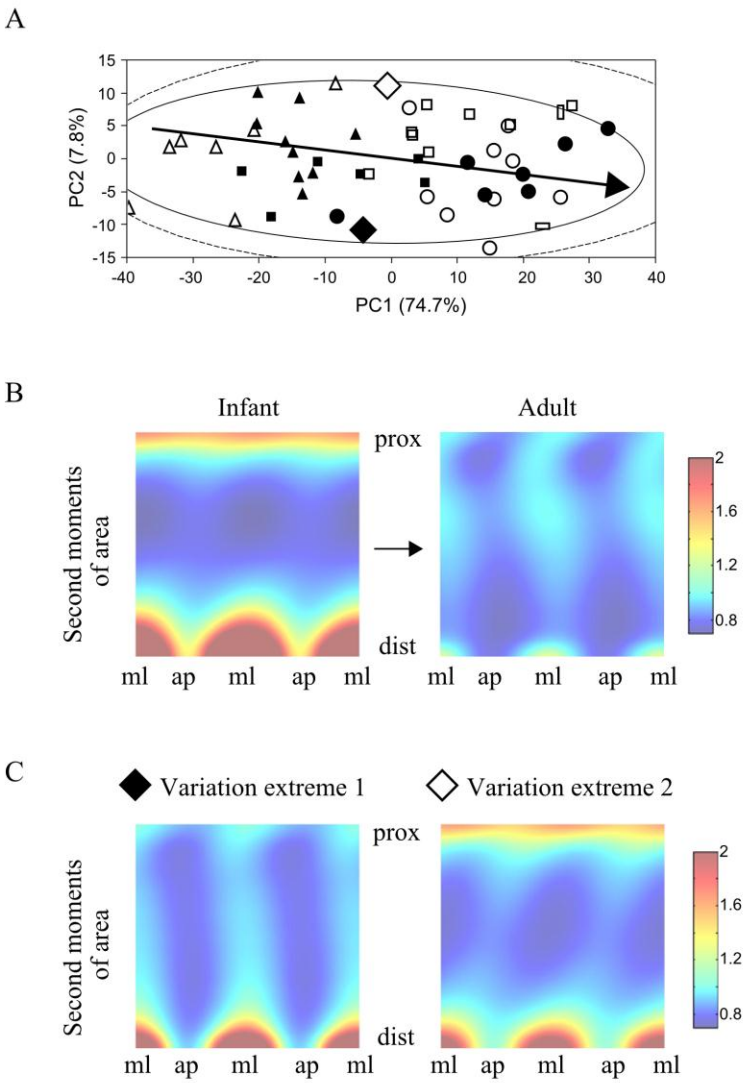

Fig. 6 Analysis of diaphyseal biomechanical properties (symbols as in Fig. 3). A, MM-based PCA of second moments of area. Captive/wild chimpanzee ontogenetic trajectories are indistinguishable in their position and orientation (see Table 1). B, corresponding average MMs visualizing ontogenetic change (infant [left] and adult [right]). C, principal patterns of intraspecific variation (extreme shapes corresponding to the diamonds in A).

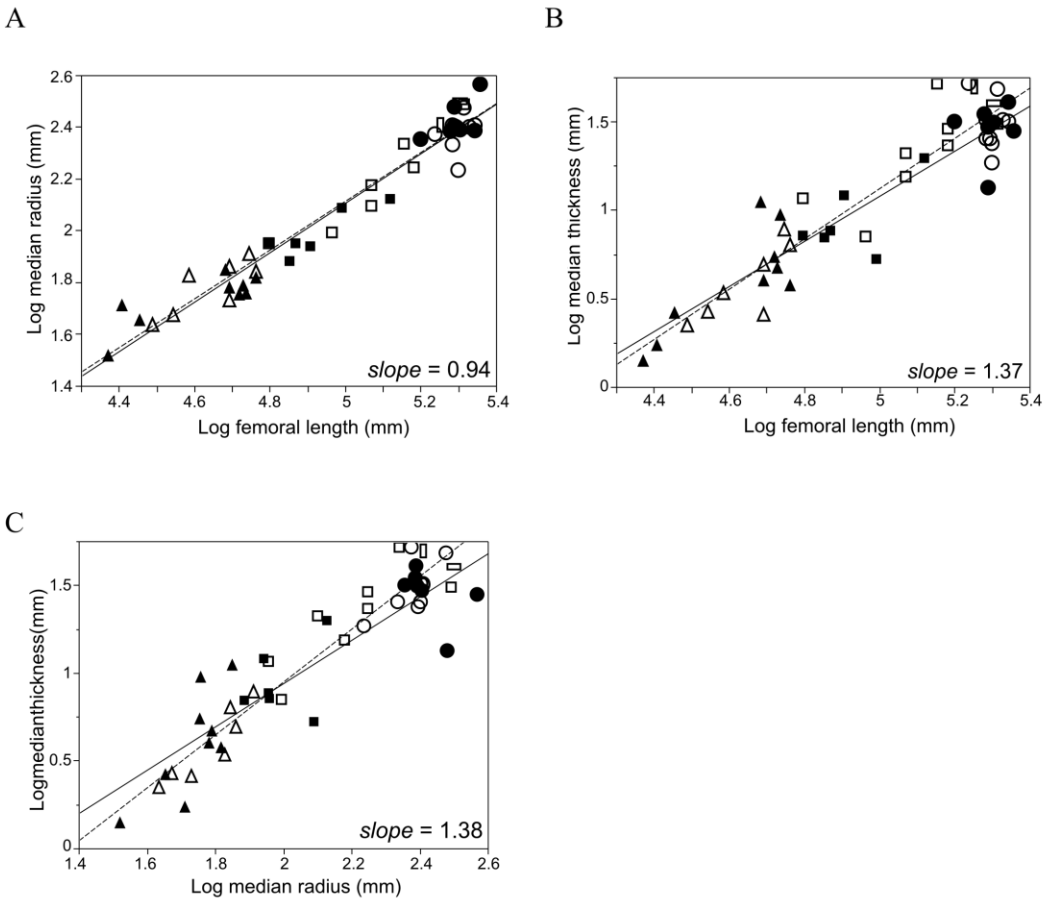

Fig. 7 Ontogenetic allometry of diaphyseal length, median cortical external radius and median bone thickness (symbols as in Fig. 3). Radius and thickness show negative and positive allometry relative to femoral length, respectively (slopes: 0.94,1.37 and 1.38 for length-radius, length-thickness and radius-thickness plots, respectively). Some adult captive individuals exhibit thicker cortical bone than wild individuals.

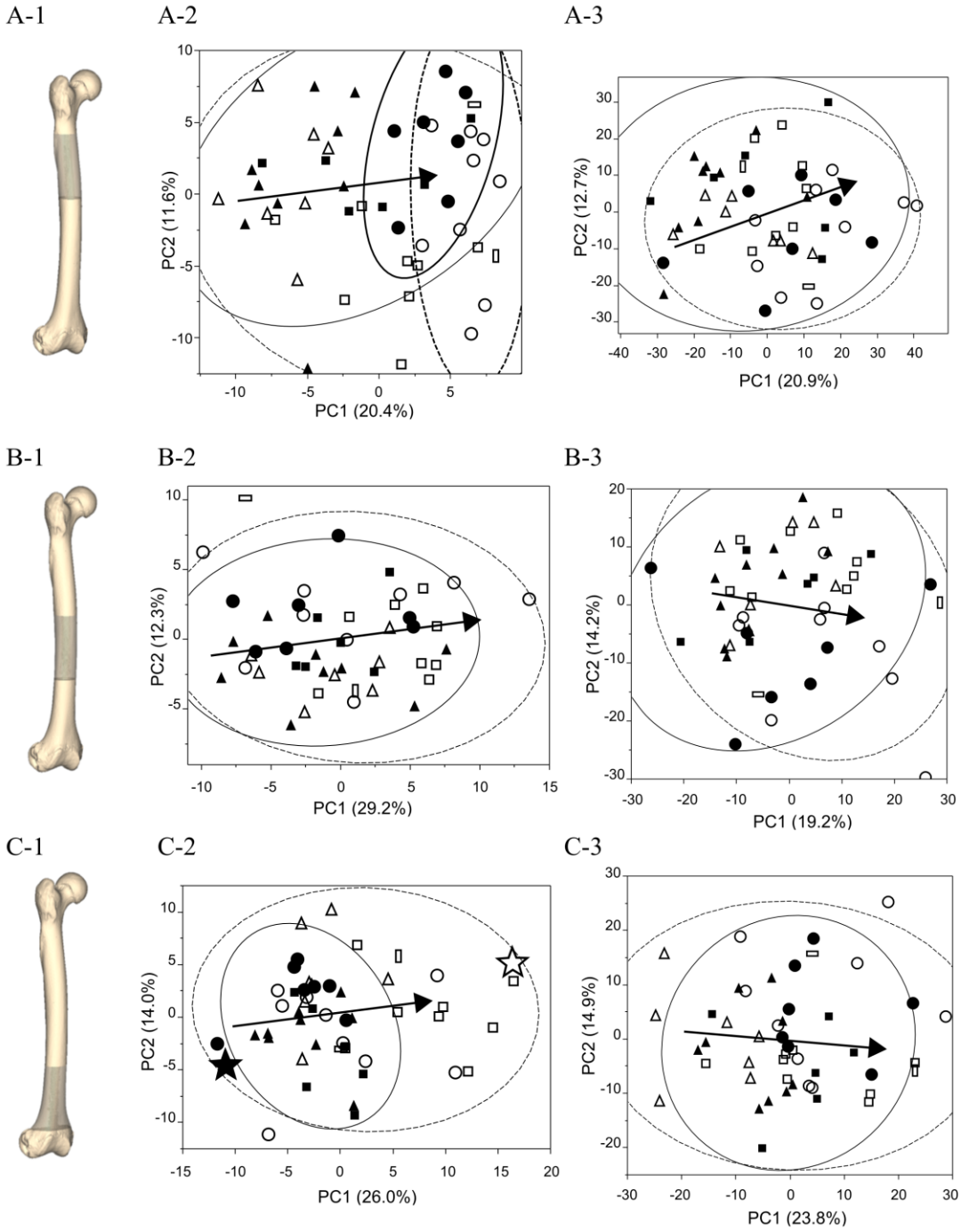

Fig. 8 MM analysis of femoral diaphyseal subregions (symbols as in Fig. 3). Proximal (A), middle (B), and distal (C) thirds were analyzed separately for cortical bone thickness (A-1 [95% density ellipses (bold lines) for adult individuals], B-1,C-1), surface curvature (A-2,B-2,C-2) by MM methods. MM-based analysis of thickness distinguishes between wild and captive chimpanzee femora at distal diaphysis (see Table 1). MM visualizations corresponding to filled/open stars are shown in Fig. 9.

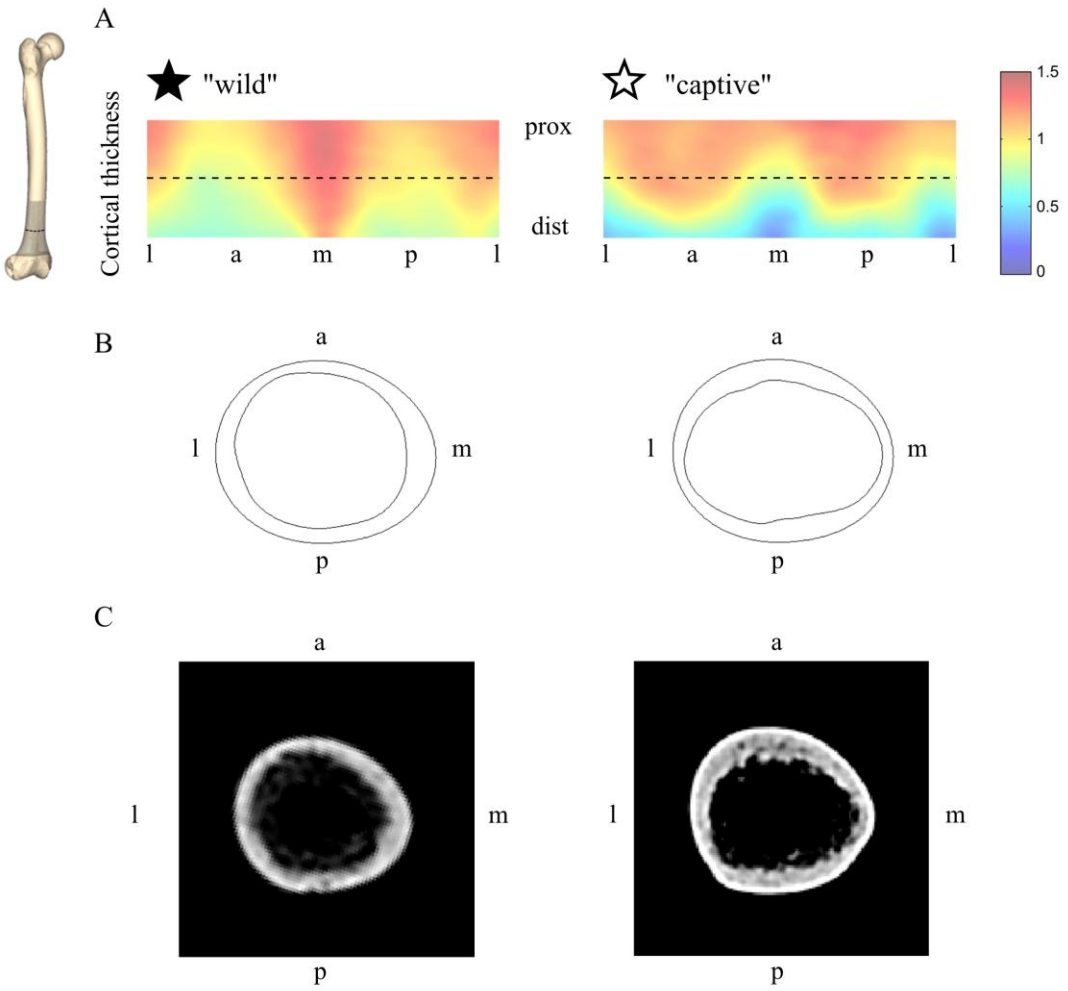

Fig. 9 Cortical bone distribution in the distal femoral diaphysis of wild (left panels) and captive (right panels) chimpanzees. A: MM of cortical bone thickness (relative value [normalized by the median]). B: corresponding cross-sectional shapes (section taken at dashed line in A). C: CT cross-sections of a wild and a captive individual (specimens closest to stars in Fig. 8C-2). Note anteroposteriorly increased thickness in captive individual.

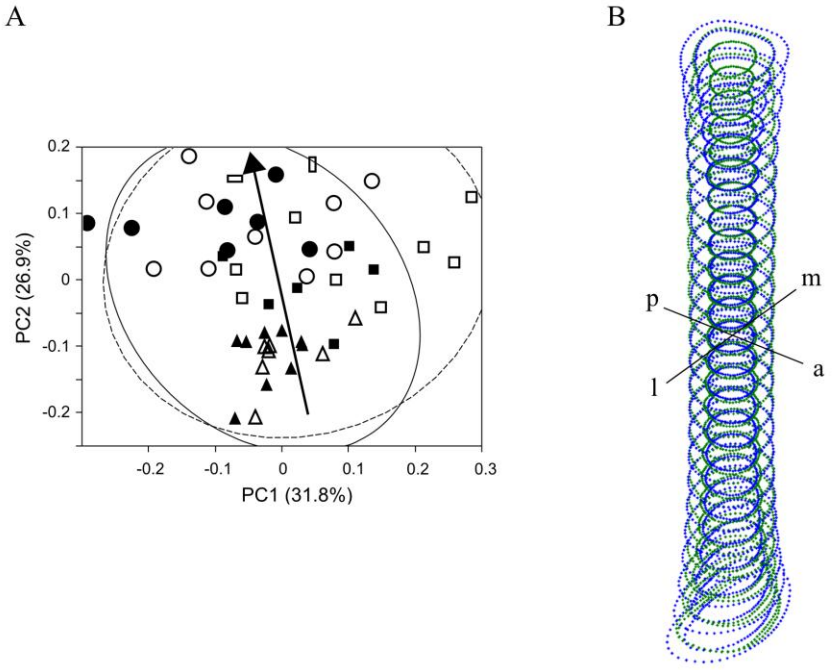

Fig. 10 GM analyses of external and internal diaphyseal surfaces (symbols as in Fig. 3). A, PC plot. Ontogenetic trajectories are indistinguishable between wild and captive groups. B, ontogenetic changes are visualized using semilandmarks (see Fig. 4 for comparison). Proximal and distal ends of the femoral diaphysis are relatively wider in infants (blue) than in adults (green) while relative midshaft shape is similar.

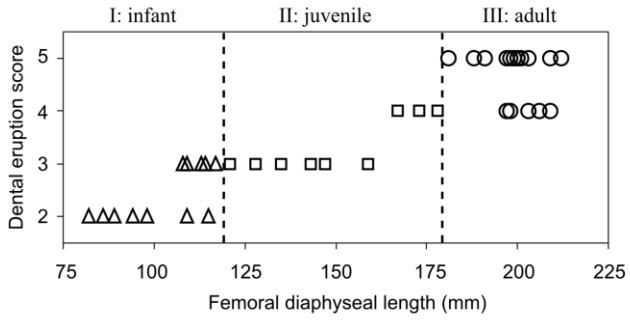

Fig. S1 Femoral diaphyseal length and dental age (wild/captive pooled; femoral length<120mm, squares: femoral length <180mm, circles: adults). Dental eruption scores correspond to the following dental eruption stages: 1: second deciduous molar erupted; 2:M1 erupted; 3: M2 erupted; 4: M3 erupted.

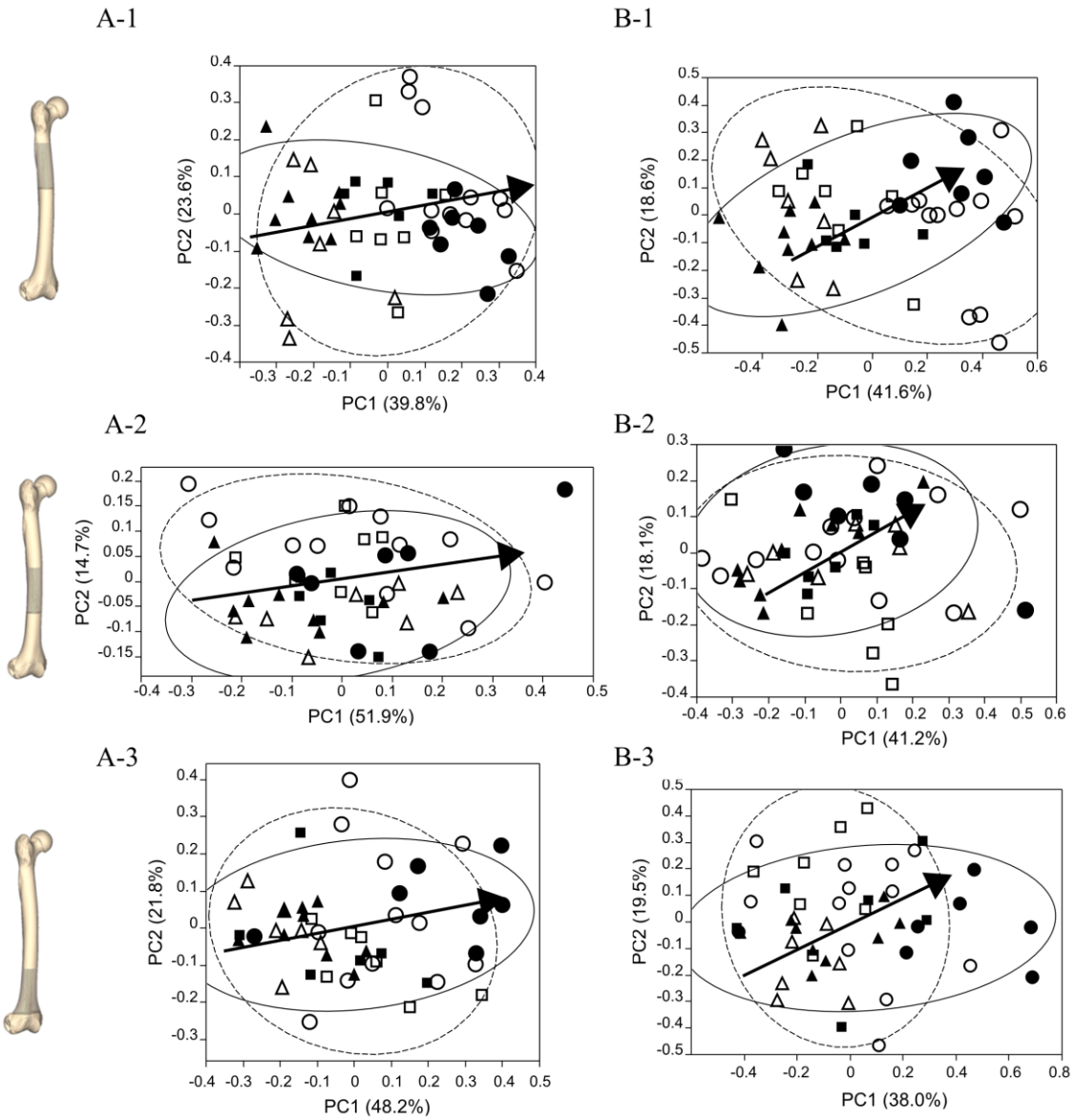

Fig. S2 PC graphs of GM analyses of diaphyseal subregions (symbols as in Fig. 3). GM analyses for external surface (A-1,B-1,C-1), and external plus internal surface (A-2,B-2,C-2) do not distinguish wild and captive groups (p>0.05).

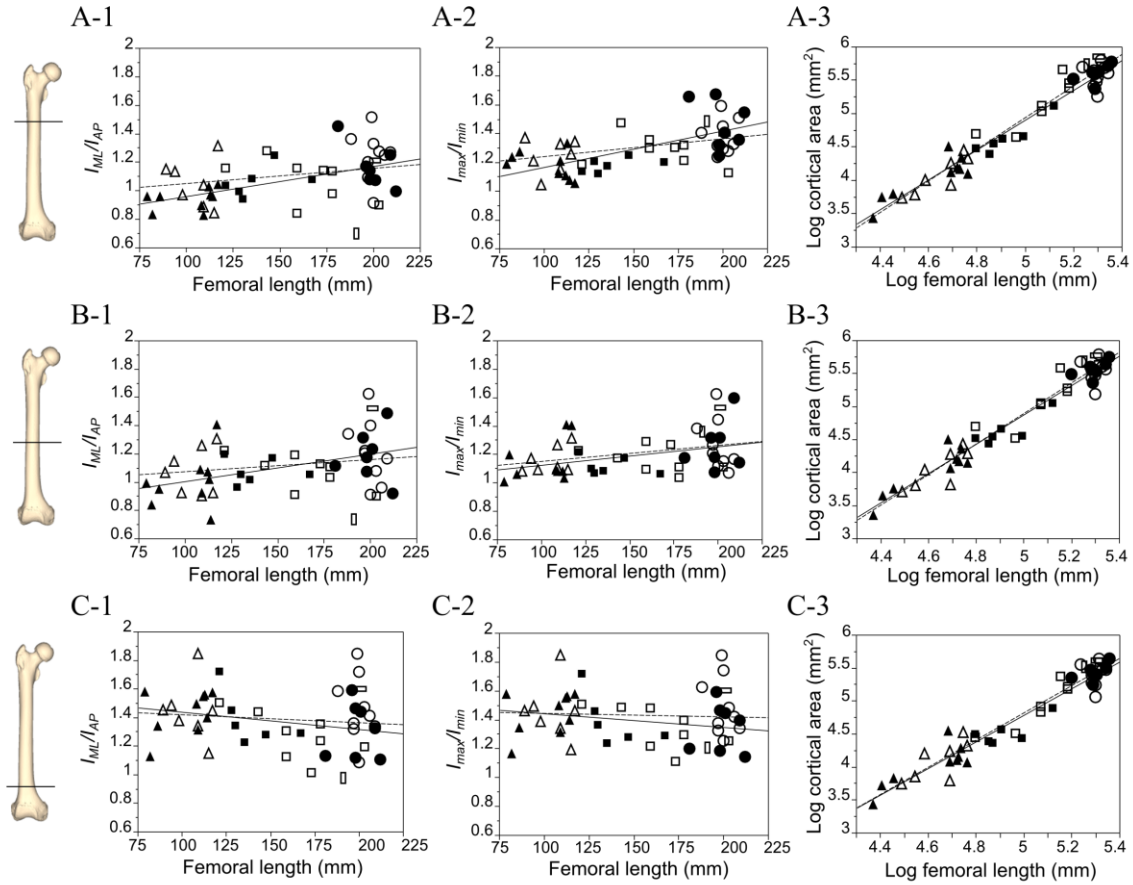

Fig. S3 Graphs of conventional cross-sectional analyses of diaphyseal subregions. Cross-sectional analyses were performed for the proximal, middle and distal shaft (at 17%, 50% and 83% of total diaphyseal length, respectively), using the ratio of mediolateral versus anteroposterior second moments of area (I_{ML}/I_{AP} corresponding to I_x/I_y of earlier analyses: A-1,B-1,C-1; the ratio of maximum/minimum second moments of area (I_{max}/I_{min}) (A-2,B-2,C-2); cortical bone area (A-3,B-3,C-3). These analyses confirm ontogenetic changes seen in corresponding MMs (Figs. 5, 6); for example, I_{max}/I_{min} increases in the proximal and midshaft, but remains constant in the distal shaft (p=0.003, 0.02 and 0.23 for least-squares regression, respectively). However, differences in the distal diaphyses between captive and wild groups cannot be detected with these methods (Table 1).

Chapter 2 Femoral morphology and femoropelvic musculoskeletal anatomy of humans and great apes: a comparative virtopsy study

Reference: *Anatomical Record* 294:1433-1445.

Abstract

The proximal femoral morphology of fossil hominins is routinely interpreted in terms of muscular topography and associated locomotor modes. However, the detailed correspondence between hard and soft tissue structures in the proximal femoral region of extant great apes is relatively unknown, because dissection protocols typically do not comprise in-depth osteological descriptions. Here we use computed tomography and virtopsy (virtual dissection) for non-invasive examination of the femoropelvic musculoskeletal anatomy in *Pan troglodytes*, *P. paniscus*, *Gorilla gorilla*, *Pongo pygmaeus*, and *Homo sapiens*. Specifically, we analyze the topographic relationship between muscle attachment sites and surface structures of the proximal femoral shaft such as the lateral spiral pilaster. Our results show that the origin of the *vastus lateralis* muscle is anterior to the insertion of *gluteus maximus* in all examined great ape specimens and humans. In gorillas and orangutans, the insertion of *gluteus maximus* is on the inferior (anterolateral) side of the lateral spiral pilaster. In chimpanzees, however, the *maximus* insertion is on its superior (posteromedial) side, similar to the situation in modern humans. These findings support the hypothesis that chimpanzees and humans exhibit a shared-derived musculoskeletal topography of the proximal femoral region, irrespective of their different locomotor modes, while gorillas and orangutans represent the primitive condition. Caution is thus warranted when inferring locomotor behavior from the surface topography of the proximal femur of fossil hominins, as the morphology of this region may contain a strong phyletic signal that tends to blur locomotor adaptation.

Keywords: virtual dissection, comparative anatomy, femoropelvic musculoskeletal anatomy, primates

Introduction

Humans are distinct from great apes in various aspects of musculoskeletal structure and organization of the femoropelvic region. Human-specific features such as an elongated femoral neck, a low position of the greater trochanter, a large bicondylar angle, a more sagittally oriented and wide ilium, and a craniocaudally shortened pelvis all indicate adaptation for bipedality because these features confer mechanical advantage for body stabilization and propulsion during bipedal locomotion (Preuschoft, 1970; Sigmon, 1974; Aiello and Dean, 1990; Lovejoy et al., 2002). Also, humans are distinct from great apes in the relative size and function of locomotor muscles. Humans have a large *gluteus maximus* (GM) relative to body mass, and large quadriceps relative to hamstring muscles (Stern, 1972; Lovejoy et al., 2002; Lieberman et al., 2006).

To study taxon-specific differences in musculoskeletal relationships, it is useful to distinguish between muscular allocation and topography. Allocation is used here to denote relative mass (strength) of muscle groups, while topography is used to denote the position and orientation of muscle origins and insertions, and the course of each muscle. The human muscular allocation pattern is thought to stabilize the hip and knee joints during bipedal locomotion (Stern and Susman, 1981), and the large human GM was recently suggested to be an adaptation for long-distance running rather than walking (Lieberman et al., 2006). On the other hand, human musculoskeletal topography, compared to the great apes, is characterized by a more posterior insertion of GM on the proximal femur, reflecting the evolutionary shift from gluteal involvement in femoral abduction to extension.

It is the human-specific *combination* of muscular allocation (*i.e.*, enlarged GM and quadriceps muscles) and topography (*i.e.*, more posteriorly situated GM) that is relevant for human extended-hip/knee bipedality. However, it is unknown whether changes of muscular topography and allocation occured in concert or independently during hominin evolution. To address this question, the proximal femoral region is of special relevance. Its morphology reflects muscular topography, and it is thought to be characteristic for great ape versus hominin modes of locomotion (Lovejoy et al., 2002; Lovejoy et al., 2009d). Comparative anatomical studies (Hepburn, 1892; Beddard, 1893; Raven, 1950; Crass, 1952; Uhlmann, 1968; Stern, 1972; Sigmon, 1974; Swindler and Wood, 1982) indicate a principal difference between human and great ape topographies, especially regarding the femoral attachment sites of the GM and *vastus lateralis* (VL) muscles. In all the great apes, GM consists of two portions. The proximal portion (GM *proprius*, GMp) originates from the sacroiliac region and blends into the proximal part of the VL aponeurosis (a part of the iliotibial tract, IT), while the distal portion (GM *ischiofemoralis*, GMi) originates from the ischial tuberosity and inserts directly along the lateral side of the distal femur, as well as into the distal portion of the IT (Stern, 1972; Aiello and Dean, 1990). Further, the GM insertion extends along the femoral diaphysis in great apes (Champneys, 1871; Hepburn, 1892; Beddard, 1893; Primrose, 1898; Raven, 1950; Crass, 1952; Uhlmann, 1968; Stern, 1972; Sigmon, 1974; Swindler and Wood, 1982). Humans lack a GMi, while the GMp is greatly increased in size and inserts directly along the proximal femoral shaft [gluteal tuberosity, third trochanter, and/or hypotrochanteric fossa (Hrdlička, 1934)], as well as into the IT (Stern, 1972).

According to Lovejoy and coauthors (Lovejoy et al., 2002; Lovejoy et al., 2009d), these differences between human and great ape muscular topography are reflected in femoral surface topography as follows:

> "The African ape posterolateral femoral shaft regularly exhibits a distomedially displaced insertion for the maximus. This is separated from a more superior attachment of the vastus lateralis [to whose tendon, however, the maximus is normally fused (Stern, 1972)] by an elevated boss on the shaft [defined as the lateral spiral pilaster (Lovejoy et al., 2002)]." (cited from Lovejoy et al., 2009d)

> "If the human specimen *also* exhibits a pilaster, the hypotrochanteric fossa lies *posteromedial* to it (the pilaster is normally the maximus insertion's anterolateral border). The ape condition contrasts starkly with this conformation. In the African pongids, the maximus insertion lies *anterior* and *inferolateral* to the spiral pilaster (which is essentially the opposite condition: the ape spiral pilaster serves as the superomedial border of the maximus insertion)." (cited from Lovejoy et al., 2002)

Among the features characterizing the surface topography of the proximal femur, the lateral spiral pilaster (LSP) is of special interest here, because it is thought to represent a reference structure for the localization of attachment sites of GM and VL in great apes versus humans with potentially important implications for locomotor function. To sum up, chimpanzee and gorilla musculoskeletal topography of GM, VL and LSP is currently recognized as follows (Lovejoy et al., 2002) (Fig. 1C)

a) LSP separates GM and VL attachment sites
b) GM insertion is distal and inferior (anterolateral) to LSP
c) VL origin is proximal and superior (posteromedial) to LSP, and extends along the femoral diaphysis in inferomedial direction, from the trochanteric origin to the superomedial border of LSP, where it blends with insertion of *adductor brevis* (Ab).

The femoropelvic musculoskeletal topography of humans has been described to differ in several respects from that of the great apes. The human proximal femoral surface exhibits a lateral pilaster (LP), which is seen as an analogous rather than homologous structure of the great ape LSP (Lovejoy et al., 2002; p. 105). The LP is situated *anterolaterally* to the gluteal tuberosity, third trochanter, and/or hypotrochanteric fossa (Hrdlička, 1934), and is oriented more vertically than the LSP. From an osteological perspective, it should be noted that the LP is visually less conspicuous than these latter structures, and this is probably why the LP does not appear in standard anatomy textbooks (e.g., Netter, 2003; Standring, 2004). However, it is a consistent structure which can readily be identified once its characteristic morphology has been recognized. As a reference structure for muscle attachment sites, the human LP forms the anterolateral border of the GM insertion (Lovejoy et al., 2002; Pickford et al., 2002). Thus, it is currently held that, due to the opposite position of GM insertion relative to L(S)P (Lovejoy et al., 2002), humans and great apes have opposite topographies of GM, VL and L(S)P. In other words, when proceeding from the posterior to the lateral side of the proximal femur, the sequence of structures is **GM**-LP-**VL** in humans, while it is **VL**-LSP-**GM** in great apes (Fig. 1C).

Various dissection-based comparative studies of great ape muscular topography provide drawings or photographs of long bones with inscribed areas of muscular attachment (Hepburn, 1892; Beddard, 1893; Boyer, 1935; Raven, 1950; Crass, 1952; Uhlmann, 1968; Stern, 1972; Sigmon, 1974; Swindler and Wood, 1982; Aiello and Dean, 1990). A detailed reading of these sources reveals, however, that there is no full correspondence between written and pictorial specifications of areas of muscular attachment, and/or that important morphological features of the proximal femoral shaft (such as LSP) and their relation to muscular topography are not considered explicitly. For example, Raven (1950) shows a detailed drawing of a gorilla femur and corresponding muscle attachment areas on the femur, and one can confirm that GM and VL attach along the lateral femoral diaphysis. However, the LSP is not explicitly depicted in these drawings such that the topographic relationship of GM and VL relative to LSP remains unclear. Overall, thus, direct information on the relationship between muscular topography and femoral surface topography for one and the same individual is typically not available from these sources, with the exception of Uhlmann (1968).

Musculoskeletal anatomy has traditionally been studied through physical dissection. However, this method of preparation has several limitations. First, full-body cadavers of great apes are relatively rare and of particular value, such that application of invasive methods is often not possible. Second, during dissection, it is often difficult to observe the skeletal (subperiosteal) morphology and the intact soft tissues of interest simultaneously, especially when bones are surrounded by strong muscles and ligamentous structures.

Virtual dissection, or "virtopsy" (from virtual autopsy) (Thali et al., 2007; Thali et al., 2009), has been proposed as a means to effectively visualize complex anatomical organization with 3D structures fully retained. The method has been successfully applied to perform non-invasive forensic and osteological analyses (Grabherr et al., 2009). Here, we use virtopsy for the simultaneous but non-invasive observation of soft- and hard-tissue structures in great ape cadavers.

This paper has two aims. The methodological aim is to demonstrate the potential of virtopsy as an alternative or complementary method to physical dissection of whole-body great ape specimens. This approach also provides a new perspective on how wet specimens in primate collections worldwide can be analyzed without sacrificing them. The anatomical aim is to use virtopsy to establish direct correspondence between femoral surface topography and muscular topography in great ape specimens. This permits to address various open questions regarding the musculoskeletal organization of the femoropelvic region. Specifically, we investigate the topography of *gluteus maximus* (GM), *vastus lateralis* (VL) and the position of their attachment sites relative to the lateral (spiral) pilaster of human, chimpanzee, gorilla, and orangutan femora. We test Lovejoy et al.'s hypothesis that humans (and fossil hominins) are distinct from all great apes in proximal femoral muscular topography and allocation. We then ask whether evolutionary changes of muscular topography and of muscular allocation in the femoropelvic region occurred simultaneously or independently during hominoid and hominin evolution. If changes in topography and allocation occurred simultaneously, this would provide evidence for a close functional coupling between muscular topography, allocation and locomotor behavior.

Materials and methods

Sample

Eight specimens of formalin-fixed/frozen cadavers of great apes (*Pan troglodytes*, *P. paniscus*, *Gorilla gorilla* and *Pongo pygmaeus*) were obtained from the collections of the Anthropological Institute and Museum of the University of Zurich (AIMUZ), the Primate Research Institute of Kyoto University (KUPRI), Kyoto City Zoo (KCZ) and Takaoka Kojo Park Zoo (TKZ) (Table 1). The CT data sets of two adult chimpanzees (KCZ-Yoko and KUPRI-9262 [TKZ-Rick]; CT data *id*: PRICT-34/218 and PRICT-320 respectively) were obtained from the Digital Morphology Museum of KUPRI (http://www.pri.kyoto-u.ac.jp/dmm/WebGallery/index.html). Comparative clinical data of living humans were from anonymized patient CT data sets publicly available on www.osirixviewer.com.

Volumetric data acquisition

Full-body volume data of great ape specimens from the AIMUZ collection were acquired using a Siemens 64-detector-array CT device with the following image reconstruction parameters: beam collimation: 1.0mm; pitch: 0.5-0.75, image reconstruction kernel: standard (B30s) and bone (B60s); slice increment: 0.2 to 0.5mm. This resulted in isotropic voxel sizes in the range of 0.2mm (neonatal and juvenile specimens) to 0.5mm (adult specimens). The adult chimpanzees from KUPRI and KCZ (KCZ-Yoko and KUPRI-9262) were scanned using a Toshiba 4-detector-array CT device with the following parameters: beam collimation: 1.0mm; slice increment: 0.8mm; image reconstruction kernel: standard and bone (FC03/FC30). This resulted in isotropic voxel size of 0.8mm.

Volume data visualization and virtopsy

Great ape and human CT data sets were processed with medical imaging software [open-source software Osirix (www.osirix-viewer.com), and Amira 4.1 (Mercury Systems, Inc.)]. Osirix was used for interactive volume visualization and manipulation, permitting X-ray density-based rendering of muscular versus bone tissue, and successive removal of outer muscle layers to visualize the deep musculature. Volume data visualization based on different X-ray densities corresponds to the workflow of physical preparation of a cadaver (Fig. 2). The software package Amira provides tools for CT-slice-based volume data segmentation, which facilitates identification of the course of single muscles and tendineous structures. Using these software tools, it is possible to establish direct links between muscular architecture, areas of muscular attachment, and femoral morphology. They also permit to visualize the subperiosteal surface topography of the femur using false-color-based mapping of its local surface curvature.

Results

The results of virtopsy are shown in Figs. 2 to 6. Virtopsy-based analysis of the human CT data set (Fig. 3A) shows musculoskeletal structures representing the well-known standard anatomy of humans (Netter, 2003; Standring, 2004). Individual muscles are clearly separated from each other, and it is possible to follow the course of each muscle while simultaneously observing the associated skeletal

morphology. This demonstrates the efficacy of virtopsy as a method of topographic anatomical analysis. Virtopsy was then applied to great ape cadavers representing different preservation conditions (frozen, formalin/alcohol/glycerine mixtures) and different age classes (birth to adulthood). Our analyses indicate that the results of virtopsy are fairly independent of methods of preservation.

As revealed by virtopsy, the musculoskeletal topography of great apes differs in several respects from the currently recognized picture (Figs. 3-6). In all great apes (as well as in humans), the origin of the VL is situated superoanteriorly relative to the insertion of GM. Furthermore, in all *Pan* specimens examined here the GM inserts on the superomedial side of the LSP, while the VL originates at its inferolateral border (Figs. 3B, 4, 5, 6). Although the LSP is less developed in immature compared to adult chimpanzees (Figs. 3B, 4D, 5; Fig. 4A,B,C, 6), this distinctive pattern of musculoskeletal topography is independent of individual age (Figs. 3B, 4, 5, 6). The LSP of chimpanzees serves as an area of insertion for the lateral intermuscular septum (LIM) of the iliotibial tract (IT; Figs. 5, 6), and thus separates the area of attachment of the GM (posteromedial) from that of the VL (anterolateral). Similar to the situation in chimpanzees, the human LP serves as an area of insertion for the proximalmost portion of the LIM, thus separating the areas of attachment of the GM and VL (Fig. 3A).

Contrasting with *Pan* and *Homo*, in all *Gorilla* and *Pongo* specimens examined here, the GM area of insertion is along the inferolateral border of the LSP, as described by Lovejoy and coauthors (Lovejoy et al., 2002; Lovejoy et al., 2009d). Hence, in gorillas and orangutans the LSP does *not* separate the areas of attachment of GM and VL, contrary to the situation in chimpanzees and humans. Accordingly, when proceeding from the posterior to the lateral side of the proximal femur of chimpanzees, the sequence of structures is GM-LSP-VL (as in humans), *not* LSP-GM-VL (as in gorillas and orangutans).

Fig. 6A shows a cross-section at the middle of LSP to illustrate the muscular topography and the corresponding morphology of the proximal femur in adult chimpanzees (KCZ-Yoko). These specimens exhibit a well-developed LSP situated between two fossae on its inferolateral and superomedial sides, respectively (Lovejoy et al., 2002). The inferolateral fossa (which typically appears as a rugose shallow depression on osteological specimens) serves as an area of attachment of VL and, in some specimens, also of the intermuscular septum (Fig. 6A, S1), while GM inserts on the *posteromedial* side of the LSP. Fig. 6B shows a cross-section immediately below lesser trochanter to illustrate the muscle attachment at the superomedial fossa in an adult chimpanzee (KCZ-Yoko). The fossa on the superomedial side of the LSP serves as an area of attachment of *adductor brevis* (Ab). The Ab, VL and GM areas of attachment are separated from each other at this level. The Ab appears to be a thin and relatively weak muscle though the superomedial fossa is well expressed in this adult chimpanzee specimen.

Superimposition of the information about muscular topography gathered during virtopsy onto corresponding 3D representations of femora (Figs. 3-6) results in Fig. 1D, which provides a comparative picture of musculoskeletal topography of the proximal femoral region in humans, chimpanzees, gorillas and orangutans.

In all human and chimpanzee individuals examined here, the vastus group is expanded compared to gorillas and orangutans, yielding a posteriorly extended area of attachment of the lateral and medial vastus muscles (Figs. 3A,B, 4). This is best seen in Fig. 4A (adult chimpanzee), where the VL attachment area is expanded toward the posterior diaphysis. Expansion of the VL area is correlated with a more posteriorly oriented insertion of *gluteus maximus*, and confinement of the

attachment areas of the adductors, *biceps femoris*, and *gluteus maximus* to a narrow strip along the femoral diaphysis (Fig. 4A). Thus, the pattern of muscular topography described here is not restricted to the proximal femur, but extends along the entire length of the femoral diaphysis.

Discussion

Virtopsy reveals patterns of muscular topography of *gluteus maximus*, *vastus lateralis*, *biceps femoris* and *adductor brevis* around proximal femur in humans and great apes which are consistent with those described in the literature (Champneys, 1871; Hepburn, 1892; Beddard, 1893; Primrose, 1898; Boyer, 1935; Raven, 1950; Crass, 1952; Uhlmann, 1968; Stern, 1972; Sigmon, 1974; Swindler and Wood, 1982). We could not, however, verify earlier reports regarding the correspondence between muscular structure and femoral surface topography (Lovejoy et al., 2002). Our results can be summarized as follows:

a) In all great apes and in humans, the origin of the VL is situated superoanteriorly relative to the GM.
b) In gorillas and orangutans, the LSP does *not* separate the areas of attachment of GM and VL, which are both situated on its anterolateral side.
c) In humans and chimpanzees, the L(S)P separates the areas of attachment of GM and VL.
d) When proceeding from the posterior to the lateral side of the proximal femur, the sequence of structures encountered is GM-**L(S)P**-VL in humans and chimpanzees, *versus* **LSP**-GM-VL in gorillas and orangutans.

The key finding of this study is that the musculoskeletal topography of the proximal femur of *Pan* deviates from that of *Gorilla/Pongo* and is similar to that of modern humans. Before any inferences can be drawn regarding the evolutionary and functional significance of this difference, its significance in terms of anatomical variability must be assessed, especially with regard to possible overlap between *Pan* and *Gorilla*/*Pongo* musculoskeletal topographies. Anatomical features such as the LSP and LP exhibit variable degrees of prominence among each species; also, muscular attachment sites exhibit variability in terms of location and surface area. Nevertheless, our data indicate that the topographic differences between *Pan* and *Gorilla*/*Pongo* are consistent:

- Patterns of muscular topography are similar in all *Pan* specimens examined here (Figs. 3B, 4, 5, 6), independent of individual age. Also, the muscular topography of the neonate orangutan of Fig. 3D is consistent with data published for orangutans of later age classes (Beddard, 1893; Primrose, 1898; Boyer, 1935; Sigmon, 1974), and the topography of the juvenile gorilla of Fig. 3C is consistent with data on juvenile (Sigmon, 1974) and adult gorillas published earlier (Raven, 1950). This indicates that the basic pattern of muscular topography is already present at a young age and does not change substantially during ontogeny. It is thus sensible to assume that the principal topographic relationships between

muscle attachment sites and femoral subperiosteal surface features are genetically determined and remain constant during species-specific ontogenies.

- In all specimens examined here, attachment sites of a given muscle are confined either to the superomedial or to the inferolateral side of the LSP, such that the LSP acts as a clear topographic divide. This indicates that the topography of GM and VL attachment sites relative to LSP represents a discrete trait, which exhibits two states: GM-LSP-VL *versus* LSP-GM-VL. The presence of the GM-LSP-VL state in all of the N=6 chimpanzees studied here (earlier studies are based on samples of $N \leq 3$) makes it highly likely that this is the standard anatomy in chimpanzees.
- In the chimpanzee specimens examined here, the GM insertion is situated more posteriorly (Figs. 3B,4,5,6) compared to gorilla and orangutan (Fig. 3C,D). This topographic difference extends along the entire length of the femoral diaphysis. In chimpanzees, VL and GM attach along a line on the posterolateral to posterior side of the diaphysis (Fig. 7A), while in gorillas and orangutans, VL and GM attach on the lateral side of the diaphysis (Fig. 7B,C). Examination of muscular attachment sites in osteological specimens (N=22 *Pan t. troglodytes*; N=20 *Gorilla g. gorilla*; N=15 *Pongo pygmaeus*) confirmed these differences between *Pan* and *Gorilla*/*Pongo*.

The similarity between human and chimpanzee femoropelvic musculoskeletal organization revealed in this study is in parallel with reported similarities of various soft tissue structures, which reflect the close phylogenetic relationship between these taxa (Gibbs et al., 2000, 2002). Considering that humans and chimpanzees exhibit substantially different locomotor modes, while chimpanzees and gorillas exhibit similar locomotor modes (knuckle-walking), our findings have several implications regarding the correlation of structure and function in the locomotor system.

Three hypotheses are proposed about the evolutionary history of femoropelvic musculoskeletal topography. The first hypothesis (H1) is that humans and chimpanzees exhibit the primitive state, while gorillas and orangutans exhibit derived states. This would imply that gorillas and orangutans reached similar femoropelvic musculoskeletal topographies via convergent evolution. Hypotheses H2 and H3 state that gorillas and orangutans represent the primitive state, while humans and chimpanzees are derived. H2 postulates that humans and chimpanzees each show a derived state, which would imply that human-chimp topographic similarities evolved independently and in parallel. H3 postulates that the human-chimpanzee topography represents a shared-derived trait, which would imply that similarities reflect the musculoskeletal topography of their last common ancestor (HC-LCA).

Among the three hypotheses, H1 and H2 are less parsimonious than H3. H1 would imply similar selective pressures acting on the locomotor system of *Pongo* and *Gorilla*, which, given their substantially different locomotor modes (obligate terrestrial versus arboreal locomotion), is unlikely. Similar arguments apply to H2. This hypothesis would imply equivalent selective pressures on human and chimpanzee locomotor systems, which is unlikely given their substantially different locomotor behaviors (habitual bipedality versus terrestrial/arboreal quadrupedality). These arguments do not

dismiss the important role of evolutionary convergence/parallelism. For example, convergent evolutionary trends have been reported for the wrist bone morphology of *Pan* and *Gorilla* (Kivell and Schmitt, 2009), but these trends are clearly associated with convergent locomotor behavior (knuckle-walking). Accordingly, convergent evolution of femoral morphology in groups exhibiting substantially different locomotor modes would be difficult to explain. We thus conclude that the evolutionary scenario suggested by H3 is the most likely one.

The notion of shared-derived femoropelvic features in humans and chimpanzees permits various evolutionary and functional inferences, but also raises further questions. For example, retention of the (inferred) HC-LCA topography in modern humans and chimpanzees, which exhibit highly divergent locomotor behaviors, indicates that these features reflect phyletic history rather than actual locomotor adaptations. Accordingly, osteologic features which are thought to be of special functional relevance for locomotor implications (Lovejoy et al., 2002; Lovejoy et al., 2009d) may have higher relevance for phyletic implications. Hypothesis 3 implies that the evolutionary modification of the GM-LSP topography in the human-chimpanzee clade occurred independent of, and prior to, the modification of muscle allocation patterns, because chimpanzees exhibit derived topography but primitive allocation patterns. Currently we can only speculate about the adaptive context and functional significance of this topographic shift. It might be indicative of an adaptive shift in locomotor behavior of the HC-LCA, which later (*i.e.*, during hominin evolution) gave rise to substantial changes in muscular allocation patterns.

Also, the functional significance of the actual human/chimpanzee versus gorilla/orangutan types of femoropelvic muscular topography remains to be elucidated, and such an endeavor has to face the challenge of dealing with highly divergent locomotor behaviors within each of these groups. One hypothesis that needs to be tested in greater detail in this context is that locomotor kinetics/kinematics differ substantially between chimpanzees and gorillas, especially in the way of how hindlimb movements result in body propulsion during locomotion (Stern and Susman, 1981; Raichlen et al., 2008; Young, 2009).

As mentioned, our results indicate that the LSP serves as a divide of muscular attachment areas. The hypothesized evolutionary shift of the GM attachment area across the LSP seems subtle but it may result in significant modification of principal directions of muscle force: insertion of GM on the anterior versus posterior sides of the LSP would imply more abduction versus more extension of the femur in the hip joint, respectively.

This hypothesis receives support from a preliminary comparative analysis of the femoral epiphyseal morphologies of chimpanzees and gorillas (Fig. 8). The surface of the greater trochanter reflects the course of GM, as it works as a pulley via the synovial bursa between greater trochanter and GM. In chimpanzees, this surface is oriented more posteriorly than in gorillas (Fig. 8C), in concert with the more posterior orientation of GM (note that part of the GM is situated posterior to greater trochanter in chimpanzees even when the femur is almost fully flexed; Figs. 4B, 6).

Our results also have implications for the interpretation of the LSP in fossil hominin femora. The LSP was originally described as a functionally and phyletically relevant character, which is present only in the great apes (Lovejoy et al., 2002). This view, however, was revised considering the *Ardipithecus* skeleton (Lovejoy et al., 2009d). Together with the evidence from *Ardipithecus*, the findings presented here lead to two alternative hypotheses about the relationship between the great ape LSP and the human LP. Hypothesis 1 postulates that the chimpanzee-hominin L(S)P and the

associated reorganization of muscular attachment are derived features of the HC-LCA. Hypothesis 2 postulates that the L(S)P is a primitive feature of all hominoids, while the HC clade is characterized by an evolutionary shift of muscular attachment sites relative to L(S)P.

Judging from the published photographs of the proximal femoral surface of *Orrorin* (Pickford et al., 2002) and *Ardipithecus* (Lovejoy et al., 2009d), it appears that characteristic rugose areas (as shown in Fig. 1) are situated laterally in both *Orrorin* and *Ardipithecus*. The topographic evidence provided here shows that three different interpretations of this area in terms of muscular attachment must be considered: 1) the area might represent the insertion of GM, which would imply closer affinities with gorilla than with the hypothetical HC-LCA; 2) it might represent the origin of VL, which would imply close affinities with the HC-LCA; 3) it might represent the hypotrochanteric fossa with blends into the third trochanter, as Lovejoy and coauthors (2009b) suggest. The currently available evidence does not permit to decide what was the case in these species, but if the topography of GM and VL attachment areas on the femur can be shown to have a functional significance, our understanding of the early evolutionary history of bipedality would be improved significantly.

Our results further indicate that currently recognized similarities of femoral morphology in chimpanzees and gorillas such as LSP and femoral epiphyseal/diaphyseal morphologies (Lovejoy et al., 2002; Ruff, 2002; Richmond and Jungers, 2008) are likely to be the consequence of convergent evolution. Caution is thus warranted when interpreting the surface topography of the proximal femur of fossil hominins in terms of locomotor function, because the HC clade exhibits a musculoskeletal topography, which represents a phyletically derived state rather than adaptation to specific locomotor functions.

Conclusion

We used virtopsy (virtual dissection) to establish direct correspondence between proximal femoral surface topography and muscular topography in *Pan troglodytes*, *P. paniscus*, *Gorilla gorilla*, *Pongo pygmaeus*, and *H. sapiens*. Our results support the hypothesis that humans and chimpanzees (HC) exhibit a shared-derived musculoskeletal topography of the proximal femoral region, while gorillas and orangutans (GO) represent the primitive condition. In HC, the lateral (spiral) pilaster (LSP) separates the areas of attachment of the *gluteus maximus* (posterior) and *vastus lateralis* (anterior), whereas in GO, attachment sites of both muscles are on the anterolateral side of the LSP. It appears from this study that the specific musculoskeletal topography of the proximal femur reflects phyletic relationships rather than adaptation to taxon-specific locomotor modes. Differences between HC and GO topographies add evidence to the hypothesis that knuckle walking in chimpanzees and gorillas has different evolutionary origins. On the other hand, the shared-derived HC topography represents divergent locomotor adaptations in H and C. Caution is thus warranted when interpreting fossil hominin proximal femoral surface topography in terms of locomotor adaptation.

This study also demonstrated that virtopsy is an optimal tool for the investigation of hominoid musculoskeletal anatomy because it permits to inspect the three-dimensional structure of hard and soft tissues simultaneously. Adopting the virtopsy approach to comparative primatology and anthropology holds great potential for further studies, because it permits in-depth analysis of valuable primate collection specimens without sacrificing them to physical dissection.

References

Aiello L, Dean C. 1990. An Introduction to Human Evolutionary Anatomy. London: Academic Press.

Alexander RM. 2004. Bipedal animals, and their differences from humans. J Anat 204:321-330.

Amtmann E, Schmitt H. 1968. Über die Verteilung der Corticalisdichte im menschlichen Femurschaft und ihre Bedeutung für die Bestimmung der Knochenfestigkeit. Zeit Anat Entwick 127:25–41.

Bass S, Saxon L, Daly R, Turner C, Robling A, Seeman E, Stuckey S. 2002. Effect of mechanical loading on the size and shape of bone in pre-, peri-, and postpubertal girls: a study in tennis players. J Bone Miner Res 17:2274-2280.

Bass SL, Eser P, Daly R. 2005. The effect of exercise and nutrition on the mechanostat. J Musculoskelet Neuronal Interact 5:239-254.

Beddard F. 1893. Contributions to the anatomy of the anthropoid apes. Trans Zool Soc London 13:177-218.

Benazet JD, Zeller R. 2009. Vertebrate limb development: moving from classical morphogen gradients to an integrated 4-dimensional patterning system. Cold Spring Harbor Perspectives in Biology 1.

Benjamin M, Kumai T, Milz S, Boszczyk BM, Boszczyk AA, Ralphs JR. 2002. The skeletal attachment of tendons - tendon 'entheses'. Comparative Biochemistry and Physiology a-Molecular and Integrative Physiology 133:931-945.

Bennett MR, Harris JWK, Richmond BG, Braun DR, Mbua E, Kiura P, Olago D, Kibunjia M, Omuombo C, Behrensmeyer AK, Huddart D, Gonzalez S. 2009. Early hominin foot morphology based on 1.5-million-year-old footprints from Ileret, Kenya. Science 323:1197-1201.

Bertram JEA, Swartz SM. 1991. The law of bone transformation - a case of crying Wolff. Biol Rev Camb Philos Soc 66:245-273.

Boehm B, Westerberg H, Lesnicar-Pucko G, Raja S, Rautschka M, Cotterell J, Swoger J, Sharpe J. 2010. The role of spatially controlled cell proliferation in limb bud morphogenesis. PLoS Biol 8:e1000420.

Bondioli L, Bayle P, Dean C, Mazurier A, Puymerail L, Ruff C, Stock J, T. , Volpato V, Zanolli C, Macchiarelli R. 2010. Technical note: Morphometric maps of long bone shafts and dental roots for imaging topographic thickness variation. Am J Phys Anthropol 142:328-334.

Bookstein F. 1991. Morphometric Tools for Landmark Data: Geometry and Biology. Cambridge: Camnridge University Press.

Boyer E. 1935. The musculature of the inferior extremity of the orang-utan *Simia satyrus*. Am J Anat 56:192-256.

Bramble DM, Lieberman DE. 2004. Endurance running and the evolution of *Homo*. Nature 432:345-352.

Brunet M, Guy F, Pilbeam D, Mackaye HT, Likius A, Ahounta D, Beauvilain A, Blondel C, Bocherens H, Boisserie JR, De Bonis L, Coppens Y, Dejax J, Denys C, Duringer P, Eisenmann VR, Fanone G, Fronty P, Geraads D, Lehmann T, Lihoreau F, Louchart A, Mahamat A, Merceron G, Mouchelin G, Otero O, Campomanes PP, De Leon MP, Rage JC, Sapanet M, Schuster M, Sudre J, Tassy P, Valentin X, Vignaud P, Viriot L, Zazzo A, Zollikofer C. 2002. A new hominid from the Upper Miocene of Chad, central Africa. Nature 418:145-151.

Burr DB, Ruff CB, Johnson C. 1989. Structural adaptations of the femur and humerus to arboreal and terrestrial environments in 3 species of macaque. Am J Phys Anthropol 79:357-367.

Butterfield NC, McGlinn E, Wicking C. 2010. The molecular regulation of vertebrate limb patterning. In: Organogenesis in Development: Elsevier. p 319-341.

Cardoso FA, Henderson CY. 2010. Enthesopathy Formation in the Humerus: Data from Known Age-at-Death and Known Occupation Skeletal Collections. Am J Phys Anthropol 141:550-560.

Carlson K, Sumner D, Morbeck M, Nishida T, Yamanaka A, Boesch C. 2008a. Role of nonbehavioral factors in adjusting long bone siaphyseal atructure in free-ranging *Pan troglodytes*. Int J Primatol 29:1401-1420.

Carlson KJ. 2005. Investigating the form-function interface in African apes: Relationships between principal moments of area and positional behaviors in femoral and humeral diaphyses. Am J Phys Anthropol 127:312-334.

Carlson KJ, Doran-Sheehy DM, Hunt KD, Nishida T, Yamanaka A, Boesch C. 2006. Locomotor behavior and long bone morphology in individual free-ranging chimpanzees. J Hum Evol 50:394-404.

Carlson KJ, Judex S. 2007. Increased non-linear locomotion alters diaphyseal bone shape. J Exp Biol 210:3117-3125.

Carlson KJ, Lublinsky S, Judex S. 2008b. Do different locomotor modes during growth modulate trabecular architecture in the murine hind limb? Integr Comp Biol 48:385-393.

Carrier DR. 1996. Ontogenetic limits on locomotor performance. Physiol Zool 69:467-488.

Carrier DR, Anders C, Schilling N. 2011. The musculoskeletal system of humans is not tuned to maximize the economy of locomotion. Proc Natl Acad Sci U S A 108:18631-18636.

Carter GJ, editor. 1990. Skeletal biomineralization: patterns, processes, and evolutionary trends. New York: Van Nostrand Reinhold.

Cavagna GA, Heglund NC, Taylor CR. 1977. Mechanical work in terrestrial locomotion: two basic mechanisms for minimizing energy expenditure. Am J Physiol 233:R243-261.

Champneys F. 1871. On the muscles and nerves of a chimpanzee (*Troglodytes niger*) and a *Cynocepalus anubis*. J Anat Lond 6:176-211.

Cobb SN, O'Higgins P. 2007. The ontogeny of sexual dimorphism in the facial skeleton of the African apes. J Hum Evol 53:176-190.

Cowgill LW. 2007. Humeral torsion revisited: A functional and ontogenetic model for populational variation. Am J Phys Anthropol 134:472-480.

Crass E. 1952. Musculature of the hip and thigh of the chimpanzee : a comparison to man and other primates. PhD thesis, Univ Wisconsin.

Crompton RH, Vereecke EE, Thorpe SKS. 2008. Locomotion and posture from the common hominoid ancestor to fully modern hominins, with special reference to the last common panin/hominin ancestor. J Anat 212:501-543.

Demes B. 2007. In vivo bone strain and bone functional adaptation. Am J Phys Anthropol 133:717-722.

Demes B, Carlson KJ. 2009. Locomotor variation and bending regimes of capuchin limb bones. Am J Phys Anthropol 139:558-571.

Demes B, Jungers WL. 1993. Long-bone cross-sectional dimensions, locomotor adaptations and body-size in prosimian primates. J Hum Evol 25:57-74.

Demes B, Larson SG, Stern JT, Jr, , Jungers WL, Biknevicius AR, Schmitt D. 1994. The kinetics of primate quadrupedalism: hindlimb drive reconsidered. J Hum Evol 26:353-374.

Demes B, Qin YX, Stern JT, Jr., Larson SG, Rubin CT. 2001. Patterns of strain in the macaque tibia during functional activity. Am J Phys Anthropol 116:257-265.

DeSilva JM. 2011. A shift toward birthing relatively large infants early in human evolution. Proc Natl Acad Sci USA 108:1022-1027.

Dillon R, Othmer HG. 1999. A mathematical model for outgrowth and spatial patterning of the vertebrate limb bud. J Theor Biol 197:295-330.

Diogo R, Wood B. 2011. Soft-tissue anatomy of the primates: phylogenetic analyses based on the muscles of the head, neck, pectoral region and upper limb, with notes on the evolution of these muscles. J Anat 219:273-359.

Doran DM. 1992. The ontogeny of chimpanzee and pygmy chimpanzee locomotor behavior - a case-study of paedomorphism and its behavioral-correlates. J Hum Evol 23:139-157.

Doran DM. 1993. Comparative locomotor behavior of chimpanzees and bonobos - the influence of morphology on locomotion. Am J Phys Anthropol 91:83-98.

Doran DM. 1996. Comparative positional behabior of the African apes. In: McGrew MC, Marchant LF, Nishida T, editors. Great Ape Societies. Cambridge: Cambridge University Press.

Doran DM. 1997. Ontogeny of locomotion in mountain gorillas and chimpanzees. J Hum Evol 32:323-344.

Doran DM, Jungers WL, Sugiyama Y, Fleagle J, Heesy C. 2002. Multivariate and phylogenetic approaches to understanding chimpanzee and bonobo behavioral diversity. In: Boesch C,

Hohmann G, Marchant LF, editors. Behavioural diversity in Chimpanzees and Bonobos. Cambridge: Cambridge University Press. p 14-34.
Drapeau MSM. 2008. Enthesis bilateral asymmetry in humans and African apes. Homo-Journal of Comparative Human Biology 59:93-109.
Elftman H. 1945. Torsion of the lower extremity. Am J Phys Anthropol-New Ser 3:255-265.
Felsenstein J. 1989. PHYLIP - Phylogeny Inference Package (Version 3.2). Cladistics 5:164-166.
Galik K, Senut B, Pickford M, Gommery D, Treil J, Kuperavage AJ, Eckhardt RB. 2004. External and internal morphology of the BAR 1002 ' 00 *Orrorin tugenensis* femur. Science 305:1450-1453.
Garland TJ, Rose MR. 2009. Experimental evolution: concepts, methods, and applications of selection experiments. Berkeley: University of California Press.
Gebo DL. 1992. Plantigrady and foot adaptation in African apes: Implications for hominid origins. Am J Phys Anthropol 89:29-58.
Gibbs S, Collard M, Wood B. 2000. Soft-tissue characters in higher primate phylogenetics. Proc Natl Acad Sci USA 97:11130-11132.
Gibbs S, Collard M, Wood B. 2002. Soft-tissue anatomy of the extant hominoids: a review and phylogenetic analysis. J Anat 200:3-49.
Gilbert CC, Rossie JB. 2007. Congruence of molecules and morphology using a narrow allometric approach. Proc Natl Acad Sci USA 104:11910-11914.
Goodall J. 1986. The Chimpanzees of Gombe. Cambridge: Harvard University Press.
Goodship AE, Lanyon LE, McFie H. 1979. Functional adaptation of bone to increased stress - experimental-study. Journal of Bone and Joint Surgery-American Volume 61:539-546.
Gould SJ, Lewontin RC. 1979. The spandrels of San Marco and the Panglossian paradigm: a critique of the adaptationist programme. Proc R Soc Lond, Ser B: Biol Sci 205:581-598.
Grabherr S, Cooper C, Ulrich-Bochsler S, Uldin T, Ross S, Oesterhelweg L, Bolliger S, Christe A, Schnyder P, Mangin P, Thali M. 2009. Estimation of sex and age of "virtual skeletons"–a feasibility study. Eur Radiol 19:419-429.
Griffin TM, Main RP, Farley CT. 2004. Biomechanics of quadrupedal walking: how do four-legged animals achieve inverted pendulum-like movements? J Exp Biol 207:3545-3558.
Groote ID, Lockwood AC, Aiello CL. 2010. Technical note: A new method for measuring long bone curvature using 3D landmarks and semi-landmarks. Am J Phys Anthropol 141:658-664.
Gunz P, Mitteroecker P, Bookstein FL. 2005. Semilandmarks in Three Dimensions. In: Slice DE, editor. Developments in Primatology: Progress and Prospects. New York: Springer.
Harmon EH. 2007. The shape of the hominoid proximal femur: a geometric morphometric analysis. J Anat 210:170-185.
Harmon EH. 2009. The shape of the early hominin proximal femur. Am J Phys Anthropol 139:154-171.
Harrison T. 2010. Apes among the tangled branches of human origins. Science 327:532-534.
Heinrich RE, Ruff CB, Adamczewski JZ. 1999. Ontogenetic changes in mineralization and bone geometry in the femur of muskoxen (Ovibos moschatus). J Zool 247:215-223.
Hepburn D. 1892. Comparative anatomy of the muscles and nerves of the superior and inferior extremities of the anthropoid apes: Part II. J Anat Physiol 26:324-356.
Hobolth A, Christensen OF, Mailund T, Schierup MH. 2007. Genomic relationships and speciation times of human, chimpanzee, and gorilla inferred from a coalescent hidden Markov model. PLoS Genet 3:294-304.
Högler W, Blimkie CJR, Cowell CT, Inglis D, Rauch F, Kemp AF, Wiebe P, Duncan CS, Farpour-Lambert N, Woodhead HJ. 2008. Sex-specific developmental changes in muscle size and bone geometry at the femoral shaft. Bone 42:982-989.
Holliday TW, Hutchinson VT, Morrow MMB, Livesay GA. 2010. Geometric morphometric analyses of hominid proximal femora: Taxonomic and phylogenetic considerations. Homo-Journal of Comparative Human Biology 61:3-15.
Holt BM. 2003. Mobility in Upper Paleolithic and Mesolithic Europe: Evidence from the lower limb. Am J Phys Anthropol 122:200-215.
Hrdlička A. 1934. The hypotrochanteric fossa of the femur. Smithon Misc Coll 92:1-49.

Hunt K. 1991. Positional behavior in the Hominoidea. Int J Primatol 12:95-118.
Hunt K, Cant J, Gebo D, Rose M, Walker S, Youlatos D. 1996. Standardized descriptions of primate locomotor and postural modes. Primates 37:363-387.
Jensvold MLA, Sanz CM, Fouts RS, Fouts DH. 2001. Effect of enclosure size and complexity on the behaviors of captive chimpanzees (*Pan troglodytes*). J Appl Anim Welf Sci 4:53- 69.
Jones HH, Priest JD, Hayes WC, Tichenor CC, Nagel DA. 1977. Humeral hypertrophy in response to exercise. J Bone Joint Surg Am 59:204-208.
Jungers WL, Minns RJ. 1979. Computed tomography and biomechanical analysis of fossil long bones. Am J Phys Anthropol 50:285-290.
Kimura M. 1968. Evolutionary rate at the molecular level. Nature 217:624-626.
Kimura T. 1991. Long and robust limb bones of primates. In: Ehara A, Kimura T, Takenaka O, Iwamoto M, editors. Primatology Today. New York: Elsevier. p 495-498.
Kimura T. 1995. Long bone characteristics of primates. Z Morphol Anthropol 80:265-280.
Kimura T, Okada M, Ishida H. 1979. Kinesiological characteristics of primate walking: its significance in human walking. In: Morbeck M, Preuschoft H, Gomberg N, editors. Environment, Behavior, and Morphology: Dynamic Interactions in Primates. New York: Gustav Fischer. p 297-312.
Kivell TL, Schmitt D. 2009. Independent evolution of knuckle-walking in African apes shows that humans did not evolve from a knuckle-walking ancestor. Proc Natl Acad Sci USA 106:14241-14246.
Kronenberg HM. 2006. PTHrP and skeletal development. Ann N Y Acad Sci 1068:1-13.
Kuhl F, Giardina C. 1982. Elliptic Fourier features of a closed contour. Computer graphics and image processing 18:236-258.
Kumar S, Filipski A, Swarna V, Walker A, Hedges SB. 2005. Placing confidence limits on the molecular age of the human-chimpanzee divergence. Proc Natl Acad Sci USA 102:18842-18847.
Kuwata T, Matsubara S, Ohkusa T, Yada Y, Suzuki M. 2011. Decreased fetal movement prompts investigation of prenatal/neonatal nemaline myopathy: The possible merit of fetal movement count. Journal of Obstetrics and Gynaecology Research 37:921-925.
Lacquaniti F, Ivanenko YP, Zago M. 2012. Development of human locomotion. Curr Opin Neurobiol 22:1-7.
Lammers AR, German RZ. 2002. Ontogenetic allometry in the locomotor skeleton of specialized half-bounding mammals. J Zool 258:485-495.
Lanyon LE. 1987. Functional strain in bone tissue as an objective, and controlling stimulus for adaptive bone remodeling. J Biomech 20:1083-1093.
Lanyon LE, Baggott DG. 1976. Mechanical function as an influence on structure and form of bone. J Bone Joint Surg-Br Vol 58:436-443.
Lanyon LE, Bourn S. 1979. Influence of mechanical function on the development and remodeling of the tibia - experimental-study in sheep. Journal of Bone and Joint Surgery-American Volume 61:263-273.
Leakey MD, Hay RL. 1979. Pliocene footprints in the Laetolil beds at Laetoli, northern Tanzania. Nature 278:317-323.
Leigh SR, Shea BT. 1996. Ontogeny of body size variation in African apes. Am J Phys Anthropol 99:43-65.
Lieberman DE, Polk JD, Demes B. 2004. Predicting long bone loading from cross-sectional geometry. Am J Phys Anthropol 123:156-171.
Lieberman DE, Raichlen DA, Pontzer H, Bramble DM, Cutright-Smith E. 2006. The human gluteus maximus and its role in running. J Exp Biol 209:2143-2155.
Lockwood CA. 1999. Homoplasy and adaptation in the atelid postcranium. Am J Phys Anthropol 108:459-482.
Lockwood CA, Fleagle JG. 2007. Homoplasy in primate and human evolution. J Hum Evol 52:471-472.
Lockwood CA, Kimbel WH, Lynch JM. 2004. Morphometrics and hominoid phylogeny: Support for a chimpanzee-human clade and differentiation among great ape subspecies. Proc Natl Acad Sci USA 101:4356-4360.

Lovejoy CO, Burstein AH, Heiple KG. 1976. Biomechanical analysis of bone strength - method and its application to platycnemia. Am J Phys Anthropol 44:489-505.

Lovejoy CO, Latimer B, Suwa G, Asfaw B, White TD. 2009a. Combining prehension and propulsion: The foot of *Ardipithecus ramidus*. Science 326:72.

Lovejoy CO, McCollum MA, Reno PL, Rosenman BA. 2003. Developmental biology and human evolution. Annu Rev Anthropol 32:85-109.

Lovejoy CO, Meindl RS, Ohman JC, Heiple KG, White TD. 2002. The Maka femur and its bearing on the antiquity of human walking: Applying contemporary concepts of morphogenesis to the human fossil record. Am J Phys Anthropol 119:97-133.

Lovejoy CO, Simpson SW, White TD, Asfaw B, Suwa G. 2009b. Careful climbing in the Miocene: The forelimbs of *Ardipithecus ramidus* and humans are primitive. Science 326:70.

Lovejoy CO, Suwa G, Simpson SW, Matternes JH, White TD. 2009c. The great divides: *Ardipithecus ramidus* reveals the postcrania of our last common ancestors with African apes. Science 326:100-106.

Lovejoy CO, Suwa G, Spurlock L, Asfaw B, White TD. 2009d. The pelvis and femur of *Ardipithecus ramidus*: The emergence of upright walking. Science 326:71.

MacKay-Lyons M. 2002. Central pattern generation of locomotion: a review of the evidence. Phys Ther 82:69-83.

Main RP, Biewener AA. 2007. Skeletal strain patterns and growth in the emu hindlimb during ontogeny. J Exp Biol 210:2676-2690.

Minetti AE, Ardig OL, Reinach E, Saibene F, Prabhakar S, Visel A, Akiyama JA, Shoukry M, Lewis KD, Holt A, Plajzer-Frick I, Morrison H, Fitzpatrick DR, Afzal V, Pennacchio LA, Rubin EM, Noonan JP, Reno PL, McCollum MA, Cohn MJ, Meindl RS, Hamrick M, Lovejoy CO. 1999. The relationship between mechanical work and energy expenditure of locomotion in horses. J Exp Biol 202:2329-2338.

Mitteroecker P, Bookstein F. 2009. The ontogenetic trajectory of the phenotypic covariance matrix, with examples from craniofacial shape in rats and humans. Evolution 63:727-737.

Mitteroecker P, Gunz P, Bookstein FL. 2005. Heterochrony and geometric morphometrics: a comparison of cranial growth in *Pan paniscus* versus *Pan troglodytes*. Evol Dev 7:244-258.

Molnar P. 2006. Tracing prehistoric activities: Musculoskeletal stress marker analysis of a stone-age population on the island of Gotland in the Baltic Sea. Am J Phys Anthropol 129:12-23.

Morimoto N, Zollikofer CPE, Ponce de León MS. 2011a. Exploring femoral diaphyseal shape variation in wild and captive chimpanzees by means of morphometric mapping: a test of Wolff's Law. Anat Rec 294:589-609.

Morimoto N, Zollikofer CPE, Ponce de León MS. 2011b. Femoral morphology and femoropelvic musculoskeletal anatomy of humans and great apes: a comparative virtopsy study. Anat Rec 294:1433-1445.

Morishita Y, Iwasa Y. 2008. Growth based morphogenesis of vertebrate limb bud. Bull Math Biol 70:1957-1978.

Moro M, vanderMeulen MCH, Kiratli BJ, Marcus R, Bachrach LK, Carter DR. 1996. Body mass is the primary determinant of midfemoral bone acquisition during adolescent growth. Bone 19:519-526.

Mosley JR, Lanyon LE. 1998. Strain rate as a controlling influence on adaptive modeling in response to dynamic loading of the ulna in growing male rats. Bone 23:313-318.

Nei M. 2007. The new mutation theory of phenotypic evolution. Proc Natl Acad Sci U S A 104:12235-12242.

Netter F. 2003. Atlas of Human Anatomy, 3 ed. Philadelphia: Saunders.

O'Higgins P, Jones N. 1998. Facial growth in Cercocebus torquatus: an application of three-dimensional geometric morphometric techniques to the study of morphological variation. J Anat 193:251-272.

O'Neill MC, Dobson SD. 2008. The degree and pattern of phylogenetic signal in primate long-bone structure. J Hum Evol 54:309-322.

Patterson N, Richter DJ, Gnerre S, Lander ES, Reich D. 2006. Genetic evidence for complex speciation of humans and chimpanzees. Nature 441:1103-1108.

Pearson OM. 2000. Postcranial remains and the origin of modern humans. Evol Anthropol 9:229-247.
Pearson OM, Lieberman DE. 2004. The aging of Wolff's "Law": Ontogeny and responses to mechanical loading in cortical bone. Yearb Phys Anthropol 47:63-99.
Penin X, Berge C, Baylac M. 2002. Ontogenetic study of the skull in modern humans and the common chimpanzees: neotenic hypothesis reconsidered with a tridimensional Procrustes analysis. Am J Phys Anthropol 118:50-62.
Pickford M, Senut B, Gommery D, Treil J. 2002. Bipedalism in *Orrorin tugenensis* revealed by its femora. C R Palevol 1:191-203.
Polk JD, Demes B, Jungers WL, Biknevicius AR, Heinrich RE, Runestad JA. 2000. A comparison of primate, carnivoran and rodent limb bone cross-sectional properties: are primates really unique? J Hum Evol 39:297 - 325.
Ponce de León MS, Zollikofer CPE. 2001. Neanderthal cranial ontogeny and its implications for late hominid diversity. Nature 412:534-538.
Pontzer H, Raichlen DA, Sockol MD. 2009. The metabolic cost of walking in humans, chimpanzees, and early hominins. J Hum Evol 56:43-54.
Preuschoft H. 1970. Functional anatomy of the lower extremity. In: Bourne GH, editor. The Chimpanzee, Vol. 3. Basel: Karger. p 221-294.
Primrose A. 1898. The anatomy of the Orang utang (*Simia satyrus*). Trans Canad Inst 6:507-598.
Raichlen DA, Pontzer H, Shapiro LJ, Sockol MD. 2008. Understanding hind limb weight support in chimpanzees with implications for the evolution of primate locomotion. Am J Phys Anthropol 138:395-402.
Rauch F. 2005. Bone growth in length and width: the Yin and Yang of bone stability. J Musculoskelet Neuronal Interact 5:194-201.
Raven H. 1950. Regional anatomy of the gorilla. In: Gregory W, editor. The Anatomy of the Gorilla. New York: Columbia University Press.
Remis M. 1995. Effects of body size and social context on the arboreal activities of lowland gorillas in the Central African Republic. Am J Phys Anthropol 97:413-433.
Remis MJ. 1998. The effects of body size and habitat on the positional behavior of lowland and mountain gorillas. In: Strasser E, Fleagle J, Rosenberger A, McHenry H, editors. Primate Locomotion -Recent Advances. New York: Plenum Press. p 95-106.
Reynolds TR. 1985. Stresses on the limbs of quadrupedal primates. Am J Phys Anthropol 67:351-362.
Rhodes JA, Knüsel CJ. 2005. Activity-related skeletal change in medieval humeri: Cross-sectional and architectural alterations. Am J Phys Anthropol 128:536-546.
Richmond BG, Begun DR, Strait DS. 2001. Origin of human bipedalism: The knuckle-walking hypothesis revisited. In: Ruff C, editor. Yearbook of Physical Anthropology, Vol 44. p 70-105.
Richmond BG, Jungers WL. 2008. *Orrorin tugenensis* femoral morphology and the evolution of hominin bipedalism. Science 319:1662-1665.
Richmond BG, Strait DS. 2000. Evidence that humans evolved from a knuckle-walking ancestor. Nature 404:382-385.
Robling AG, Hinant FM, Burr DB, Turner CH. 2002. Improved bone structure and strength after long-term mechanical loading is greatest if loading is separated into short bouts. J Bone Miner Res 17:1545-1554.
Rodman PS, McHenry HM. 1980. Bioenergetics and the origin of hominid bipedalism. Am J Phys Anthropol 52:103-106.
Rohlf FJ. 1990. Rotational fit (Procrustes) methods. In: Rohlf F, Bookstein F, editors. Proceedings of the Michigan Morphometrics Workshop: Univ.of Michigan Museum of Zoology (Special Publication no. 2). p 227–236.
Rook L, Bondioli L, Kohler M, Moya-Sola S, Macchiarelli R. 1999. *Oreopithecus* was a bipedal ape after all: Evidence from the iliac cancellous architecture. Proc Natl Acad Sci USA 96:8795-8799.
Ruff CB. 1988. Hindlimb articular surface allometry in hominoidea and *Macaca*, with comparisons to diaphyseal scaling. J Hum Evol 17:687-714.
Ruff CB. 2002. Long bone articular and diaphyseal structure in old world monkeys and apes. I: Locomotor effects. Am J Phys Anthropol 119:305-342.

Ruff CB. 2003a. Growth in bone strength, body size, and muscle size in a juvenile longitudinal sample. Bone 33:317-329.
Ruff CB. 2003b. Ontogenetic adaptation to bipedalism: age changes in femoral to humeral length and strength proportions in humans, with a comparison to baboons. J Hum Evol 45:317-349.
Ruff CB. 2009. Relative limb strength and locomotion in *Homo habilis*. Am J Phys Anthropol 138:90-100.
Ruff CB, Hayes WC. 1983. Cross-sectional geometry of Pecos Pueblo femora and tibiae--a biomechanical investigation: I. Method and general patterns of variation. Am J Phys Anthropol 60:359-381.
Ruff CB, Holt B, Trinkaus E. 2006. Who's afraid of the big bad wolff? "Wolff is law" and bone functional adaptation. Am J Phys Anthropol 129:484-498.
Ruff CB, McHenry HM, Thackeray JF. 1999. Cross-sectional morphology of the SK 82 and 97 proximal femora. Am J Phys Anthropol 109:509-521.
Ruff CB, Runestad JA. 1992. Primate limb bone structural adaptations. Annu Rev Anthropol 21:407-433.
Ruff CB, Trinkaus E, Walker A, Larsen CS. 1993. Postcranial robusticity in *Homo*. I: Temporal trends and mechanical interpretation. Am J Phys Anthropol 91:21-53.
Ruff CB, Walker A, Trinkaus E. 1994. Postcranial robusticity in *Homo*. III: ontogeny. Am J Phys Anthropol 93:35-54.
Scheuer L, Black S, Christie A. 2000. Developmental Juvenile Osteology. San Diego, San Francisco, New York, Boston, London, Sydney, Tokyo: Academic Press.
Schmitt D. 2003. Insights into the evolution of human bipedalism from experimental studies of humans and other primates. J Exp Biol 206:1437-1448.
Schmitt D, Lemelin P. 2002. The origins of primate locomotion: gait mechanics of the woolly opossum. Am J Phys Anthropol 118:231-238.
Schultz AH. 1937. Proportions, variability and asymmetries of the long bones of the limbs and the clavicles in man and apes. Hum Biol 9:281-328.
Schultz AH. 1969. The skeleton of the chimpanzee. In: Bourne GH, editor. The Chimpanzee, Vol. 1. Basel: Karger. p 50-103.
Schultz AH. 1973. Age changes, variability and generic differences in body proportions of recent hominoids. Folia Primatol 19:338-359.
Schwartz JH. 1995. Skeleton Keys: An Introduction to Human Skeletal Morphology, Development, and Analysis. Oxford: Oxford University Press.
Senut B, Pickford M, Gommery D, Mein P, Cheboi K, Coppens Y. 2001. First hominid from the Miocene (Lukeino Formation, Kenya). C R Acad Sci Paris Ser II a 332:137-144.
Serrat MA, King D, Lovejoy CO. 2008. Temperature regulates limb length in homeotherms by directly modulating cartilage growth. Proc Natl Acad Sci USA 105:19348-19353.
Serrat MA, Lovejoy CO, King D. 2007. Age- and site-specific decline in insulin-like growth factor-I receptor expression is correlated with differential growth plate activity in the mouse hindlimb. The Anatomical Record: Advances in Integrative Anatomy and Evolutionary Biology 290:375-381.
Shea BT. 1981. Relative growth of the limbs and trunk in the African apes. Am J Phys Anthropol 56:179-201.
Sigmon BA. 1974. A functional analysis of pongid hip and thigh musculature. J Hum Evol 3:161-185.
Smith RJ, Leigh SR. 1998. Sexual dimorphism in primate neonatal body mass. J Hum Evol 34:173-201.
Sockol MD, Raichlen DA, Pontzer H. 2007. Chimpanzee locomotor energetics and the origin of human bipedalism. Proc Natl Acad Sci USA 104:12265-12269.
Sparacello V, Marchi D. 2008. Mobility and subsistence economy: A diachronic comparison between two groups settled in the same geographical area (Liguria, Italy). Am J Phys Anthropol 136:485-495.
Sparacello VS, Pearson OM. 2010. The importance of accounting for the area of the medullary cavity in cross-sectional geometry: A test based on the femoral midshaft. Am J Phys Anthropol 143:612–624.

Specht M, Lebrun R, Zollikofer CPE. 2007. Visualizing shape transformation between chimpanzee and human braincases. Visual Computer 23:743-751.
Standring S, editor. 2004. Gray's Anatomy, 39 ed. Edinburgh/London/New York: Churchill Livingstone.
Standring S, editor. 2005. Gray's anatomy: Churchill Livingstone.
Stern JT. 1972. Anatomical and functional specializations of human gluteus maximus. Am J Phys Anthropol 36:315-338.
Stern JT, Susman RL. 1981. Electromyography of the gluteal muscles in *Hylobates*, *Pongo*, and *Pan* - implications for the evolution of hominid bipedality. Am J Phys Anthropol 55:153-166.
Sumner DR, Andriacchi TP. 1996. Adaptation to differential loading: Comparison of growth-related changes in cross-sectional properties of the human femur and humerus. Bone 19:121-126.
Sutherland DH, Olshen R, Cooper L, Woo SL. 1980. The development of mature gait. J Bone Joint Surg Am 62:336-353.
Swindler D, Wood C. 1982. An Atlas of Primate Gross Anatomy. Malabar: Robert E. Krieger Publishing Company.
Szivek JA, Johnson EM, Magee FP. 1992. *In vivo* strain analysis of the greyhound femoral diaphysis. Journal of Investigative Surgery 5:91-108.
Thali MJ, Dirnhofer R, Vock P, editors. 2009. The Virtopsy Approach. New York: CRC Press.
Thali MJ, Jackowski C, Oesterhelweg L, Ross SG, Dirnhofer R. 2007. Virtopsy - The Swiss virtual autopsy approach. Legal Med 9:100-104.
Thorpe SK, Crompton RH. 2005. Locomotor ecology of wild orangutans (*Pongo pygmaeus abelii*) in the Gunung Leuser Ecosystem, Sumatra, Indonesia: a multivariate analysis using log-linear modelling. Am J Phys Anthropol 127:58-78.
Thorpe SK, Crompton RH. 2006. Orangutan positional behavior and the nature of arboreal locomotion in Hominoidea. Am J Phys Anthropol 131:384-401.
Thorpe SKS, Holder RL, Crompton RH. 2007. Origin of human bipedalism as an adaptation for locomotion on flexible branches. Science 316:1328-1331.
Trinkaus E, Churchill SE, Ruff CB. 1994. Postcranial robusticity in *Homo*. II: Humeral bilateral asymmetry and bone plasticity. Am J Phys Anthropol 93:1-34.
Turley K, Guthrie EH, Frost SR. 2011. Geometric Morphometric Analysis of Tibial Shape and Presentation Among Catarrhine Taxa. The Anatomical Record: Advances in Integrative Anatomy and Evolutionary Biology 294:217-230.
Turner CH, Forwood MR, Otter MW. 1994. Mechanotransduction in bone - do bone-cells act as sensors of fluid-flow. FASEB J 8:875-878.
Turner CH, Owan I, Takano Y. 1995. Mechanotransduction in bone - role of strain-rate. American Journal of Physiology-Endocrinology and Metabolism 269:E438-E442.
Tuttle RH, Watts DP. 1985. The positional behavior and adaptive complexes of *Pan gorilla*. In: Kondo S, Ishida S, Okada M, Kimura T, Yamazaki M, editors. Primate Morphophysiology, Locomotor Analyses and Human Bipedalism. Tokyo: University of Tokyo Press. p 261-288.
Uhlmann K. 1968. Hüft- und Oberschenkelmuskulatur: Systematische und vergleichende Anatomie. In: Hofer H, Schultz AH, Starck D, editors. Primatologia: Handbuch der Primatenkunde. Basel: Karger.
Van der Eerden BCJ, Karperien M, Gevers EF, Löwik CWGM, Wit JM. 2000. Expression of indian hedgehog, parathyroid hormone-related protein, and their receptors in the postnatal growth plate of the rat: evidence for a locally acting growth restraining feedback loop after birth. J Bone Miner Res 15:1045-1055.
van der Meulen MCH, Ashford MW, Kiratli BJ, Bachrach LK, Carter DR. 1996. Determinants of femoral geometry and structure during adolescent growth. J Orth Res 14:22-29.
Villotte S, Castex D, Couallier V, Dutour O, Knusel CJ, Henry-Gambier D. 2010. Enthesopathies as occupational stress markers: evidence from the upper limb. Am J Phys Anthropol 142:224-234.
Wallace IJ, Middleton KM, Lublinsky S, Kelly SA, Judex S, Garland T, Demes B. 2010a. Functional significance of genetic variation underlying limb bone diaphyseal structure. Am J Phys Anthropol 143:21-30.

Wallace IJ, Middleton KM, Svetlana L, Kelly SA, Stefan J, Theodore G, Jr., Brigitte D. 2010b. Functional significance of genetic variation underlying limb bone diaphyseal structure. In.
Wallace IJ, Tommasini SM, Judex S, Garland T, Demes B. 2012. Genetic variations and physical activity as determinants of limb bone morphology: An experimental approach using a mouse model. Am J Phys Anthropol 148:24-35.
Ward CV. 2002. Interpreting the posture and locomotion of *Australopithecus afarensis*: where do we stand? Am J Phys Anthropol Suppl 35:185-215.
Warden SJ, Hurst JA, Sanders MS, Turner CH, Burr DB, Li J. 2005. Bone adaptation to a mechanical loading program significantly increases skeletal fatigue resistance. J Bone Miner Res 20:809-816.
Weiss E. 2004. Understanding muscle markers: Lower limbs. Am J Phys Anthropol 125:232-238.
White TD, Asfaw B, Beyene Y, Haile-Selassie Y, Lovejoy CO, Suwa G, WoldeGabriel G. 2009. *Ardipithecus ramidus* and the paleobiology of early hominids. Science 326:75-86.
Wolff J. 1892. Das Gesetz der Transformation der Knochen. Berlin: A. Hirschwald.
Wolff J. 1986. The law of bone remodeling. Berlin: Springer-Verlag.
Wood B, Harrison T. 2011. The evolutionary context of the first hominins. Nature 470:347-352.
Wood B, Richmond BG. 2000. Human evolution: taxonomy and paleobiology. J Anat 197 (Pt 1):19-60.
Yamanaka A, Gunji H, Ishida H. 2005. Curvature, length, and cross-sectional geometry of the femur and humerus in anthropoid primates. Am J Phys Anthropol 127:46-57.
Young JW. 2009. Ontogeny of joint mechanics in squirrel monkeys (*Saimiri boliviensis*): functional implications for mammalian limb growth and locomotor development. J Exp Biol 212:1576-1591.
Young JW, Fernandez D, Fleagle JG. 2009. Ontogeny of long bone geometry in capuchin monkeys (Cebus albifrons and Cebus apella): implications for locomotor development and life history. Biol Lett 6:197-200.
Young NM, Hallgrimsson B. 2005. Serial homology and the evolution of mammalian limb covariation structure. Evolution 59:2691-2704.
Young NM, Wagner GP, Hallgrímsson B. 2010. Development and the evolvability of human limbs. Proc Natl Acad Sci USA 107:3400-3405.
Zollikofer CPE, de Leon MSP, Lieberman DE, Guy F, Pilbeam D, Likius A, Mackaye HT, Vignaud P, Brunet M. 2005. Virtual cranial reconstruction of *Sahelanthropus tchadensis*. Nature 434:755-759.
Zollikofer CPE, Ponce de León MS. 2001. Computer-assisted morphometry of hominoid fossils: the role of morphometric maps. In: De Bonis L, Koufos G, Andrews P, editors. Phylogeny of the Neogene Hominoid Primates of Eurasia. Cambridge: Cambridge University Press. p 50-59.
Zollikofer CPE, Ponce de León MS. 2006. Neanderthals and modern humans - chimps and bonobos: similarities and differences in development and evolution. In: Harvati K, Harrison T, editors. Neanderthals Revisited: New Approaches and Perspectives. New York: Springer. p 71-88.

Acknowledgements

We thank P. Jans for help with sample preparation and CT scanning. We are grateful to Kyoto City Zoo, Takaoka Kojo Park Zoo and the GAIN (Great Ape Information Network) project of Japan for data of Yoko and Rick. Research funded by the Swiss National Science Foundation (grant # 31003A-109344 to C.P.E.Z.) We are also grateful to the two anonymous reviewers for valuable comments and suggestions.

Abbreviations

Ab: *adductor brevis*

BF: *biceps femoris*

GM: *gluteus maximus*

GMi: *gluteus maximus ischiofemoralis*

GMp: *gluteus maximus proprius*

Gmd: *gluteus medius*

VL: *vastus lateralis*

IT: iliotibial tract

LIM: lateral intermuscular septum

LP: lateral pilaster

LSP: lateral spiral pilaster

Table 1. List of specimens

specimen id	*taxon*	*individual age*	*sex*	*dental eruption*	*preservation*	*Figure number*
Clinical data #1	*Homo sapiens*	adult	m	M3 erupted	−	Fig. 3A
AIMUZH-7283	*Pan troglodytes*	infant	m	DCM2* erupted	formalin	Fig. 2, 3B
AIMUZH-n10003	*Pan troglodytes*	infant	f	DCM2 erupted	frozen	Fig. 5
AIMUZH-n10001	*Pan troglodytes*	adult	f	M3 erupted	formalin	Fig. 4A
KCZ-Yoko (PRICT-34/218)	*Pan troglodytes*	adult (20y)	f	M3 erupted	frozen	Fig. 4B, 6
KUPRI-9262 (TKZ-Rick; PRICT-320)	*Pan troglodytes*	adult (22y)	m	M3 erupted	frozen	Fig. 4C, S1
AIMUZH-n10006	*Pan paniscus*	infant	−	DCM2 erupted	frozen	Fig. 4D
AIMUZH-n10004	*Gorilla gorilla*	juvenile	m	M1 erupted	formalin	Fig. 3C
AIMUZH-11427	*Pongo pygmaeus*	neonate	m	−	formalin	Fig. 3D

* second deciduous molar

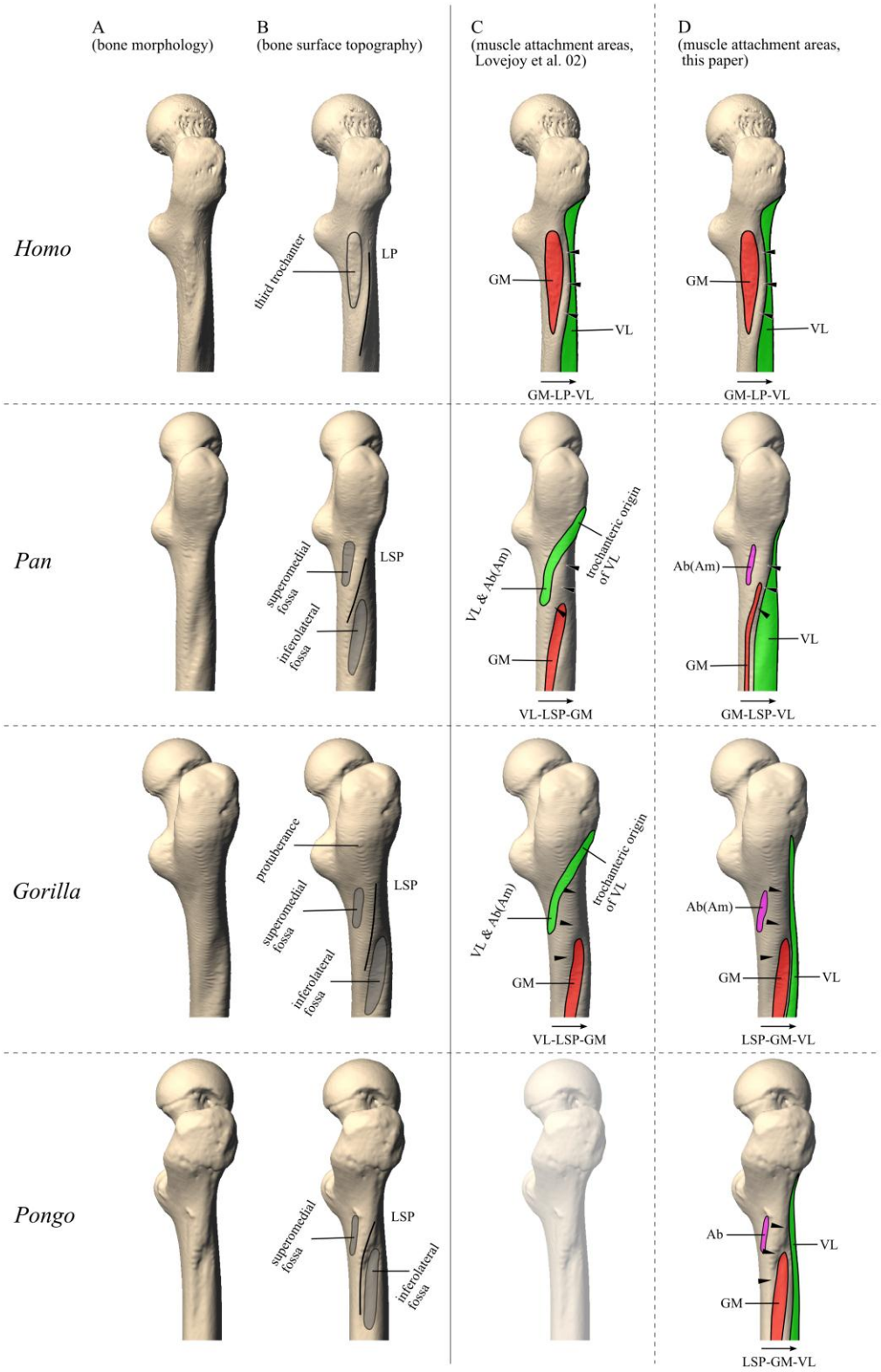

Fig. 1 Topographic relationships between structures of the proximal femoral shaft and areas of muscular attachment. A: bone morphology. B: bone surface topography. C: topographic relationships suggested by Lovejoy et al. (2002). D: topographic relationships as derived from virtopsy data of this study. GM: *gluteus maximus*, VL: *vastus lateralis*, Ab: *adductor brevis*, Am: *adductor minimus*, LSP: lateral spiral pilaster. Arrowheads indicate lateral spiral pilaster.

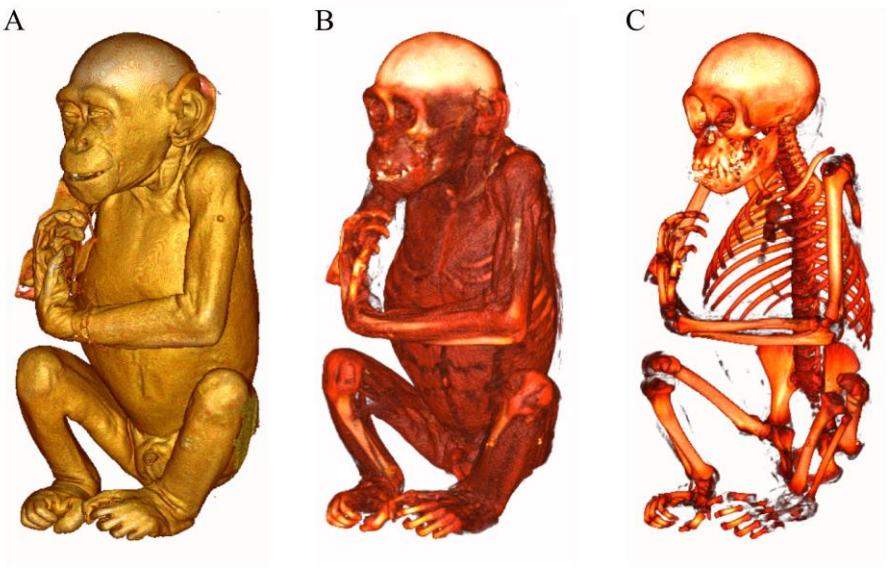

Fig. 2 Scheme of virtual dissection (virtopsy). Volume data visualization was performed for CT data of a formalin-preserved juvenile chimpanzee (*id*: AIMUZH-7283) to visualize the skin (A), muscles (B) and skeleton (C).

Fig. 3 (legend see next page)

Fig. 3 Virtual dissection of the femoropelvic region of humans and great apes (right lateral views). A: adult human (clinical data set, *id*: Clinical data #1); B: juvenile *Pan troglodytes* (*id*: AIMUZH-7283, frozen specimen); C: juvenile *Gorilla gorilla* (*id*: AIMUZH-n10004); D: neonate *Pongo pygmaeus* (*id*: AIMUZH-11427) (gorilla and orangutan specimens are formalin-preserved). Left graphs: muscle topography (GM: *gluteus maximus*, GMi: *gluteus maximus ischiofemoralis*, GMp: *gluteus maximus proprius*, Gmd: *gluteus medius*, VL: *vastus lateralis*, VI: *vastus intermedius*, BF: *biceps femoris*, ST: *semitendinosus*, TFL: *tensor fasciae latae*); middle graphs: superposition of muscles (outlines) and skeletal parts; right graphs: bone visualization (arrowheads indicate LP/LSP [lateral pilaster/lateral spiral pilaster]). In humans/chimpanzees, the GM inserts postero-(supero-)medially relative to the LP/LSP; in gorillas and orangutans, the GM inserts antero-(infero-)laterally relative to the LSP (note that in individual A, the LP is situated close to the third trochanter).

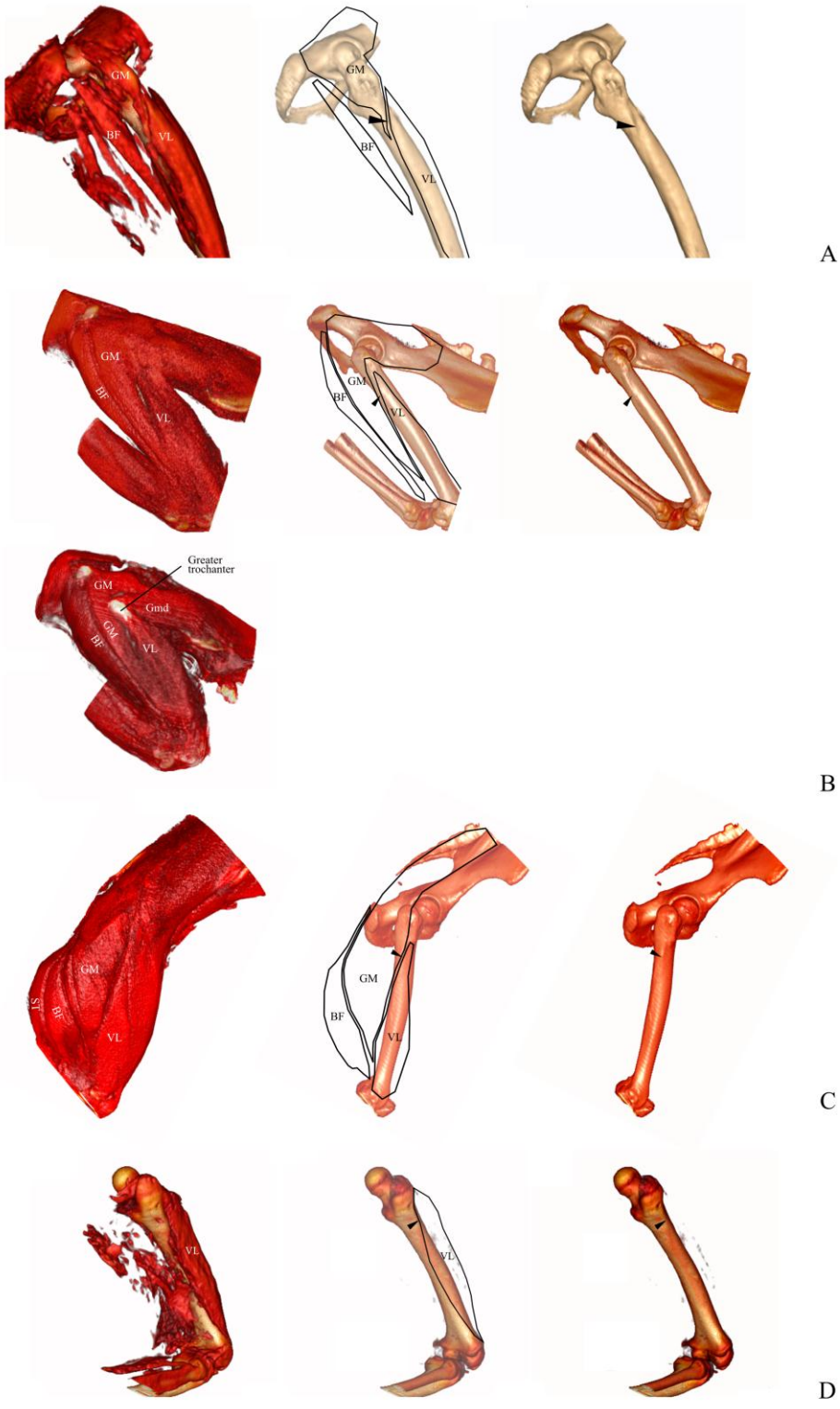

Fig. 4 (legend see next page)

Fig. 4 Topographic relationship between *gluteus maximus* (GM) and *vastus lateralis* (VL) in *Pan* (right lateral views). Left graphs: muscles (GM: *gluteus maximus*, Gmd: *gluteus medius*, VL: *vastus lateralis*, BF: *biceps femoris*); middle graphs: superposition of muscles (outlines) and skeletal parts; right graphs: bone visualization (arrowheads indicate LP/LSP). A, B, C: adult *P. troglodytes* (A: formalin-preserved specimen [*id*: AIMUZH-n10001], B: frozen specimen [*id*: KCZ-Yoko], C: frozen specimen [*id*: KUPRI-9262]); D: juvenile *P. paniscus* (frozen specimen [*id*: AIMUZH-n10006]). In B, superficial part of GM is removed to expose the attachment area of GM and VL, and course of GM. Posterior portion of GM is situated posterior to greater trochanter. In A, B, note the groove between GM and VL, which is formed by the LIM, and which coincides with the location of the LSP (arrowheads).

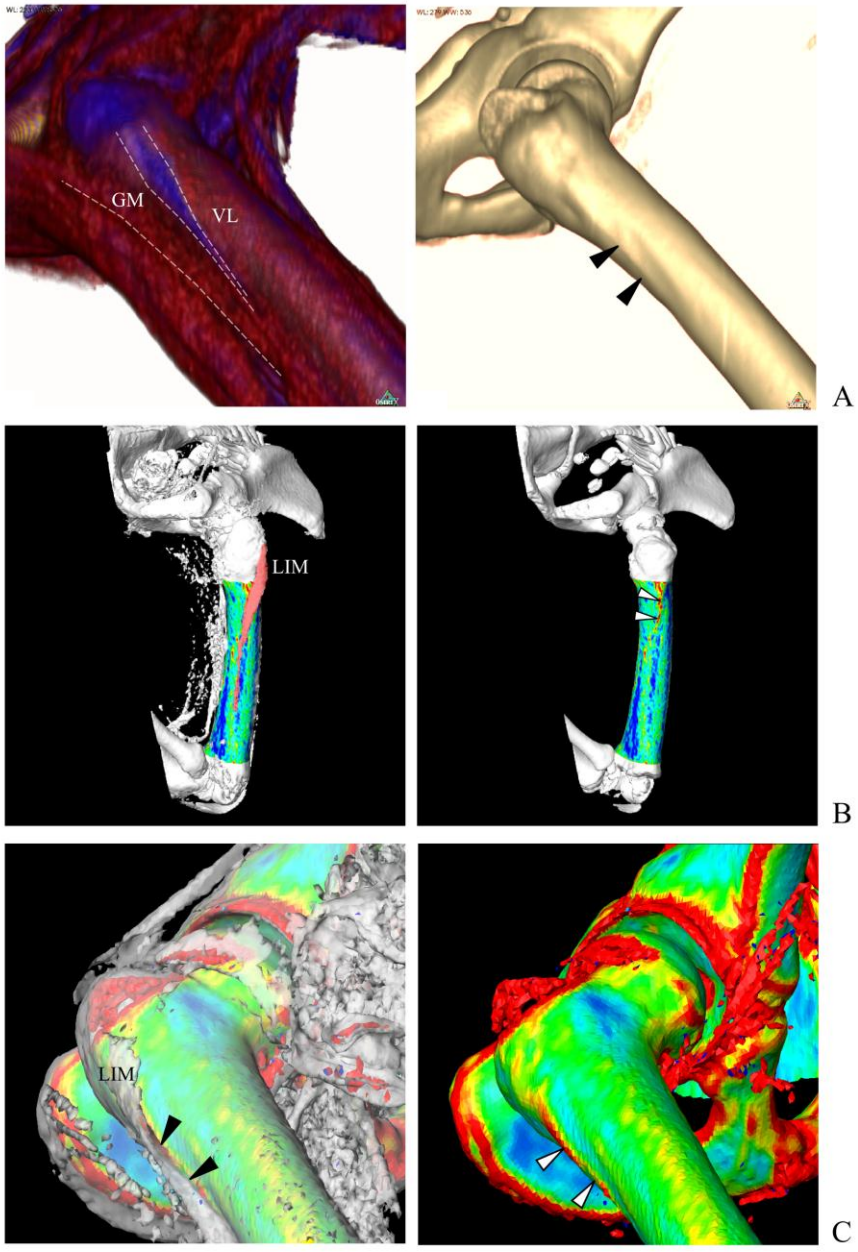

Fig. 5 Topographic relationship between lateral intermuscular septum (LIM) and lateral spiral pilaster (LSP) in a juvenile chimpanzee (frozen specimen [*id*: AIMUZH-n10003]). A: Visualization of muscles (left graph) and underlying skeletal parts (right graph); right lateral view. B, C: Visualization of LIM (light red in left graph of B) and skeletal parts (right graph); right lateral (B) and right anterolateral (C) views. Femoral surface curvature is visualized with false colors. The LIM appears as an aponeurotic flap, which is attached to the LSP (red-yellow, indicated by arrows), and blends distally into the VL aponeurosis running along the linea aspera (yellow-green). Arrowheads indicate LSP.

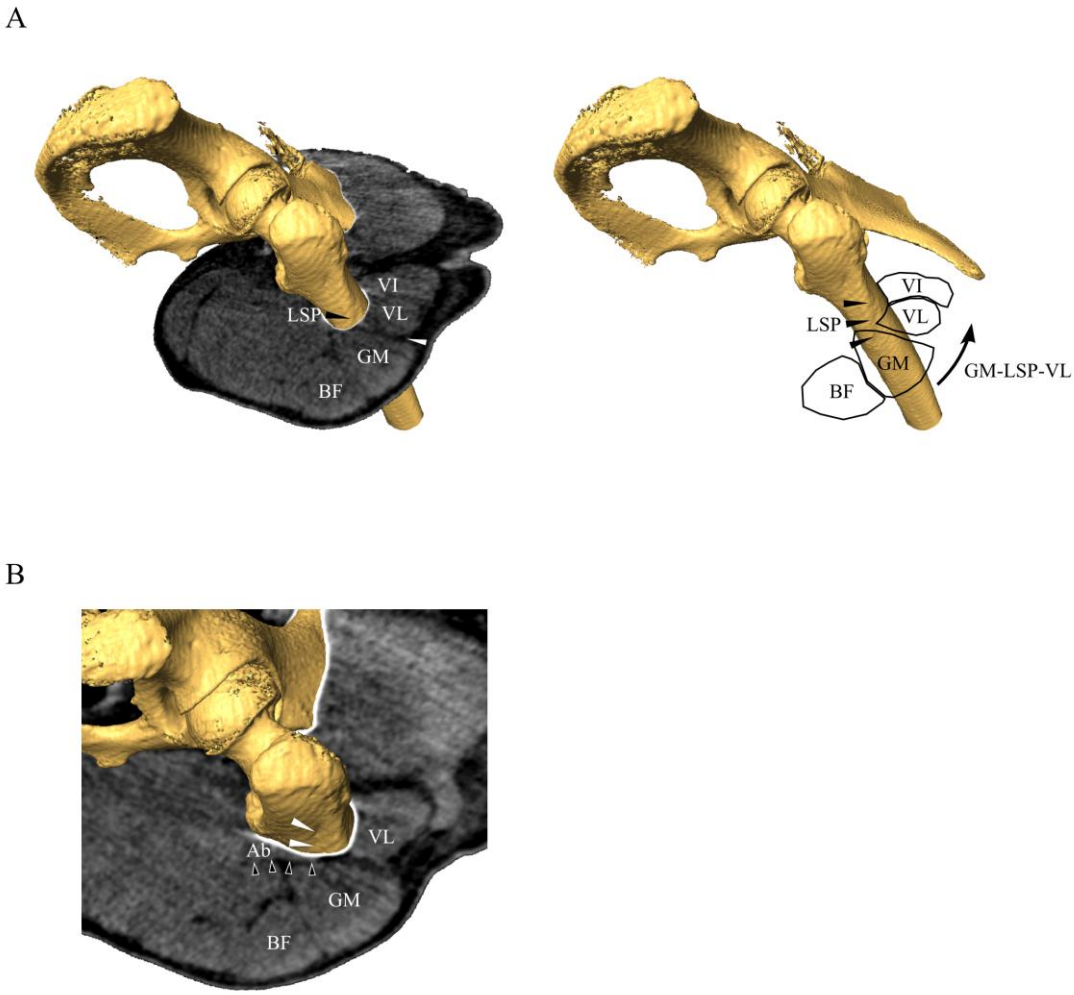

Fig. 6 Topographic relationship between structures of the proximal femoral shaft and areas of muscular attachment of adult chimpanzees (KCZ-Yoko). A: cross-section at the middle of lateral spiral pilaster (LSP). The fossa on the infero-anterior side of LSP is the attachment site of VL (not of GM). Black and white arrowheads indicate LSP and the groove between GM and VL respectively. B: cross-section immediately below the lesser trochanter. Black and white arrowheads indicate the course of *adductor brevis* and a fossa superomedial to LSP respectively. The fossa superomedial to LSP is inserted by *adductor brevis*. GM: *gluteus maximus*, VL: *vastus lateralis*, VI: *vastus intermedius*, BF: *biceps femoris*.

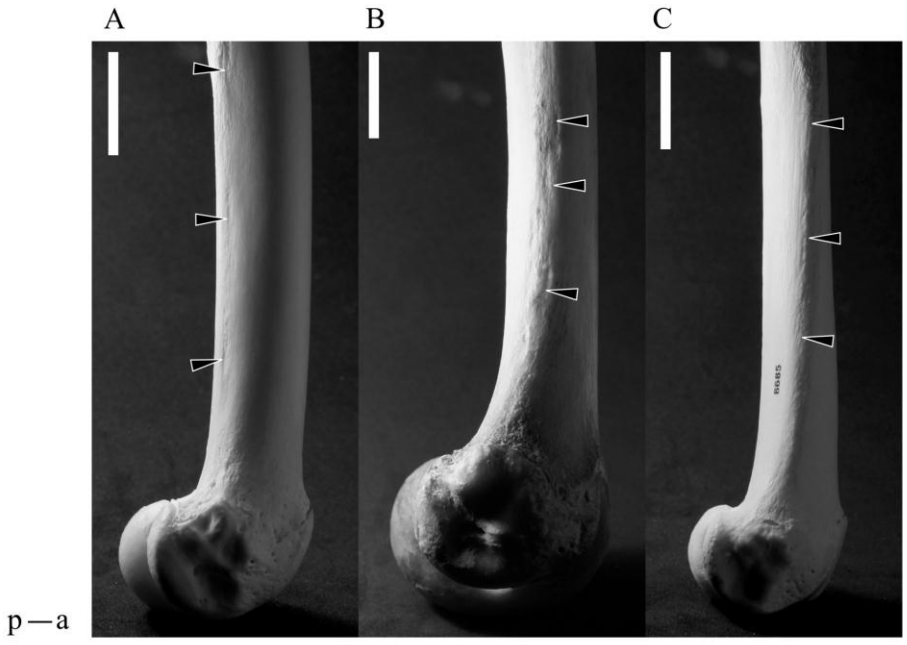

Fig. 7 Areas of attachment of VL (*vastus lateralis*) and GM (*gluteus maximus*) on distal femoral diaphysis of great apes (photographs of right femora in lateral view). A: chimpanzee; VL/GM attach along a line on posterior diaphysis (black arrowheads). B, gorillas, and C: orangutans; VL/GM attach on lateral diaphysis. Scale bar: 2.5cm.

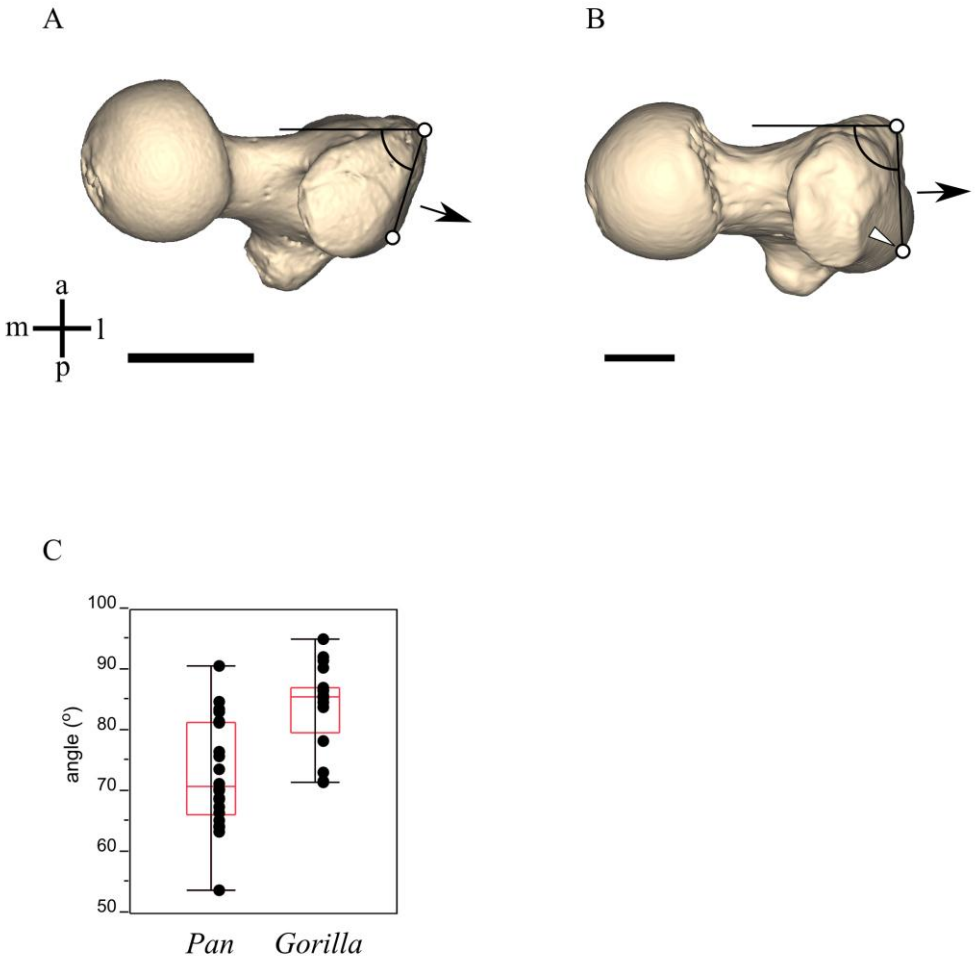

Fig. 8 Orientation of greater trochanter in chimpanzees and gorillas. Proximal view of the right femur of a male adult chimpanzee (A) and gorilla (B). Scale bar: 2.5cm. Greater trochanter is oriented in posterolateral direction in chimpanzees (A), while it is oriented in a more lateral direction in gorillas. Gorillas show marked protuberance on the posterolateral trochanteric surface (white arrowhead). C: box-plot of the angle of greater trochanter orientation (angle between femoral transverse axis and a line through most anterolateral and posterolateral points on the greater trochanter).

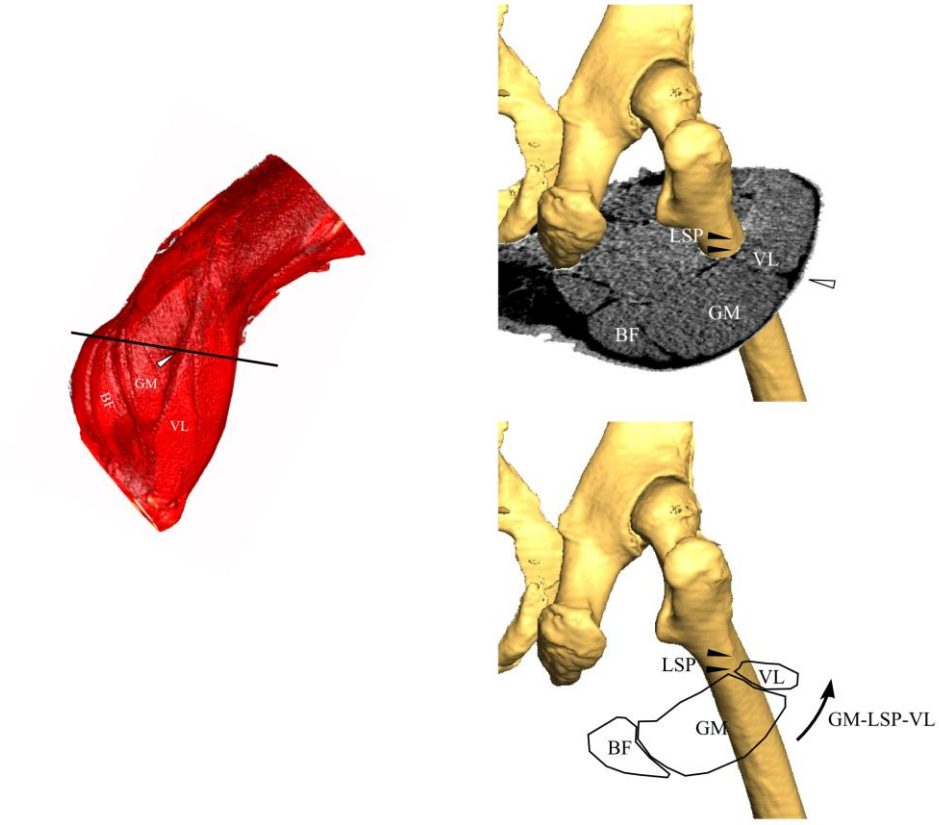

Fig. S1 Topographic relationship between structures of the proximal femoral shaft and areas of muscular attachment of adult chimpanzees (*id*: KUPRI-9262). Cross-section at the middle of lateral spiral pilaster (LSP). The fossa on the infero-anterior side of LSP is the attachment site of VL (not of GM). Black and white arrowheads indicate LSP and the groove between GM and VL respectively. GM: *gluteus maximus*, VL: *vastus lateralis*, BF: *biceps femoris*.

Chapter 3 Shared human-chimpanzee pattern of perinatal femoral shaft morphology and its implications for the evolution of hominin locomotor adaptations

Reference: *PLoS ONE* 7(7): e41980

Abstract

Background

Acquisition of bipedality is a hallmark of human evolution. How bipedality evolved from great ape-like locomotor behaviors, however, is still highly debated. This is mainly because it is difficult to infer locomotor function, and even more so locomotor kinematics, from fossil hominin long bones. Structure-function relationships are complex, as long bone morphology reflects phyletic history, developmental programs, and loading history during an individual's lifetime. Here we discriminate between these factors by investigating the morphology of long bones in fetal and neonate great apes and humans, before the onset of locomotion.

Methodology/Principal Findings

Comparative morphometric analysis of the femoral diaphysis indicates that its morphology reflects phyletic relationships between hominoid taxa to a greater extent than taxon-specific locomotor adaptations. Diaphyseal morphology in humans and chimpanzees exhibits several shared-derived features, despite substantial differences in locomotor adaptations. Orangutan and gorilla morphologies are largely similar, and likely represent the primitive hominoid state.

Conclusions/Significance

These findings are compatible with two possible evolutionary scenarios. Diaphyseal morphology may reflect retained adaptive traits of ancestral taxa, hence human-chimpanzee shared-derived features may be indicative of the locomotor behavior of our last common ancestor. Alternatively, diaphyseal morphology might reflect evolution by genetic drift (neutral evolution) rather than selection, and might thus be more informative about phyletic relationships between taxa than about locomotor adaptations. Both scenarios are consistent with the hypothesis that knuckle-walking in chimpanzees and gorillas resulted from convergent evolution, and that the evolution of human bipedality is unrelated to extant great ape locomotor specializations.

Introduction

Humans and extant great apes exhibit a pattern of locomotor diversification (Hunt, 1991; Hunt et al., 1996; Thorpe and Crompton, 2006; Crompton et al., 2008), which stands in contrast with their phyletic relationships. While humans are obligate terrestrial bipeds, our closest living relatives, the chimpanzees, exhibit a wide range of arboreal locomotor behaviors (Doran, 1992, 1993), and their peculiar mode of terrestrial quadrupedal locomotion – knuckle-walking – differs substantially from human bipedal locomotion (Gebo, 1992; Richmond et al., 2001). The more distantly-related gorillas also exhibit various arboreal locomotor behaviors, as well as terrestrial knuckle-walking (Tuttle and Watts, 1985; Remis, 1995; Doran, 1997). Because knuckle-walking occurs in chimpanzees and gorillas, it has been proposed as an ancestral mode of locomotion from which human bipedality evolved (Richmond and Strait, 2000). This hypothesis has been challenged on anatomical, developmental and behavioral grounds (Gibbs et al., 2002; Thorpe et al., 2007; Kivell and Schmitt, 2009), and the orangutan has been proposed, instead, as a model for the evolution of bipedality from a generalized bipedal/quadrupedal arboreal repertoire of locomotion (Thorpe et al., 2007). In contrast to both hypotheses, the phyletic and functional analysis of the skeleton of *Ardipithecus ramidus* (Lovejoy et al., 2009a; Lovejoy et al., 2009b; Lovejoy et al., 2009c; Lovejoy et al., 2009d; White et al., 2009) provided evidence that hominin bipedality might have evolved from a locomotor mode no longer present in extant great apes.

During reconstruction of the evolutionary history of hominin bipedalism, fossil evidence from hind limb elements, especially from the femur, has played a central role. The surface topography of the proximal femoral diaphysis of *Ardipithecus ramidus* (Lovejoy et al., 2009d) and *Australopithecus afarensis* (Lovejoy et al., 2002) has provided evidence for reorganization of the femoropelvic musculature toward bipedal locomotor behaviors (Lieberman et al., 2006; Pontzer et al., 2009). Likewise, the proximal femoral morphology of *Orrorin tugenensis* indicates bipedal locomotor adaptations (Richmond and Jungers, 2008). Form-function relationships of the femur are complex, however, as femoral morphology results from both long-term processes of selection and adaptation, and short-term processes of bone remodeling during an individual's lifetime (Wolff's Law (Wolff, 1892) or bone functional adaptation (Pearson and Lieberman, 2004; Ruff et al., 2006)). Femoral morphology thus typically reflects a combination of (a) the impact of an individual's locomotor history on its musculoskeletal system, (b) taxon-specific adaptation of the musculoskeletal system to specialized locomotor behaviors, and (c) phyletic history not directly related to a taxon's actual locomotor adaptations (phyletic inertia) (Lovejoy et al., 2003; Pearson and Lieberman, 2004; Ruff et al., 2006; Wallace et al., 2010a; Morimoto et al., 2011a; Wallace et al., 2012). Discrimination between these factors is especially difficult in fossil specimens, for which *in-vivo* patterns of locomotion and species-specific locomotor behavior are unknown, and taxon affiliation is often uncertain.

Here we address these questions by studying femoral morphology in fetuses and neonates of extant great apes and humans. Phyletic relationships and locomotor behaviors of these taxa are well known. Great ape taxa show a remarkable variety of arboreal and terrestrial, quadrupedal and bipedal locomotor behaviors (Doran, 1992, 1993, 1996, 1997; Remis, 1998; Thorpe and Crompton, 2006), the frequencies of which depend on taxon-specific, environmental and life-history factors (Doran et al., 2002; Thorpe and Crompton, 2005, 2006). While various modes of terrestrial locomotion are an important component of the locomotor repertoire of chimpanzees and gorillas (Doran, 1996, 1997), orangutans are highly restricted to arboreal habitats and are unique among great apes in showing pronograde suspensory behaviors and fist-walking (Hunt et al., 1996; Thorpe and Crompton, 2006).

Studying long bone morphology in fetuses and neonates permits analysis of the effects of the developmental program before the onset of locomotion, that is, before the skeletal morphology is modified by taxon-specific and/or individual mechanical loading regimes, and by environmental factors. Because epiphyses are not yet ossified around the time of birth, we focus on diaphyseal morphology. We ask whether perinatal femoral diaphyseal morphology reflects phyletic relationships independent of an extant taxon's locomotor adaptation (H0), or whether it reflects adaptation to taxon-specific locomotor behaviors (H1). According to hypothesis H0, humans and chimpanzees should exhibit similar femoral morphologies, to the exclusion of gorillas; according to H1, chimpanzees and gorillas are expected to exhibit largely similar diaphyseal morphologies, while modern human femoral diaphyses should be clearly distinct.

Long bone morphology is brought about by growth in longitudinal and radial directions. During this process, bone is deposited at diaphyseal growth plates and subperiosteal surfaces, respectively, and resorbed at endosteal surfaces (Schwartz, 1995; Scheuer et al., 2000; Van der Eerden et al., 2000; Rauch, 2005; Kronenberg, 2006; Serrat et al., 2007). Young et al. (Young and Hallgrimsson, 2005; Young et al., 2010) have shown that hominoid long bone longitudinal relative to radial growth is more variable than in other primate taxa, and reflects taxon-specific locomotor adaptations. In hominoids, taxon-specific limb proportions are almost fully established at birth (Schultz, 1973), indicating distinct taxon-specific longitudinal growth characteristics already before birth. Longitudinal diaphyseal growth characteristics and morphology thus provide support for hypothesis H1.

Here we complement this study by investigating radial diaphyseal morphology. Variability in radial growth results in variability in external (subperiosteal) surface morphology and cortical bone thickness. These features are correlated with musculoskeletal topography (Lovejoy et al., 2002; Morimoto et al., 2011b) and cross-sectional biomechanical properties (Ruff, 2003b, 2003a; Högler et al., 2008), respectively. Specifically, we ask whether prenatal subperiosteal morphology of the hominoid femoral diaphysis reflects phyletic history (H0) or taxon-specific locomotor adaptations (H1). In the first case (H0), human and chimpanzee morphologies should exhibit several shared-derived features compared to gorilla and orangutan morphologies. In the second case (H1), the fetal/neonate diaphyseal surface morphology of humans should be distinct from that of all great ape taxa, while chimpanzees and gorillas should be more similar to each other than to orangutans.

Three-dimensional data of femoral diaphyses were acquired with computed tomography (CT) from a sample of late fetal to neonate humans, chimpanzees, gorillas, and orangutans (see Materials and Methods). Data were analyzed with methods of morphometric mapping (MM), which are well suited to quantify the morphology of relatively featureless cylindroid structures such as long bone diaphyses (Morimoto et al., 2011a). In contrast to standard geometric-morphometric techniques, MM does not require pre-defined morphological features such as anatomical landmarks. Rather, morphological features characterizing the sample as a whole, or subsamples, are identified by means of the MM analysis. Here, the shape of the external diaphyseal surface is quantified by its transverse curvature (=curvature around the shaft), which closely reflects the topography of muscular attachment sites (Morimoto et al., 2011a, 2011b) (during the fetal period the internal (endosteal) surface is not yet fully ossified and hence cannot be quantified reliably (Scheuer et al., 2000; Standring, 2004)). Hereafter we use *diaphyseal surface morphology* to denote the resulting MMs (see Materials and Methods, Fig. S1). MMs of all specimens of the sample were aligned so as to minimize differences in rotation around the diaphyseal longitudinal axis. The aligned MMs were then submitted to 2D Fourier

Analysis. Principal Components Analysis (PCA) was used to reduce the high dimensionality of the data in Fourier space. This procedure permits to characterize principal patterns of shape variation in the sample (Fig. 1A), to quantify phenetic similarity between taxa (Lockwood et al., 2004) (Fig. 1B), and to visualize commonalities and differences between taxon-specific diaphyseal morphologies (Fig. 1C).

Results and Discussion

MM-based analysis shows that taxon-specific femoral diaphyseal surface morphologies are already present before birth (Fig. 1). Graphing the first two shape components (SC1 and SC2), which account for 23.9% and 15.1% of the total shape variation in the sample indicates that diaphyseal surface morphologies of gorillas (G) and orangutans (O) are more similar to each other than to any other taxon, while diaphyseal morphologies of chimpanzees (C) and humans (H) are approximately equally distant from GO morphologies (Table 1). Differences between taxa along SC1 partly reflect differences in neonatal body mass (Fig. S2A), while differences along shape component 2 are independent of body mass (Fig. S2B). Furthermore, taxon-specific differences in diaphyseal shape are not due to differences in diaphyseal length and cross-sectional area (Fig. S3). Also, sex-specific shape differences could not be found at this early stage of development.

Using orangutans as an outgroup, a phyletic tree evaluated from the data of Fig. 1A clearly groups humans with chimpanzees (HC), versus gorillas (Fig. 1B). Tree topology is well supported by bootstrapping (999 replications of the given tree out of 1000 resamplings). This phene-based tree is consistent with molecular trees of human and great ape phyletic divergence (Kumar et al., 2005; Patterson et al., 2006; Hobolth et al., 2007), supporting hypothesis H0 that femoral diaphyseal surface morphology in the fetal/neonatal period reflects hominoid phylogeny.

Taxon-specific perinatal femoral diaphyseal surface morphologies are visualized in Fig. 1C. The proximal femoral diaphysis of G and O is characterized by the presence of a prominent lateral spiral pilaster (*lp*) (Lovejoy et al., 2002; Lovejoy et al., 2009d), which is delimited by fossae on its inferolateral and superomedial sides (*ilf* and *smf*) (Morimoto et al., 2011b). Also, GO femora are characterized by a marked lateral ridge (*lr*) on the distal diaphysis. H and C femoral diaphyses also exhibit a *lp*, but it is only weakly expressed compared to GO. Most notably, the HC femur is characterized by the presence of a linea aspera (*la*) along the posterolateral diaphysis. This feature has a similar position and orientation in humans and chimpanzees, and is not present on GO femora (Fig. 1C).

Which evolutionary processes gave rise to this pattern of morphological similarity and dissimilarity between taxa? Before this question can be addressed, the potential influence of environmental factors and associated loading regimes on fetal long bone development has to be considered. In the uterus, the effects of gravitation are neutralized by buoyancy, but the fetal skeleton experiences loads through spontaneous fetal limb movements, as well as reactive and inertial forces elicited by maternal movements. Clinical evidence shows that spontaneous fetal limb movements are important for normal limb development (Kuwata et al., 2011). These movements are mediated by central pattern generators (MacKay-Lyons, 2002), i.e., genetically programmed neural networks. Fetal movements thus reflect the developmental state of the neuromotor system rather than environmental factors (Lacquaniti et al., 2012). Also, our results make it unlikely that taxon-specific maternal locomotor/postural behaviors influence fetal long bone morphology. For example,

chimpanzee and gorilla neonatal femora have a clearly distinct morphology (Fig. 1) despite largely similar neonatal body size (Table S1) (Leigh and Shea, 1996; Smith and Leigh, 1998; DeSilva, 2011) and maternal locomotor behaviors, while gorilla and orangutan neonates have similar femoral diaphyseal morphology, despite significant differences in maternal locomotor behaviors. Overall, it appears unlikely that differences in intrauterine loading regimes contribute substantially to taxon-specific differences in femoral diaphyseal morphology.

The following evolutionary scenarios bringing about the observed differences between taxa may thus be considered (Fig. 2): (a) H and C similarities in femoral diaphyseal morphology represent shared-derived features, which go back to the last common ancestor (HC-LCA) (Fig. 2A), (b) H and C morphologies evolved independently from an African great ape ancestor (Fig. 2B), and (c) G and O morphologies represent derived states, while the HC-LCA represents the primitive state (Fig. 2C);

Scenarios (b) and (c) imply that similar morphologies result from parallel and convergent evolution, respectively. This is unlikely, given the substantial differences between H and C with respect to locomotor behaviors and associated selective pressures (obligate bipedalism versus predominant quadrupedalism), and between G and O (mostly terrestrial versus predominantly arboreal locomotion).

Scenario (a) is more parsimonious. Adopting this scenario as the most likely one, we may thus infer that, in HC, prenatal femoral diaphyseal ontogeny follows a derived mode, while GO represent the primitive mode. It has been suggested that chimpanzee and gorilla femoral diaphyseal morphologies reflect a shared femoropelvic musculoskeletal organization (Lovejoy et al., 2002; Lovejoy et al., 2009d). In contrast, our results indicate that chimpanzee and gorilla femoral morphologies are distinct already during early development. Together with evidence from musculoskeletal anatomy of ref. (Morimoto et al., 2011b), this adds to the growing evidence that HC phenetic similarities reflect their close phylogenetic relationship (Gibbs et al., 2000, 2002; Lockwood et al., 2004; Morimoto et al., 2011b). This is consistent with the hypothesis that knuckle-walking and associated skeletal adaptations of chimpanzees and gorillas evolved independently (Kivell and Schmitt, 2009).

It remains to be clarified to which extent the inferred derived HC-LCA diaphyseal surface morphology resulted from neutral evolution (i.e., evolution by drift (Kimura, 1968; Nei, 2007)), and/or from adaptation to taxon-specific locomotor behaviors, respectively. Since close links exist between femoral diaphyseal surface morphology and muscle topography (Morimoto et al., 2011b), we hypothesize that the HC-LCA underwent an adaptive shift in femoropelvic musculoskeletal organization. Inferences on possible HC-LCA locomotor specialization must remain speculative. If we assume that the posteriorly-located *la* of H and C neonate femora (Fig. 1C) represents a shared-derived feature, its inferred presence in the HC-LCA might indicate a modified function of the muscles inserting along this structure (e.g. the *gluteus maximus*) during hind limb-mediated body propulsion (Morimoto et al., 2011b).

While our data imply that H and C exhibit shared-derived femoral diaphyseal features relative to G, they also show that morphologies of both H and C diverged from the HC-LCA morphology, probably to a greater extent in H than in C (Figs. 1A,B). This is in concordance with fossil evidence from *Ardipithecus* indicating taxon-specific evolution of femoral morphology not only in hominins

but also in panins since their split from the HC-LCA (Lovejoy et al., 2009b; Lovejoy et al., 2009c; Lovejoy et al., 2009d; White et al., 2009).

Human and chimpanzee femoral diaphyseal features unique to each taxon (Figs. 1A,C) most likely reflect taxon-specific locomotor adaptations. For example, humans differ from chimpanzees in exhibiting a prominent anteromedial ridge (*amr*) and a ridge along the medial diaphysis (*mmr*; Fig. 1C) while chimpanzees show a more prominent posteromedial ridge (*pmr*). These morphological differences might reflect differences in the relative size and attachment areas of locomotor muscles around the femur (e.g. large vastus muscles relative to adductor/hamstring muscles in humans compared to chimpanzees (Lovejoy et al., 2002)). In addition to phyletic divergence, diaphyseal morphologies of H and C also diverge during postnatal development, with the effect that the morphology of the proximal femoral diaphysis of C becomes more similar to G, e.g. regarding the expression of the lateral spiral pilaster (*lsp*) (Lovejoy et al., 2002; Morimoto et al., 2011a). It remains to be elucidated in greater detail to which extent each of the diaphyseal features identified in Fig. 1C reflects taxon-specific locomotor function, and to which extent they reflect homology versus homoplasy.

Our data provide evidence that the surface morphology of the perinatal hominoid femoral diaphysis reflects phylogenetic affinities (hypothesis H0) to a greater extent than locomotor adaptation (hypothesis H1). The underlying processes of prenatal radial diaphyseal ontogeny appear to be evolutionarily more conservative than those of longitudinal ontogeny. The latter have been shown to reflect taxon-specific locomotor adaptations in terms of limb segment lengths and proportions (Schultz, 1973; Young and Hallgrimsson, 2005; Young et al., 2010). While the elongation of the hind limb ‑ which is a key feature of human bipedality (Young et al., 2010) ‑ could have been effected by a relatively minor modification of the developmental program (Serrat et al., 2007), radial ontogeny and associated femoral diaphyseal surface morphology seem to be constrained by muscular topography, which has been reported to reflect phyletic relationships in the hominoids (Gibbs et al., 2000, 2002; Morimoto et al., 2011b).

Materials and methods

Sample structure. The sample consists of femora of *Homo sapiens* (*N*=22; femoral diaphyseal length: 41.6-63.4mm), *Pan troglodytes* (*N*=17; 32.2-55.1mm), *Gorilla gorilla* (*N*=10; 20.0-59.9mm) and *Pongo pygmaeus* (*N*=8; 30.8-46.8mm) from late fetal stages (3 months pre-term) to neonate stages (before the eruption of the first deciduous molar; <2 months). Since femoral shape does not exhibit significant sex-specific differences at this early stage of development, we used taxon-specific pooled-sex samples. All specimens are from the Collections of the Anthropological Institute and Museum of the University of Zurich.

Volumetric data acquisition. Femora of wet (formalin-preserved, frozen or fresh cadaver) specimens were scanned using a Siemens 64-detector-array CT device (beam collimation 1.0mm; standard/bone kernels [B30/B60]; serial cross-sections reconstructed at 0.2mm intervals). Small specimens were scanned using a micro-CT scanner (µCT80, Scanco Medical, Switzerland; volume data reconstructed at an isotropic voxel resolution of 75 µm). Cross sections orthogonal to the principal axis of the femoral shaft were obtained by resampling the original volumetric data using the software Amira 4.1 (Mercury Systems).

Morphometric data acquisition. In immature specimens, unfused epiphyses are often missing, or their position relative to the diaphysis cannot be reconstructed reliably. We thus focus here on diaphyseal morphology. The femoral diaphysis was extracted from the CT volume data using epiphyseal lines as proximal and distal delimiters. Femoral diaphyseal length was measured as the distance between proximal and distal epiphyseal lines. Subperiosteal (external) outlines of each cross section were parameterized with elliptical Fourier analysis (EFA) (Kuhl and Giardina, 1982). EFA was used to reduce noise, and to define parametric outline functions. The curvature of the external diaphyseal surface (k_{ext}) was calculated analytically using the parametric functions of EFA. Resulting positive/negative values of the curvature k_{ext} denote convex/concave regions, respectively (see ref. (Morimoto et al., 2011a) for details).

Morphometric analysis. For each specimen, measurements of k_{ext} were sampled around each cross-sectional outline, and along the entire diaphyseal shaft. These data were normalized to their respective median values, and mapped onto a cylindrical coordinate system (ρ, θ, z), where $\rho=1/(2\pi)$=constant denotes the radius of the cylinder. Specimens were prealigned manually such that angle θ denotes the anatomical direction ($\theta=0^o \rightarrow 360^o$: anterior $\rightarrow$ medial $\rightarrow$ posterior $\rightarrow$ lateral $\rightarrow$ anterior), and z denotes the normalized position along the diaphysis ($z=0 \rightarrow 1$: distal $\rightarrow$ proximal) (Zollikofer and Ponce de León, 2001; Bondioli et al., 2010). Since ρ=constant, data can be visualized as two-dimensional morphometric maps $\mathbf{M}(\theta, z)$, and distributions $k_{ext}(\theta, z)$ (Fig. S1) can be represented as $K \times L$ matrices, where K and L denote the number of elements along z and θ, respectively ($K=L=300$).

For the comparative analysis of the morphometric maps $\mathbf{M}_i$ of all specimens $i=1 \ldots N$, differences between specimens in orientation around the diaphyseal long axis (θ) had to be minimized. This procedure is analogous to the Procrustes superposition used in anatomical landmark-based geometric morphometric analyses. However, because the morphometric maps of the femoral diaphysis do not contain predefined anatomical features, the alignment was performed in Fourier space. To this end, 2D-Fourier transforms $F(\mathbf{M}_i)$ of all $\mathbf{M}_i$ were calculated ($\mathbf{M}$ has a natural periodicity in θ), yielding $K \times L$ sets of Fourier coefficients, which define a specimen's diaphyseal shape as a point in multidimensional Fourier space. Specimens were aligned to each other by minimizing inter-specimen distances in Fourier space through rotation around θ (diaphyseal axis).

To reduce the high dimensionality of the data in Fourier space, and to identify principal patterns of shape variability in the sample, Fourier coefficient sets were submitted to Principal Components Analysis (PCA). To facilitate visual inspection and anatomical interpretation of the results of PCA, real-space morphometric maps were reconstructed by transforming a given point $\mathbf{P}^*$ in PC space into its corresponding set of Fourier coefficients $F(\mathbf{M}^*)$, and applying an inverse Fourier transform to obtain a morphometric map $\mathbf{M}^*$. This method was used to produce the MMs of Fig. 1C. Morphometric maps were false-color coded. All calculations were performed with MATLAB7.7 (MathWorks) (see ref. (Morimoto et al., 2011a) for details).

Similarity analysis. Dissimilarity matrices $\mathbf{D}$ were evaluated to represent all between-taxon distances D (quantified as Euclidean distances between taxon mean points; see Table 1) in shape space. Phenetic trees were evaluated for $\mathbf{D}$ with PHYLIP 3.69 (Felsenstein, 1989), using the neighbor-joining method.

References

Aiello L, Dean C. 1990. An Introduction to Human Evolutionary Anatomy. London: Academic Press.
Alexander RM. 2004. Bipedal animals, and their differences from humans. J Anat 204:321-330.
Amtmann E, Schmitt H. 1968. Über die Verteilung der Corticalisdichte im menschlichen Femurschaft und ihre Bedeutung für die Bestimmung der Knochenfestigkeit. Zeit Anat Entwick 127:25–41.
Bass S, Saxon L, Daly R, Turner C, Robling A, Seeman E, Stuckey S. 2002. Effect of mechanical loading on the size and shape of bone in pre-, peri-, and postpubertal girls: a study in tennis players. J Bone Miner Res 17:2274-2280.
Bass SL, Eser P, Daly R. 2005. The effect of exercise and nutrition on the mechanostat. J Musculoskelet Neuronal Interact 5:239-254.
Beddard F. 1893. Contributions to the anatomy of the anthropoid apes. Trans Zool Soc London 13:177-218.
Benazet JD, Zeller R. 2009. Vertebrate limb development: moving from classical morphogen gradients to an integrated 4-dimensional patterning system. Cold Spring Harbor Perspectives in Biology 1.
Benjamin M, Kumai T, Milz S, Boszczyk BM, Boszczyk AA, Ralphs JR. 2002. The skeletal attachment of tendons - tendon 'entheses'. Comparative Biochemistry and Physiology a-Molecular and Integrative Physiology 133:931-945.
Bennett MR, Harris JWK, Richmond BG, Braun DR, Mbua E, Kiura P, Olago D, Kibunjia M, Omuombo C, Behrensmeyer AK, Huddart D, Gonzalez S. 2009. Early hominin foot morphology based on 1.5-million-year-old footprints from Ileret, Kenya. Science 323:1197-1201.
Bertram JEA, Swartz SM. 1991. The law of bone transformation - a case of crying Wolff. Biol Rev Camb Philos Soc 66:245-273.
Boehm B, Westerberg H, Lesnicar-Pucko G, Raja S, Rautschka M, Cotterell J, Swoger J, Sharpe J. 2010. The role of spatially controlled cell proliferation in limb bud morphogenesis. PLoS Biol 8:e1000420.
Bondioli L, Bayle P, Dean C, Mazurier A, Puymerail L, Ruff C, Stock J, T. , Volpato V, Zanolli C, Macchiarelli R. 2010. Technical note: Morphometric maps of long bone shafts and dental roots for imaging topographic thickness variation. Am J Phys Anthropol 142:328-334.
Bookstein F. 1991. Morphometric Tools for Landmark Data: Geometry and Biology. Cambridge: Camnridge University Press.
Boyer E. 1935. The musculature of the inferior extremity of the orang-utan *Simia satyrus*. Am J Anat 56:192-256.
Bramble DM, Lieberman DE. 2004. Endurance running and the evolution of *Homo*. Nature 432:345-352.
Brunet M, Guy F, Pilbeam D, Mackaye HT, Likius A, Ahounta D, Beauvilain A, Blondel C, Bocherens H, Boisserie JR, De Bonis L, Coppens Y, Dejax J, Denys C, Duringer P, Eisenmann VR, Fanone G, Fronty P, Geraads D, Lehmann T, Lihoreau F, Louchart A, Mahamat A, Merceron G, Mouchelin G, Otero O, Campomanes PP, De Leon MP, Rage JC, Sapanet M, Schuster M, Sudre J, Tassy P, Valentin X, Vignaud P, Viriot L, Zazzo A, Zollikofer C. 2002. A new hominid from the Upper Miocene of Chad, central Africa. Nature 418:145-151.
Burr DB, Ruff CB, Johnson C. 1989. Structural adaptations of the femur and humerus to arboreal and terrestrial environments in 3 species of macaque. Am J Phys Anthropol 79:357-367.
Butterfield NC, McGlinn E, Wicking C. 2010. The molecular regulation of vertebrate limb patterning. In: Organogenesis in Development: Elsevier. p 319-341.
Cardoso FA, Henderson CY. 2010. Enthesopathy Formation in the Humerus: Data from Known Age-at-Death and Known Occupation Skeletal Collections. Am J Phys Anthropol 141:550-560.
Carlson K, Sumner D, Morbeck M, Nishida T, Yamanaka A, Boesch C. 2008a. Role of nonbehavioral factors in adjusting long bone siaphyseal atructure in free-ranging *Pan troglodytes*. Int J Primatol 29:1401-1420.

Carlson KJ. 2005. Investigating the form-function interface in African apes: Relationships between principal moments of area and positional behaviors in femoral and humeral diaphyses. Am J Phys Anthropol 127:312-334.

Carlson KJ, Doran-Sheehy DM, Hunt KD, Nishida T, Yamanaka A, Boesch C. 2006. Locomotor behavior and long bone morphology in individual free-ranging chimpanzees. J Hum Evol 50:394-404.

Carlson KJ, Judex S. 2007. Increased non-linear locomotion alters diaphyseal bone shape. J Exp Biol 210:3117-3125.

Carlson KJ, Lublinsky S, Judex S. 2008b. Do different locomotor modes during growth modulate trabecular architecture in the murine hind limb? Integr Comp Biol 48:385-393.

Carrier DR. 1996. Ontogenetic limits on locomotor performance. Physiol Zool 69:467-488.

Carrier DR, Anders C, Schilling N. 2011. The musculoskeletal system of humans is not tuned to maximize the economy of locomotion. Proc Natl Acad Sci U S A 108:18631-18636.

Carter GJ, editor. 1990. Skeletal biomineralization: patterns, processes, and evolutionary trends. New York: Van Nostrand Reinhold.

Cavagna GA, Heglund NC, Taylor CR. 1977. Mechanical work in terrestrial locomotion: two basic mechanisms for minimizing energy expenditure. Am J Physiol 233:R243-261.

Champneys F. 1871. On the muscles and nerves of a chimpanzee (*Troglodytes niger*) and a *Cynocepalus anubis*. J Anat Lond 6:176-211.

Cobb SN, O'Higgins P. 2007. The ontogeny of sexual dimorphism in the facial skeleton of the African apes. J Hum Evol 53:176-190.

Cowgill LW. 2007. Humeral torsion revisited: A functional and ontogenetic model for populational variation. Am J Phys Anthropol 134:472-480.

Crass E. 1952. Musculature of the hip and thigh of the chimpanzee : a comparison to man and other primates. PhD thesis, Univ Wisconsin.

Crompton RH, Vereecke EE, Thorpe SKS. 2008. Locomotion and posture from the common hominoid ancestor to fully modern hominins, with special reference to the last common panin/hominin ancestor. J Anat 212:501-543.

Demes B. 2007. In vivo bone strain and bone functional adaptation. Am J Phys Anthropol 133:717-722.

Demes B, Carlson KJ. 2009. Locomotor variation and bending regimes of capuchin limb bones. Am J Phys Anthropol 139:558-571.

Demes B, Jungers WL. 1993. Long-bone cross-sectional dimensions, locomotor adaptations and body-size in prosimian primates. J Hum Evol 25:57-74.

Demes B, Larson SG, Stern JT, Jr, , Jungers WL, Biknevicius AR, Schmitt D. 1994. The kinetics of primate quadrupedalism: hindlimb drive reconsidered. J Hum Evol 26:353-374.

Demes B, Qin YX, Stern JT, Jr., Larson SG, Rubin CT. 2001. Patterns of strain in the macaque tibia during functional activity. Am J Phys Anthropol 116:257-265.

DeSilva JM. 2011. A shift toward birthing relatively large infants early in human evolution. Proc Natl Acad Sci USA 108:1022-1027.

Dillon R, Othmer HG. 1999. A mathematical model for outgrowth and spatial patterning of the vertebrate limb bud. J Theor Biol 197:295-330.

Diogo R, Wood B. 2011. Soft-tissue anatomy of the primates: phylogenetic analyses based on the muscles of the head, neck, pectoral region and upper limb, with notes on the evolution of these muscles. J Anat 219:273-359.

Doran DM. 1992. The ontogeny of chimpanzee and pygmy chimpanzee locomotor behavior - a case-study of paedomorphism and its behavioral-correlates. J Hum Evol 23:139-157.

Doran DM. 1993. Comparative locomotor behavior of chimpanzees and bonobos - the influence of morphology on locomotion. Am J Phys Anthropol 91:83-98.

Doran DM. 1996. Comparative positional behabior of the African apes. In: McGrew MC, Marchant LF, Nishida T, editors. Great Ape Societies. Cambridge: Cambridge University Press.

Doran DM. 1997. Ontogeny of locomotion in mountain gorillas and chimpanzees. J Hum Evol 32:323-344.

Doran DM, Jungers WL, Sugiyama Y, Fleagle J, Heesy C. 2002. Multivariate and phylogenetic approaches to understanding chimpanzee and bonobo behavioral diversity. In: Boesch C, Hohmann G, Marchant LF, editors. Behavioural diversity in Chimpanzees and Bonobos. Cambridge: Cambridge University Press. p 14-34.

Drapeau MSM. 2008. Enthesis bilateral asymmetry in humans and African apes. Homo-Journal of Comparative Human Biology 59:93-109.

Elftman H. 1945. Torsion of the lower extremity. Am J Phys Anthropol-New Ser 3:255-265.

Felsenstein J. 1989. PHYLIP - Phylogeny Inference Package (Version 3.2). Cladistics 5:164-166.

Galik K, Senut B, Pickford M, Gommery D, Treil J, Kuperavage AJ, Eckhardt RB. 2004. External and internal morphology of the BAR 1002 ' 00 *Orrorin tugenensis* femur. Science 305:1450-1453.

Garland TJ, Rose MR. 2009. Experimental evolution: concepts, methods, and applications of selection experiments. Berkeley: University of California Press.

Gebo DL. 1992. Plantigrady and foot adaptation in African apes: Implications for hominid origins. Am J Phys Anthropol 89:29-58.

Gibbs S, Collard M, Wood B. 2000. Soft-tissue characters in higher primate phylogenetics. Proc Natl Acad Sci USA 97:11130-11132.

Gibbs S, Collard M, Wood B. 2002. Soft-tissue anatomy of the extant hominoids: a review and phylogenetic analysis. J Anat 200:3-49.

Gilbert CC, Rossie JB. 2007. Congruence of molecules and morphology using a narrow allometric approach. Proc Natl Acad Sci USA 104:11910-11914.

Goodall J. 1986. The Chimpanzees of Gombe. Cambridge: Harvard University Press.

Goodship AE, Lanyon LE, McFie H. 1979. Functional adaptation of bone to increased stress - experimental-study. Journal of Bone and Joint Surgery-American Volume 61:539-546.

Gould SJ, Lewontin RC. 1979. The spandrels of San Marco and the Panglossian paradigm: a critique of the adaptationist programme. Proc R Soc Lond, Ser B: Biol Sci 205:581-598.

Grabherr S, Cooper C, Ulrich-Bochsler S, Uldin T, Ross S, Oesterhelweg L, Bolliger S, Christe A, Schnyder P, Mangin P, Thali M. 2009. Estimation of sex and age of "virtual skeletons"–a feasibility study. Eur Radiol 19:419-429.

Griffin TM, Main RP, Farley CT. 2004. Biomechanics of quadrupedal walking: how do four-legged animals achieve inverted pendulum-like movements? J Exp Biol 207:3545-3558.

Groote ID, Lockwood AC, Aiello CL. 2010. Technical note: A new method for measuring long bone curvature using 3D landmarks and semi-landmarks. Am J Phys Anthropol 141:658-664.

Gunz P, Mitteroecker P, Bookstein FL. 2005. Semilandmarks in Three Dimensions. In: Slice DE, editor. Developments in Primatology: Progress and Prospects. New York: Springer.

Harmon EH. 2007. The shape of the hominoid proximal femur: a geometric morphometric analysis. J Anat 210:170-185.

Harmon EH. 2009. The shape of the early hominin proximal femur. Am J Phys Anthropol 139:154-171.

Harrison T. 2010. Apes among the tangled branches of human origins. Science 327:532-534.

Heinrich RE, Ruff CB, Adamczewski JZ. 1999. Ontogenetic changes in mineralization and bone geometry in the femur of muskoxen (Ovibos moschatus). J Zool 247:215-223.

Hepburn D. 1892. Comparative anatomy of the muscles and nerves of the superior and inferior extremities of the anthropoid apes: Part II. J Anat Physiol 26:324-356.

Hobolth A, Christensen OF, Mailund T, Schierup MH. 2007. Genomic relationships and speciation times of human, chimpanzee, and gorilla inferred from a coalescent hidden Markov model. PLoS Genet 3:294-304.

Högler W, Blimkie CJR, Cowell CT, Inglis D, Rauch F, Kemp AF, Wiebe P, Duncan CS, Farpour-Lambert N, Woodhead HJ. 2008. Sex-specific developmental changes in muscle size and bone geometry at the femoral shaft. Bone 42:982-989.

Holliday TW, Hutchinson VT, Morrow MMB, Livesay GA. 2010. Geometric morphometric analyses of hominid proximal femora: Taxonomic and phylogenetic considerations. Homo-Journal of Comparative Human Biology 61:3-15.

Holt BM. 2003. Mobility in Upper Paleolithic and Mesolithic Europe: Evidence from the lower limb. Am J Phys Anthropol 122:200-215.

Hrdlička A. 1934. The hypotrochanteric fossa of the femur. Smithon Misc Coll 92:1-49.
Hunt K. 1991. Positional behavior in the Hominoidea. Int J Primatol 12:95-118.
Hunt K, Cant J, Gebo D, Rose M, Walker S, Youlatos D. 1996. Standardized descriptions of primate locomotor and postural modes. Primates 37:363-387.
Jensvold MLA, Sanz CM, Fouts RS, Fouts DH. 2001. Effect of enclosure size and complexity on the behaviors of captive chimpanzees (*Pan troglodytes*). J Appl Anim Welf Sci 4:53- 69.
Jones HH, Priest JD, Hayes WC, Tichenor CC, Nagel DA. 1977. Humeral hypertrophy in response to exercise. J Bone Joint Surg Am 59:204-208.
Jungers WL, Minns RJ. 1979. Computed tomography and biomechanical analysis of fossil long bones. Am J Phys Anthropol 50:285-290.
Kimura M. 1968. Evolutionary rate at the molecular level. Nature 217:624-626.
Kimura T. 1991. Long and robust limb bones of primates. In: Ehara A, Kimura T, Takenaka O, Iwamoto M, editors. Primatology Today. New York: Elsevier. p 495-498.
Kimura T. 1995. Long bone characteristics of primates. Z Morphol Anthropol 80:265-280.
Kimura T, Okada M, Ishida H. 1979. Kinesiological characteristics of primate walking: its significance in human walking. In: Morbeck M, Preuschoft H, Gomberg N, editors. Environment, Behavior, and Morphology: Dynamic Interactions in Primates. New York: Gustav Fischer. p 297-312.
Kivell TL, Schmitt D. 2009. Independent evolution of knuckle-walking in African apes shows that humans did not evolve from a knuckle-walking ancestor. Proc Natl Acad Sci USA 106:14241-14246.
Kronenberg HM. 2006. PTHrP and skeletal development. Ann N Y Acad Sci 1068:1-13.
Kuhl F, Giardina C. 1982. Elliptic Fourier features of a closed contour. Computer graphics and image processing 18:236-258.
Kumar S, Filipski A, Swarna V, Walker A, Hedges SB. 2005. Placing confidence limits on the molecular age of the human-chimpanzee divergence. Proc Natl Acad Sci USA 102:18842-18847.
Kuwata T, Matsubara S, Ohkusa T, Yada Y, Suzuki M. 2011. Decreased fetal movement prompts investigation of prenatal/neonatal nemaline myopathy: The possible merit of fetal movement count. Journal of Obstetrics and Gynaecology Research 37:921-925.
Lacquaniti F, Ivanenko YP, Zago M. 2012. Development of human locomotion. Curr Opin Neurobiol 22:1-7.
Lammers AR, German RZ. 2002. Ontogenetic allometry in the locomotor skeleton of specialized half-bounding mammals. J Zool 258:485-495.
Lanyon LE. 1987. Functional strain in bone tissue as an objective, and controlling stimulus for adaptive bone remodeling. J Biomech 20:1083-1093.
Lanyon LE, Baggott DG. 1976. Mechanical function as an influence on structure and form of bone. J Bone Joint Surg-Br Vol 58:436-443.
Lanyon LE, Bourn S. 1979. Influence of mechanical function on the development and remodeling of the tibia - experimental-study in sheep. Journal of Bone and Joint Surgery-American Volume 61:263-273.
Leakey MD, Hay RL. 1979. Pliocene footprints in the Laetolil beds at Laetoli, northern Tanzania. Nature 278:317-323.
Leigh SR, Shea BT. 1996. Ontogeny of body size variation in African apes. Am J Phys Anthropol 99:43-65.
Lieberman DE, Polk JD, Demes B. 2004. Predicting long bone loading from cross-sectional geometry. Am J Phys Anthropol 123:156-171.
Lieberman DE, Raichlen DA, Pontzer H, Bramble DM, Cutright-Smith E. 2006. The human gluteus maximus and its role in running. J Exp Biol 209:2143-2155.
Lockwood CA. 1999. Homoplasy and adaptation in the atelid postcranium. Am J Phys Anthropol 108:459-482.
Lockwood CA, Fleagle JG. 2007. Homoplasy in primate and human evolution. J Hum Evol 52:471-472.

Lockwood CA, Kimbel WH, Lynch JM. 2004. Morphometrics and hominoid phylogeny: Support for a chimpanzee-human clade and differentiation among great ape subspecies. Proc Natl Acad Sci USA 101:4356-4360.

Lovejoy CO, Burstein AH, Heiple KG. 1976. Biomechanical analysis of bone strength - method and its application to platycnemia. Am J Phys Anthropol 44:489-505.

Lovejoy CO, Latimer B, Suwa G, Asfaw B, White TD. 2009a. Combining prehension and propulsion: The foot of *Ardipithecus ramidus*. Science 326:72.

Lovejoy CO, McCollum MA, Reno PL, Rosenman BA. 2003. Developmental biology and human evolution. Annu Rev Anthropol 32:85-109.

Lovejoy CO, Meindl RS, Ohman JC, Heiple KG, White TD. 2002. The Maka femur and its bearing on the antiquity of human walking: Applying contemporary concepts of morphogenesis to the human fossil record. Am J Phys Anthropol 119:97-133.

Lovejoy CO, Simpson SW, White TD, Asfaw B, Suwa G. 2009b. Careful climbing in the Miocene: The forelimbs of *Ardipithecus ramidus* and humans are primitive. Science 326:70.

Lovejoy CO, Suwa G, Simpson SW, Matternes JH, White TD. 2009c. The great divides: *Ardipithecus ramidus* reveals the postcrania of our last common ancestors with African apes. Science 326:100-106.

Lovejoy CO, Suwa G, Spurlock L, Asfaw B, White TD. 2009d. The pelvis and femur of *Ardipithecus ramidus*: The emergence of upright walking. Science 326:71.

MacKay-Lyons M. 2002. Central pattern generation of locomotion: a review of the evidence. Phys Ther 82:69-83.

Main RP, Biewener AA. 2007. Skeletal strain patterns and growth in the emu hindlimb during ontogeny. J Exp Biol 210:2676-2690.

Minetti AE, Ardig OL, Reinach E, Saibene F, Prabhakar S, Visel A, Akiyama JA, Shoukry M, Lewis KD, Holt A, Plajzer-Frick I, Morrison H, Fitzpatrick DR, Afzal V, Pennacchio LA, Rubin EM, Noonan JP, Reno PL, McCollum MA, Cohn MJ, Meindl RS, Hamrick M, Lovejoy CO. 1999. The relationship between mechanical work and energy expenditure of locomotion in horses. J Exp Biol 202:2329-2338.

Mitteroecker P, Bookstein F. 2009. The ontogenetic trajectory of the phenotypic covariance matrix, with examples from craniofacial shape in rats and humans. Evolution 63:727-737.

Mitteroecker P, Gunz P, Bookstein FL. 2005. Heterochrony and geometric morphometrics: a comparison of cranial growth in *Pan paniscus* versus *Pan troglodytes*. Evol Dev 7:244-258.

Molnar P. 2006. Tracing prehistoric activities: Musculoskeletal stress marker analysis of a stone-age population on the island of Gotland in the Baltic Sea. Am J Phys Anthropol 129:12-23.

Morimoto N, Zollikofer CPE, Ponce de León MS. 2011a. Exploring femoral diaphyseal shape variation in wild and captive chimpanzees by means of morphometric mapping: a test of Wolff's Law. Anat Rec 294:589-609.

Morimoto N, Zollikofer CPE, Ponce de León MS. 2011b. Femoral morphology and femoropelvic musculoskeletal anatomy of humans and great apes: a comparative virtopsy study. Anat Rec 294:1433-1445.

Morishita Y, Iwasa Y. 2008. Growth based morphogenesis of vertebrate limb bud. Bull Math Biol 70:1957-1978.

Moro M, vanderMeulen MCH, Kiratli BJ, Marcus R, Bachrach LK, Carter DR. 1996. Body mass is the primary determinant of midfemoral bone acquisition during adolescent growth. Bone 19:519-526.

Mosley JR, Lanyon LE. 1998. Strain rate as a controlling influence on adaptive modeling in response to dynamic loading of the ulna in growing male rats. Bone 23:313-318.

Nei M. 2007. The new mutation theory of phenotypic evolution. Proc Natl Acad Sci U S A 104:12235-12242.

Netter F. 2003. Atlas of Human Anatomy, 3 ed. Philadelphia: Saunders.

O'Higgins P, Jones N. 1998. Facial growth in Cercocebus torquatus: an application of three-dimensional geometric morphometric techniques to the study of morphological variation. J Anat 193:251-272.

O'Neill MC, Dobson SD. 2008. The degree and pattern of phylogenetic signal in primate long-bone structure. J Hum Evol 54:309-322.

Patterson N, Richter DJ, Gnerre S, Lander ES, Reich D. 2006. Genetic evidence for complex speciation of humans and chimpanzees. Nature 441:1103-1108.

Pearson OM. 2000. Postcranial remains and the origin of modern humans. Evol Anthropol 9:229-247.

Pearson OM, Lieberman DE. 2004. The aging of Wolff's "Law": Ontogeny and responses to mechanical loading in cortical bone. Yearb Phys Anthropol 47:63-99.

Penin X, Berge C, Baylac M. 2002. Ontogenetic study of the skull in modern humans and the common chimpanzees: neotenic hypothesis reconsidered with a tridimensional Procrustes analysis. Am J Phys Anthropol 118:50-62.

Pickford M, Senut B, Gommery D, Treil J. 2002. Bipedalism in *Orrorin tugenensis* revealed by its femora. C R Palevol 1:191-203.

Polk JD, Demes B, Jungers WL, Biknevicius AR, Heinrich RE, Runestad JA. 2000. A comparison of primate, carnivoran and rodent limb bone cross-sectional properties: are primates really unique? J Hum Evol 39:297 - 325.

Ponce de León MS, Zollikofer CPE. 2001. Neanderthal cranial ontogeny and its implications for late hominid diversity. Nature 412:534-538.

Pontzer H, Raichlen DA, Sockol MD. 2009. The metabolic cost of walking in humans, chimpanzees, and early hominins. J Hum Evol 56:43-54.

Preuschoft H. 1970. Functional anatomy of the lower extremity. In: Bourne GH, editor. The Chimpanzee, Vol. 3. Basel: Karger. p 221-294.

Primrose A. 1898. The anatomy of the Orang utang (*Simia satyrus*). Trans Canad Inst 6:507-598.

Raichlen DA, Pontzer H, Shapiro LJ, Sockol MD. 2008. Understanding hind limb weight support in chimpanzees with implications for the evolution of primate locomotion. Am J Phys Anthropol 138:395-402.

Rauch F. 2005. Bone growth in length and width: the Yin and Yang of bone stability. J Musculoskelet Neuronal Interact 5:194-201.

Raven H. 1950. Regional anatomy of the gorilla. In: Gregory W, editor. The Anatomy of the Gorilla. New York: Columbia University Press.

Remis M. 1995. Effects of body size and social context on the arboreal activities of lowland gorillas in the Central African Republic. Am J Phys Anthropol 97:413-433.

Remis MJ. 1998. The effects of body size and habitat on the positional behavior of lowland and mountain gorillas. In: Strasser E, Fleagle J, Rosenberger A, McHenry H, editors. Primate Locomotion -Recent Advances. New York: Plenum Press. p 95-106.

Reynolds TR. 1985. Stresses on the limbs of quadrupedal primates. Am J Phys Anthropol 67:351-362.

Rhodes JA, Knüsel CJ. 2005. Activity-related skeletal change in medieval humeri: Cross-sectional and architectural alterations. Am J Phys Anthropol 128:536-546.

Richmond BG, Begun DR, Strait DS. 2001. Origin of human bipedalism: The knuckle-walking hypothesis revisited. In: Ruff C, editor. Yearbook of Physical Anthropology, Vol 44. p 70-105.

Richmond BG, Jungers WL. 2008. *Orrorin tugenensis* femoral morphology and the evolution of hominin bipedalism. Science 319:1662-1665.

Richmond BG, Strait DS. 2000. Evidence that humans evolved from a knuckle-walking ancestor. Nature 404:382-385.

Robling AG, Hinant FM, Burr DB, Turner CH. 2002. Improved bone structure and strength after long-term mechanical loading is greatest if loading is separated into short bouts. J Bone Miner Res 17:1545-1554.

Rodman PS, McHenry HM. 1980. Bioenergetics and the origin of hominid bipedalism. Am J Phys Anthropol 52:103-106.

Rohlf FJ. 1990. Rotational fit (Procrustes) methods. In: Rohlf F, Bookstein F, editors. Proceedings of the Michigan Morphometrics Workshop: Univ.of Michigan Museum of Zoology (Special Publication no. 2). p 227–236.

Rook L, Bondioli L, Kohler M, Moya-Sola S, Macchiarelli R. 1999. *Oreopithecus* was a bipedal ape after all: Evidence from the iliac cancellous architecture. Proc Natl Acad Sci USA 96:8795-8799.

Ruff CB. 1988. Hindlimb articular surface allometry in hominoidea and *Macaca*, with comparisons to diaphyseal scaling. J Hum Evol 17:687-714.
Ruff CB. 2002. Long bone articular and diaphyseal structure in old world monkeys and apes. I: Locomotor effects. Am J Phys Anthropol 119:305-342.
Ruff CB. 2003a. Growth in bone strength, body size, and muscle size in a juvenile longitudinal sample. Bone 33:317-329.
Ruff CB. 2003b. Ontogenetic adaptation to bipedalism: age changes in femoral to humeral length and strength proportions in humans, with a comparison to baboons. J Hum Evol 45:317-349.
Ruff CB. 2009. Relative limb strength and locomotion in *Homo habilis*. Am J Phys Anthropol 138:90-100.
Ruff CB, Hayes WC. 1983. Cross-sectional geometry of Pecos Pueblo femora and tibiae--a biomechanical investigation: I. Method and general patterns of variation. Am J Phys Anthropol 60:359-381.
Ruff CB, Holt B, Trinkaus E. 2006. Who's afraid of the big bad wolff? "Wolff is law" and bone functional adaptation. Am J Phys Anthropol 129:484-498.
Ruff CB, McHenry HM, Thackeray JF. 1999. Cross-sectional morphology of the SK 82 and 97 proximal femora. Am J Phys Anthropol 109:509-521.
Ruff CB, Runestad JA. 1992. Primate limb bone structural adaptations. Annu Rev Anthropol 21:407-433.
Ruff CB, Trinkaus E, Walker A, Larsen CS. 1993. Postcranial robusticity in *Homo*. I: Temporal trends and mechanical interpretation. Am J Phys Anthropol 91:21-53.
Ruff CB, Walker A, Trinkaus E. 1994. Postcranial robusticity in *Homo*. III: ontogeny. Am J Phys Anthropol 93:35-54.
Scheuer L, Black S, Christie A. 2000. Developmental Juvenile Osteology. San Diego, San Francisco, New York, Boston, London, Sydney, Tokyo: Academic Press.
Schmitt D. 2003. Insights into the evolution of human bipedalism from experimental studies of humans and other primates. J Exp Biol 206:1437-1448.
Schmitt D, Lemelin P. 2002. The origins of primate locomotion: gait mechanics of the woolly opossum. Am J Phys Anthropol 118:231-238.
Schultz AH. 1937. Proportions, variability and asymmetries of the long bones of the limbs and the clavicles in man and apes. Hum Biol 9:281-328.
Schultz AH. 1969. The skeleton of the chimpanzee. In: Bourne GH, editor. The Chimpanzee, Vol. 1. Basel: Karger. p 50-103.
Schultz AH. 1973. Age changes, variability and generic differences in body proportions of recent hominoids. Folia Primatol 19:338-359.
Schwartz JH. 1995. Skeleton Keys: An Introduction to Human Skeletal Morphology, Development, and Analysis. Oxford: Oxford University Press.
Senut B, Pickford M, Gommery D, Mein P, Cheboi K, Coppens Y. 2001. First hominid from the Miocene (Lukeino Formation, Kenya). C R Acad Sci Paris Ser II a 332:137-144.
Serrat MA, King D, Lovejoy CO. 2008. Temperature regulates limb length in homeotherms by directly modulating cartilage growth. Proc Natl Acad Sci USA 105:19348-19353.
Serrat MA, Lovejoy CO, King D. 2007. Age- and site-specific decline in insulin-like growth factor-I receptor expression is correlated with differential growth plate activity in the mouse hindlimb. The Anatomical Record: Advances in Integrative Anatomy and Evolutionary Biology 290:375-381.
Shea BT. 1981. Relative growth of the limbs and trunk in the African apes. Am J Phys Anthropol 56:179-201.
Sigmon BA. 1974. A functional analysis of pongid hip and thigh musculature. J Hum Evol 3:161-185.
Smith RJ, Leigh SR. 1998. Sexual dimorphism in primate neonatal body mass. J Hum Evol 34:173-201.
Sockol MD, Raichlen DA, Pontzer H. 2007. Chimpanzee locomotor energetics and the origin of human bipedalism. Proc Natl Acad Sci USA 104:12265-12269.
Sparacello V, Marchi D. 2008. Mobility and subsistence economy: A diachronic comparison between two groups settled in the same geographical area (Liguria, Italy). Am J Phys Anthropol 136:485-495.

Sparacello VS, Pearson OM. 2010. The importance of accounting for the area of the medullary cavity in cross-sectional geometry: A test based on the femoral midshaft. Am J Phys Anthropol 143:612–624.

Specht M, Lebrun R, Zollikofer CPE. 2007. Visualizing shape transformation between chimpanzee and human braincases. Visual Computer 23:743-751.

Standring S, editor. 2004. Gray's Anatomy, 39 ed. Edinburgh/London/New York: Churchill Livingstone.

Standring S, editor. 2005. Gray's anatomy: Churchill Livingstone.

Stern JT. 1972. Anatomical and functional specializations of human gluteus maximus. Am J Phys Anthropol 36:315-338.

Stern JT, Susman RL. 1981. Electromyography of the gluteal muscles in *Hylobates*, *Pongo*, and *Pan* - implications for the evolution of hominid bipedality. Am J Phys Anthropol 55:153-166.

Sumner DR, Andriacchi TP. 1996. Adaptation to differential loading: Comparison of growth-related changes in cross-sectional properties of the human femur and humerus. Bone 19:121-126.

Sutherland DH, Olshen R, Cooper L, Woo SL. 1980. The development of mature gait. J Bone Joint Surg Am 62:336-353.

Swindler D, Wood C. 1982. An Atlas of Primate Gross Anatomy. Malabar: Robert E. Krieger Publishing Company.

Szivek JA, Johnson EM, Magee FP. 1992. *In vivo* strain analysis of the greyhound femoral diaphysis. Journal of Investigative Surgery 5:91-108.

Thali MJ, Dirnhofer R, Vock P, editors. 2009. The Virtopsy Approach. New York: CRC Press.

Thali MJ, Jackowski C, Oesterhelweg L, Ross SG, Dirnhofer R. 2007. Virtopsy - The Swiss virtual autopsy approach. Legal Med 9:100-104.

Thorpe SK, Crompton RH. 2005. Locomotor ecology of wild orangutans (*Pongo pygmaeus abelii*) in the Gunung Leuser Ecosystem, Sumatra, Indonesia: a multivariate analysis using log-linear modelling. Am J Phys Anthropol 127:58-78.

Thorpe SK, Crompton RH. 2006. Orangutan positional behavior and the nature of arboreal locomotion in Hominoidea. Am J Phys Anthropol 131:384-401.

Thorpe SKS, Holder RL, Crompton RH. 2007. Origin of human bipedalism as an adaptation for locomotion on flexible branches. Science 316:1328-1331.

Trinkaus E, Churchill SE, Ruff CB. 1994. Postcranial robusticity in *Homo*. II: Humeral bilateral asymmetry and bone plasticity. Am J Phys Anthropol 93:1-34.

Turley K, Guthrie EH, Frost SR. 2011. Geometric Morphometric Analysis of Tibial Shape and Presentation Among Catarrhine Taxa. The Anatomical Record: Advances in Integrative Anatomy and Evolutionary Biology 294:217-230.

Turner CH, Forwood MR, Otter MW. 1994. Mechanotransduction in bone - do bone-cells act as sensors of fluid-flow. FASEB J 8:875-878.

Turner CH, Owan I, Takano Y. 1995. Mechanotransduction in bone - role of strain-rate. American Journal of Physiology-Endocrinology and Metabolism 269:E438-E442.

Tuttle RH, Watts DP. 1985. The positional behavior and adaptive complexes of *Pan gorilla*. In: Kondo S, Ishida S, Okada M, Kimura T, Yamazaki M, editors. Primate Morphophysiology, Locomotor Analyses and Human Bipedalism. Tokyo: University of Tokyo Press. p 261-288.

Uhlmann K. 1968. Hüft- und Oberschenkelmuskulatur: Systematische und vergleichende Anatomie. In: Hofer H, Schultz AH, Starck D, editors. Primatologia: Handbuch der Primatenkunde. Basel: Karger.

Van der Eerden BCJ, Karperien M, Gevers EF, Löwik CWGM, Wit JM. 2000. Expression of indian hedgehog, parathyroid hormone-related protein, and their receptors in the postnatal growth plate of the rat: evidence for a locally acting growth restraining feedback loop after birth. J Bone Miner Res 15:1045-1055.

van der Meulen MCH, Ashford MW, Kiratli BJ, Bachrach LK, Carter DR. 1996. Determinants of femoral geometry and structure during adolescent growth. J Orth Res 14:22-29.

Villotte S, Castex D, Couallier V, Dutour O, Knusel CJ, Henry-Gambier D. 2010. Enthesopathies as occupational stress markers: evidence from the upper limb. Am J Phys Anthropol 142:224-234.

Wallace IJ, Middleton KM, Lublinsky S, Kelly SA, Judex S, Garland T, Demes B. 2010a. Functional significance of genetic variation underlying limb bone diaphyseal structure. Am J Phys Anthropol 143:21-30.

Wallace IJ, Middleton KM, Svetlana L, Kelly SA, Stefan J, Theodore G, Jr., Brigitte D. 2010b. Functional significance of genetic variation underlying limb bone diaphyseal structure. In.

Wallace IJ, Tommasini SM, Judex S, Garland T, Demes B. 2012. Genetic variations and physical activity as determinants of limb bone morphology: An experimental approach using a mouse model. Am J Phys Anthropol 148:24-35.

Ward CV. 2002. Interpreting the posture and locomotion of *Australopithecus afarensis*: where do we stand? Am J Phys Anthropol Suppl 35:185-215.

Warden SJ, Hurst JA, Sanders MS, Turner CH, Burr DB, Li J. 2005. Bone adaptation to a mechanical loading program significantly increases skeletal fatigue resistance. J Bone Miner Res 20:809-816.

Weiss E. 2004. Understanding muscle markers: Lower limbs. Am J Phys Anthropol 125:232-238.

White TD, Asfaw B, Beyene Y, Haile-Selassie Y, Lovejoy CO, Suwa G, WoldeGabriel G. 2009. *Ardipithecus ramidus* and the paleobiology of early hominids. Science 326:75-86.

Wolff J. 1892. Das Gesetz der Transformation der Knochen. Berlin: A. Hirschwald.

Wolff J. 1986. The law of bone remodeling. Berlin: Springer-Verlag.

Wood B, Harrison T. 2011. The evolutionary context of the first hominins. Nature 470:347-352.

Wood B, Richmond BG. 2000. Human evolution: taxonomy and paleobiology. J Anat 197 (Pt 1):19-60.

Yamanaka A, Gunji H, Ishida H. 2005. Curvature, length, and cross-sectional geometry of the femur and humerus in anthropoid primates. Am J Phys Anthropol 127:46-57.

Young JW. 2009. Ontogeny of joint mechanics in squirrel monkeys (*Saimiri boliviensis*): functional implications for mammalian limb growth and locomotor development. J Exp Biol 212:1576-1591.

Young JW, Fernandez D, Fleagle JG. 2009. Ontogeny of long bone geometry in capuchin monkeys (Cebus albifrons and Cebus apella): implications for locomotor development and life history. Biol Lett 6:197-200.

Young NM, Hallgrimsson B. 2005. Serial homology and the evolution of mammalian limb covariation structure. Evolution 59:2691-2704.

Young NM, Wagner GP, Hallgrímsson B. 2010. Development and the evolvability of human limbs. Proc Natl Acad Sci USA 107:3400-3405.

Zollikofer CPE, de Leon MSP, Lieberman DE, Guy F, Pilbeam D, Likius A, Mackaye HT, Vignaud P, Brunet M. 2005. Virtual cranial reconstruction of *Sahelanthropus tchadensis*. Nature 434:755-759.

Zollikofer CPE, Ponce de León MS. 2001. Computer-assisted morphometry of hominoid fossils: the role of morphometric maps. In: De Bonis L, Koufos G, Andrews P, editors. Phylogeny of the Neogene Hominoid Primates of Eurasia. Cambridge: Cambridge University Press. p 50-59.

Zollikofer CPE, Ponce de León MS. 2006. Neanderthals and modern humans - chimps and bonobos: similarities and differences in development and evolution. In: Harvati K, Harrison T, editors. Neanderthals Revisited: New Approaches and Perspectives. New York: Springer. p 71-88.

Acknowledgements

We thank P. Jans for help with sample preparation and CT scanning. The comments of C. Finlayson and M. Walker are greatly acknowledged. We are also grateful to the two anonymous reviewers for their valuable comments and suggestions.

Table 1. Morphometric distances between taxon-specific mean shapes

	H (*Homo*)	C (*Pan*)	G (*Gorilla*)
C (*Pan*)	3.41*	–	–
G (*Gorilla*)	3.32*	3.00*	–
O (*Pongo*)	3.10*	2.57*	0.64 (p=0.41)

* p<0.001

Table S1. Neonatal body mass of hominoids

Taxon	**Body mass (g)**	***N***	**Source**
Homo sapiens	3111.3*	11317	DeSilva, 2011
Pan troglodytes	1766	45	Leigh and Shea, 1996
Pan troglodytes	1766	68	DeSilva, 2011
Pan troglodytes mean	1766*	113	
Gorilla gorilla	2327	136	Leigh and Shea, 1996
Gorilla gorilla	2251(m), 1996 (f)	56, 55	Smith and Leigh, 1998
Gorilla gorilla mean	2236.1*	247	
Pongo pygmaeus	1965 (m), 1653 (f)	27, 28	Smith and Leigh, 1998
Pongo pygmaeus mean	1806.2*	55	

*used in Fig. S2

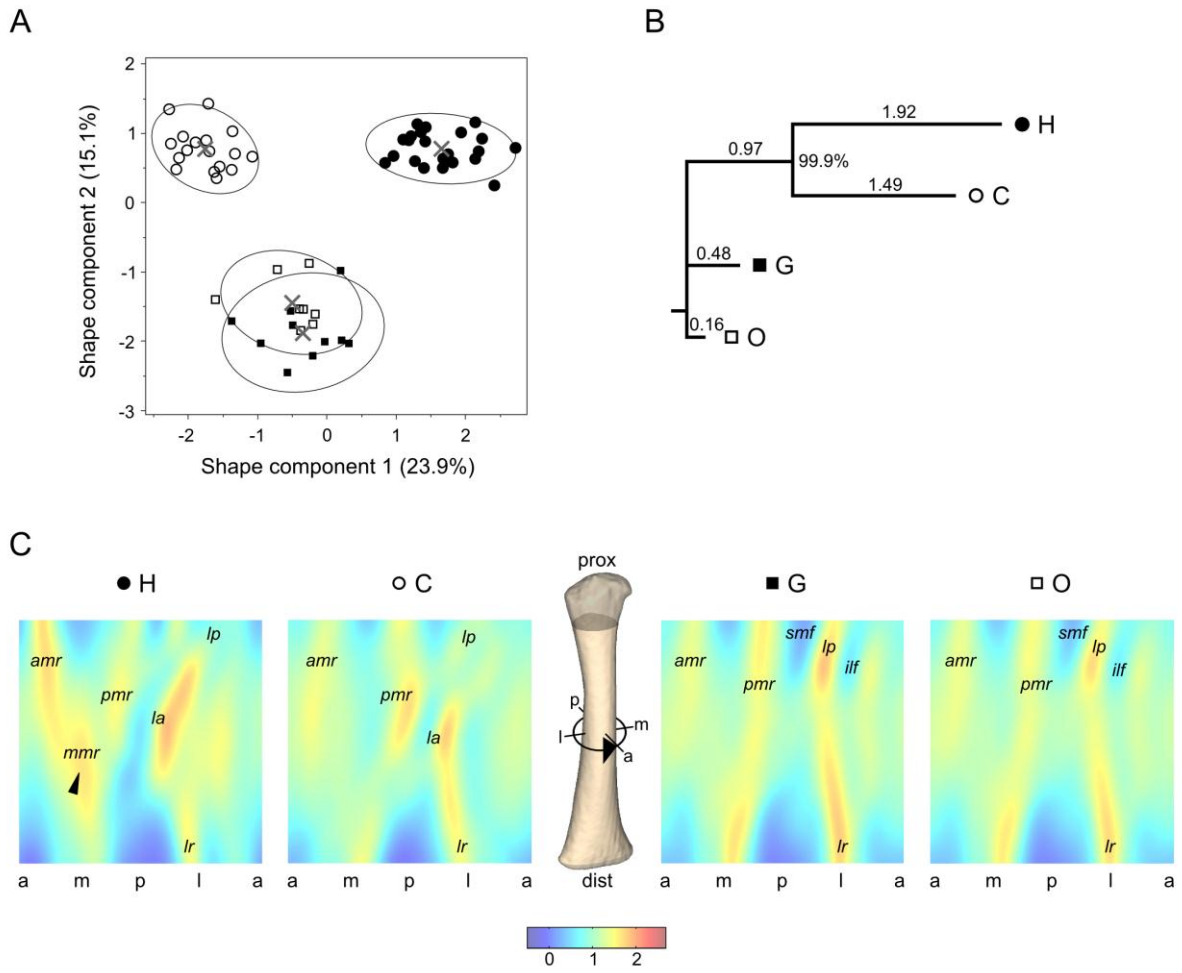

Fig. 1 Femoral diaphyseal shape variation in hominoids. A, variation along shape components 1 and 2 of morphospace (humans: filled circles, chimpanzees: open circles, gorillas: filled squares, orangutans: open squares; crosses/ellipses indicate taxon-specific means/90%-density ellipses). B, neighbor-joining tree based on between-taxon distances (see Table 1); numbers above branches indicate branch lengths; number at the branch node indicates bootstrap support (999 of 1000 replications); H: humans, C: chimpanzees, G: gorillas, O: orangutans. C, morphometric maps [false-color images of external surface curvature (relative units)] visualizing taxon-specific mean morphologies (a-m-p-l: anterior-medial-posterior-lateral); *la*: linea aspera, *lp*: lateral pilaster, *ilf*: inferolateral fossa, *smf*: superomedial fossa, *lr*: lateral ridge, *amr*: anteromedial ridge, *pmr*: posteromedial ridge, *mmr*: midshaft medial ridge.

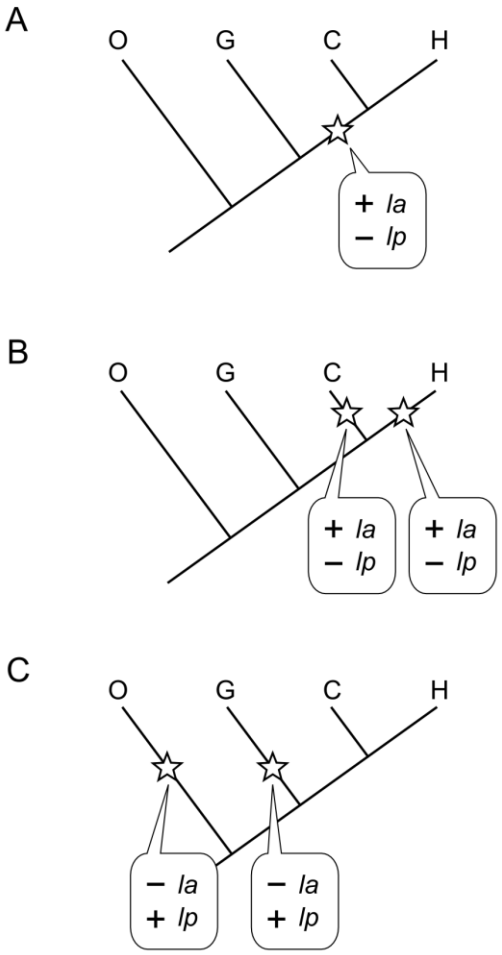

Fig. 2 Hypothetical scenarios of femoral diaphyseal shape evolution. Scenario A: shared-derived formation of linea aspera and reduction of lateral pilaster in humans and chimpanzees. Scenario B: parallel evolution of *la* and reduction of *lp*. Scenario C: convergent evolution of similar orangutan/gorilla features (see Fig. 1C for feature codes).

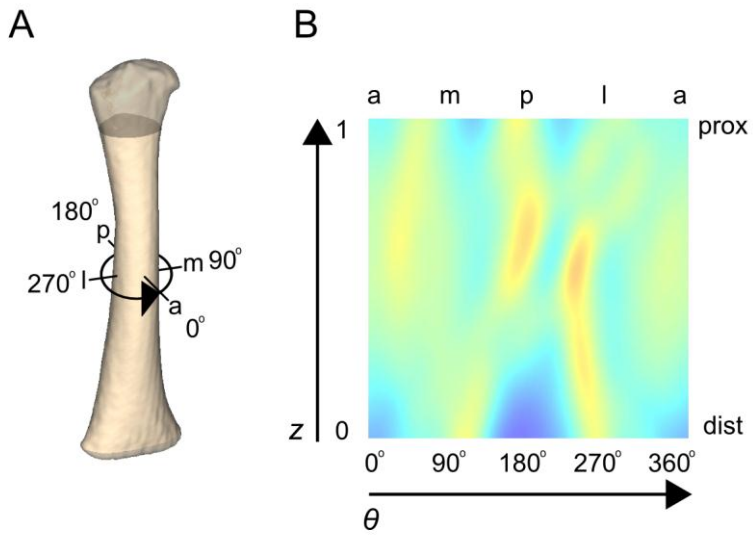

Fig. S1 Principle of morphometric mapping. A, 3D representation of the right femur. B, principle of cylindrical projection (anterior [0°] → medial [90°] → posterior [180°] → lateral [270°] → anterior [0°]).

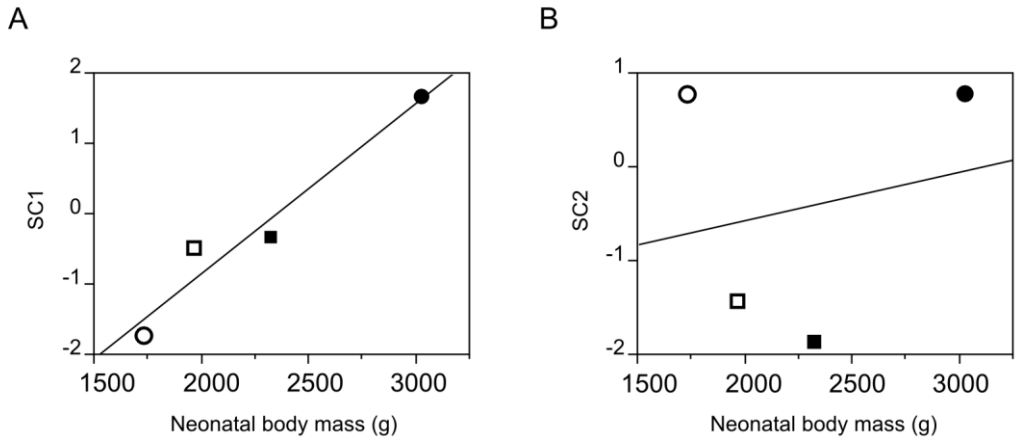

Fig. S2 Correlation between taxon-specific means of shape component scores and means of neonatal body mass (data summarized in Table S1; humans: filled circles, chimpanzees: open circles, gorillas: filled squares, orangutans: open squares). SC1 is weakly correlated with neonatal body mass (p=0.06, R^2=0.88) (A). SC2, which distinguishes between human-chimpanzee and gorilla-orangutan, is not correlated with neonatal body mass (B).

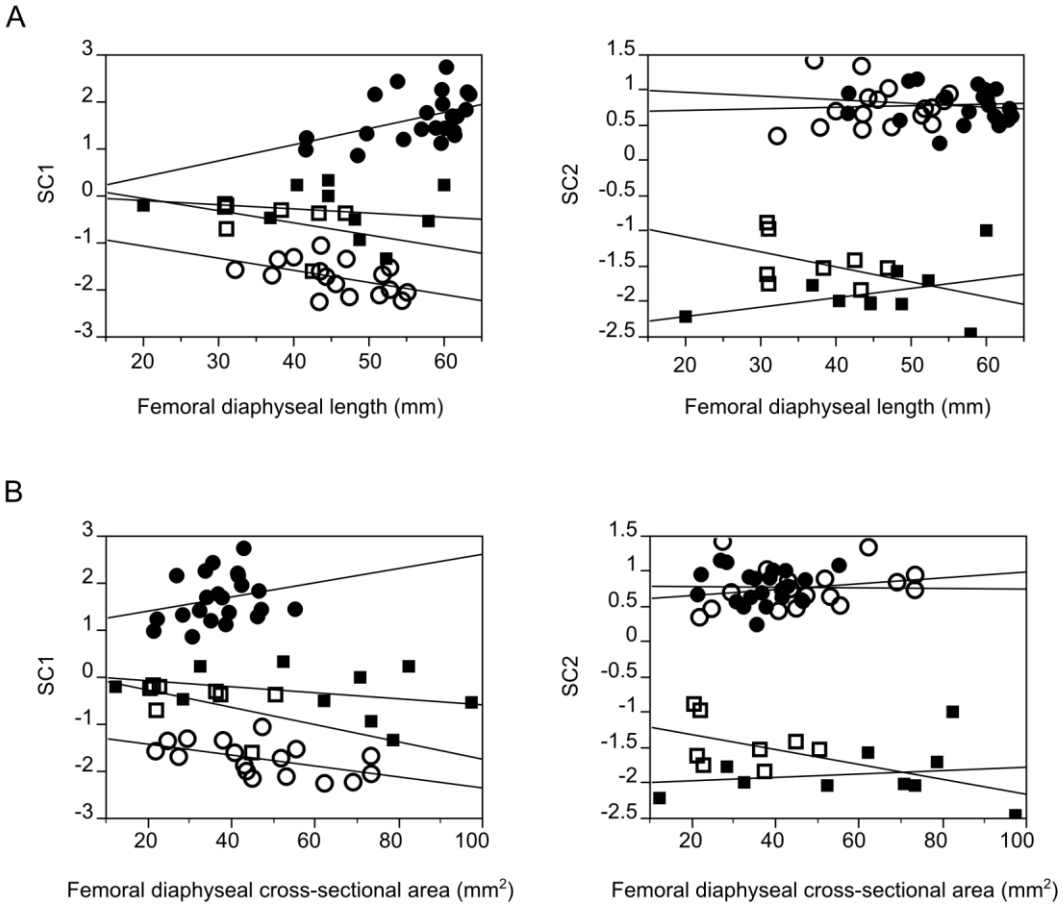

Fig. S3 Correlation between femoral diaphyseal shape component scores (SC1, SC2) and femoral size (humans: filled circles, chimpanzees: open circles, gorillas: filled squares, orangutans: open squares). Shape component scores are plotted against femoral diaphyseal length (A), and median femoral diaphyseal cross-sectional area (B). Each cross-sectional area was calculated as the total area of bone marrow-filled cross-section. Overall, taxon-specific differences in femoral diaphyseal length are not correlated with femoral diaphyseal morphology. Humans exhibit a weak correlation of SC1 with femoral diaphyseal length ($p<0.05$, $R^2=0.20$); chimpanzees exhibit a weak correlation of SC1 with femoral diaphyseal cross-sectional area ($p<0.05$, $R^2=0.28$).

Materials and methods

Specimen list

The following specimens are used in the studies of this thesis. Dental eruption scores represent the following ontogenetic stages; 1: Deciduous molar (DC) 1 erupted, 2: DC2 erupted, 3: M1 erupted, 4: M2 erupted, 5: M3 erupted.

Chapter 1

ID	Taxon	Individual life history	Femoral diaphyseal length (mm)	Dental eruption score
AM9968	*Pan troglodytes*	wild	79	–
AM7659	*Pan troglodytes*	wild	82	2
AS1813	*Pan troglodytes*	wild	86	2
AM6695	*Pan troglodytes*	wild	108	3
AM6613	*Pan troglodytes*	wild	109	3
AM6614	*Pan troglodytes*	wild	112	–
AS1786	*Pan troglodytes*	wild	113	3
AM6615	*Pan troglodytes*	wild	114	3
AM7480	*Pan troglodytes*	wild	117	3
AM7421	*Pan troglodytes*	wild	121	3
AM7056	*Pan troglodytes*	wild	128	3
AM9967	*Pan troglodytes*	wild	130	3
AM7009	*Pan troglodytes*	wild	135	3
AM6972	*Pan troglodytes*	wild	147	3
AM6616	*Pan troglodytes*	wild	167	4
PAL9	*Pan troglodytes*	wild	181	5
AM7078	*Pan troglodytes*	wild	198	5
AM6938	*Pan troglodytes*	wild	198	4
AM6876	*Pan troglodytes*	wild	201	5
MRAC29074	*Pan troglodytes*	wild	211	–
AS1586	*Pan troglodytes*	wild	212	5
AM7127	*Pan troglodytes*	wild	209	5
AM6670	*Pan troglodytes*	captive	89	2
AS1571	*Pan troglodytes*	captive	94	2
AS1662	*Pan troglodytes*	captive	98	2
AS1760	*Pan troglodytes*	captive	109	2
AS1787	*Pan troglodytes*	captive	109	3
AS788	*Pan troglodytes*	captive	115	2
PAL221	*Pan troglodytes*	captive	117	–
AS310	*Pan troglodytes*	captive	121	–
AS1808	*Pan troglodytes*	captive	143	3
AS1686	*Pan troglodytes*	captive	159	3
PAL194	*Pan troglodytes*	captive	159	3

ID	Taxon	Individual life history	Femoral diaphyseal length (mm)	Dental eruption score
PAL110	*Pan troglodytes*	captive	173	4
AS1687	*Pan troglodytes*	captive	178	4
PAL106	*Pan troglodytes*	captive	178	4
PAL217	*Pan troglodytes*	captive	181	5
PAL219	*Pan troglodytes*	captive	188	5
PAL191	*Pan troglodytes*	captive	191	–
AS1785	*Pan troglodytes*	captive	197	4
PAL96	*Pan troglodytes*	captive	197	5
AS1784	*Pan troglodytes*	captive	199	5
PAL175	*Pan troglodytes*	captive	200	5
AS1745	*Pan troglodytes*	captive	200	5
AM5920	*Pan troglodytes*	captive	203	4
AM10280	*Pan troglodytes*	captive	203	5
AS1789	*Pan troglodytes*	captive	206	4
AS1680	*Pan troglodytes*	captive	209	4

Chapter 2

ID	Taxon	Individual age	Sex	Dental eruption score	Preservation
Clinical data #1	*Homo sapiens*	adult	m	3	–
AIMUZH-7283	*Pan troglodytes*	infant	m	2	formalin
AIMUZH-n10003	*Pan troglodytes*	infant	f	2	frozen
AIMUZH-n10001	*Pan troglodytes*	adult	f	5	formalin
KCZ-Yoko (PRICT-34/218)	*Pan troglodytes*	adult (20y)	f	5	frozen
KUPRI-9262 (TKZ-Rick; PRICT-320)	*Pan troglodytes*	adult (22y)	m	5	frozen
AIMUZH-n10006	*Pan paniscus*	infant	–	2	frozen
AIMUZH-n10004	*Gorilla gorilla*	juvenile	m	4	formalin
AIMUZH-11427	*Pongo pygmaeus*	neonate	m	–	formalin

Chapter 3

ID	Taxon	Individual age	Femoral diaphyseal length (mm)
AM-HF1263-1	*Homo sapiens*	fetus	54
AM-HF1277 1a-1-1	*Homo sapiens*	fetus	58
AN697	*Homo sapiens*	fetus	59
AM1649	*Homo sapiens*	fetus	60
AM-HF1277-1-a1-9	*Homo sapiens*	fetus	61
AS195	*Homo sapiens*	fetus	61
AM-HF1277-1a-1-8	*Homo sapiens*	fetus	62
AM-HF1267-1	*Homo sapiens*	fetus	63
AM-HF1277-1a-1-2	*Homo sapiens*	fetus	63
AM-HF1277 1a 1-7	*Homo sapiens*	fetus	63
AM-HF1276_2_2	*Homo sapiens*	fetus	60
AM_Limb2	*Homo sapiens*	fetus	42
AM_Limb4	*Homo sapiens*	fetus	42
AM-HF1274_2_2	*Homo sapiens*	fetus	57
AM-HF1275_3_1	*Homo sapiens*	fetus	49
AM-HF1275_1	*Homo sapiens*	fetus	60
AM-HF1275_2	*Homo sapiens*	fetus	55
AM-HF1269A_1_1	*Homo sapiens*	fetus	60
AM-HF1277_1c_1	*Homo sapiens*	fetus	61
AM-HF1277_1c_5	*Homo sapiens*	fetus	50
AM-HF1278_2_1	*Homo sapiens*	fetus	60
AM-HF1278_2_2	*Homo sapiens*	fetus	51
AM6807	*Pan troglodytes*	neonate	32
AS445	*Pan troglodytes*	fetus	37
AM6830	*Pan troglodytes*	fetus	38
AM7529	*Pan troglodytes*	neonate	40
AM13308	*Pan troglodytes*	neonate	43
AS443	*Pan troglodytes*	neonate	44
AM13302	*Pan troglodytes*	neonate	44
AM13306	*Pan troglodytes*	neonate	46
AM13303	*Pan troglodytes*	neonate	47
AM6866	*Pan troglodytes*	neonate	47
AM13310	*Pan troglodytes*	neonate	53
AS1666	*Pan troglodytes*	neonate	53
AM13304	*Pan troglodytes*	neonate	54
AM5559	*Pan troglodytes*	neonate	55
AM9404	*Pan troglodytes*	neonate	44
AM9361	*Pan troglodytes*	neonate	51
AM11451	*Pan troglodytes*	neonate	52
MRAC76064	*Gorilla gorilla*	fetus	20
AM11455	*Gorilla gorilla*	fetus	37

ID	Taxon	Individual age	Femoral diaphyseal length (mm)
AM10045	*Gorilla gorilla*	neonate	41
AM10144	*Gorilla gorilla*	neonate	45
AM9290	*Gorilla gorilla*	neonate	45
AM10218	*Gorilla gorilla*	neonate	48
AM11440	*Gorilla gorilla*	neonate	49
AM11228	*Gorilla gorilla*	fetus	52
AM6674	*Gorilla gorilla*	fetus	58
AM Zoo Baby 1	*Gorilla gorilla*	neonate	60
AS1642	*Pongo pygmaeus*	fetus	31
AS1647	*Pongo pygmaeus*	fetus	31
AM2142	*Pongo pygmaeus*	fetus	31
AM8664	*Pongo pygmaeus*	neonate	43
AS1603	*Pongo pygmaeus*	neonate	43
AM1592	*Pongo pygmaeus*	neonate	47
AM11427	*Pongo pygmaeus*	neonate	38
APE381	*Pongo pygmaeus*	fetus	31

CT parameters

Femora of dry and wet (formalin-preserved, frozen or fresh cadaver) specimens are scanned using medical and micro CT scanners using the following parameters respectively:

Medical CT parameters

Device: Siemens 64-detector-array CT
Beam collimation (slice thickness): 1.0mm
Pitch: 0.5-0.75
Slice increment: 0.2-0.5mm
Reconstruction kernels: B30s (standard) and B60s/B70s (bone filter)

Micro CT parameters

Device: µCT80 (Scanco Medical, Switzerland)
Beam energy: 70kV
Beam intensity: 114µA
Integration time: 500ms
Image matrix: 1024×1024
Data are reconstructed at an isotropic voxel resolution of 75µm

Morphometric data acquisition and analysis

Details of morphometric data acquisition and analyses is documented in Chapter 1 (and in its appendix section), and in the appendix of this thesis. The program code implemented during this PhD thesis is available on request. All programs run on Matlab (Mathworks).

Conclusions

In this thesis, I asked whether long bone diaphyseal morphology and corresponding musculature reflect taxon-specific locomotor adaptations or phylogenetic relationships of hominoids (Fig. 1). The specific questions asked to tackle this issue, and the major conclusions drawn from the studies presented here can be summarized as follows:

a) How can the featureless long bone diaphyseal morphology be analyzed quantitatively?

To quantify, visualize and analyze the „landmark-depleted“ morphology of long bone diaphyses, the concept of Morphometric Mapping (MM) was extended from a visualization tool to an analytical toolkit, using concepts of elliptical Fourier analysis, 2D and multi-dimensional Fourier analysis, and principal components analysis. The proposed methods permit dense sampling and detailed quantitative analyses of geometric and biomechanical properties of long bone diaphyses, giving insights into subtle patterns of shape variation not detectable with traditional geometric morphometric methods.

(Chapter 1)

b) *In-vivo* loading history: does Wolff's Law apply to the ontogeny of long bone diaphyses?

Patterns of ontogenetic shape variation of femoral diaphyses were compared between wild and captive chimpanzees to examine the influence of *in-vivo* loading histories on adult shape variation. The results show that average patterns of femoral diaphyseal ontogeny are statistically indistinguishable between wild and captive groups. The results indicate that femoral diaphyseal morphology is determined dominantly by the genetically defined developmental program rather than *in-vivo* locomotor behavior, and that possible *in-vivo* effects of individual locomotor behaviors are cancelled out in overall developmental patterns.

(Chapter 1)

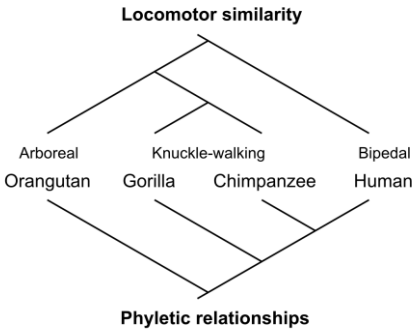

Fig. 1 Central hypotheses about possible causes underlying similarity of long bone shaft morphology among hominoid taxa

c) To which extent do femoropelvic musculoskeletal structures reflect phylogeny versus locomotor adaptation?

Two lines of evidence lend support to the hypothesis that long bone diaphyseal morphology and corresponding musculature reflect phyletic relationships and taxon-specific developmental programs rather than the actual locomotor adaptations of extant hominoid taxa.

First, femoropelvic musculoskeletal anatomy in modern humans and great apes was explored using methods of virtual dissection (virtopsy). Specifically, the topographic relationships between the attachment sites of *gluteus maximus*, *vastus lateralis* and the lateral pilaster were investigated in modern humans and great apes. The topography of the femoropelvic musculature is similar in humans and chimpanzees, despite substantially different locomotor adaptations. Also, topography is similar in gorillas and orangutans, despite different locomotor adaptations. On the other hand, gorillas and chimpanzees show substantially different topography of the femoropelvic musculature despite similar modes of terrestrial locomotion. This indicates that muscular topography and corresponding femoral surface topography reflect phylogenetic relationships rather than taxon-specific locomotor behaviors.

Second, femoral diaphyseal morphology of modern humans and great apes in the perinatal period was analyzed to investigate the morphological variability free from taxon-specific postnatal loading regimes. Femoral diaphyseal morphology of gorillas and orangutans is similar despite substantial differences in locomotor adaptation (obligate terrestrial versus arboreal locomotion). Gorillas and chimpanzees exhibit substantially different femoral diaphyseal morphologies despite similar modes of terrestrial locomotion (knuckle-walking). Humans and chimpanzees share several features of femoral diaphyseal morphology despite substantial differences in locomotor adaptations. These data indicate that femoral diaphyseal morphology reflects phyletic relationships rather than taxon-specific locomotor adaptations.

(Chapter 2, 3)

d) Taxon-specific developmental program: when do taxon-specific femoral diaphyseal features appear during ontogeny?

In hominoids, the basic taxon-specific patterns of femoral diaphyseal morphology and corresponding femoropelvic muscular topography are present already early during ontogeny (i.e., at birth) and are maintained throughout ontogeny. This indicates that long bone diaphyseal morphology and corresponding femoropelvic musculature largely reflect taxon-specific developmental programs.

(Chapter 1, 2, 3)

Collectively, the results of these studies converge in the conclusion that, in the hominoids, femoral diaphyseal morphology and corresponding topography of major locomotor muscles reflect phylogenetic relationships and taxon-specific developmental programs to a greater extent than taxon-specific locomotor adaptation (Fig. 1; lower tree).

Femoral morphology and human bipedality

What do the results of these studies mean for the evolution of human bipedality?

Analyzing possible form-function relationship of long bones is an important starting point to investigate the evolution of human bipedality and great ape locomotion. The femur, a functional key locomotor element, can be expected to have undergone substantial structural modifications during the acquisition of bipedality. The results of this thesis indicate that the classical form-function approach must be complemented by a form-function-*phylogeny* approach to long bone evolutionary morphology, which unifies form-function and phylogenetic questions.

The form-function-phylogeny approach takes into account the effects of evolutionary inertia as a top-down constraint, in a sense that "form follows phylogeny" rather than "form follows function". Function could then be explored with a bottom-up approach in a sense that biomechanical adaptation and *in-vivo* modification occurs within the framework of taxon-specific developmental constraints. For example, the inferred function/role of each locomotor muscle such as *gluteus maximus* in relation to skeletal morphology would be a relevant target in such an approach (e.g., whether a muscle functions more as extensor or abductor).

On the other hand, the results of this thesis contain „good news" for morphological studies: skeletal morphology and corresponding soft tissue structures are a golden mine to seek not only for function but also for phylogenetic relationships. It will be of special relevance to merge genetic evidence and detailed morphological evidence on long bone development and function to better understand the evolutionary diversification of the human and great ape locomotor system, and of the locomotor behavioral reaction norms made possible by these systems.

Appendix

A. Matlab-based toolkit implementation

Matlab basics

Matlab (Mathworks) is a program and a program language which is designed primarily for matrix calculations and is universally used in many disciplines today. Matlab offers a collection of tool-kits of data analysis and visualization. When starting Matlab, basic operations can be performed in two windows (Fig. 1). One can run calculations directly in the command window (Fig. 1A), but it is often more practical to create so-called script files (*.m files) that contain flows of functions (Fig. 1B-D).

Fig 1.B-D shows an example of the structure of scripts. One script (Fig. 1B) can be the core script of a program, and other scripts (Fig. 1C, D) can be the scripts that contain the parameters of the core script. For example, the core script can be the program that generates Morphometric Maps (MM), and parameters can be the specification of the dataset of PC (Principal Component) scores or the kind of false-color mapping scheme used to visualize the results.

Flow chart of the matlab-based codes

The procedure of *morphometric mapping analysis* consists of three steps: (a) image processing, (b) elliptic Fourier analysis and (c) multi-dimensional Fourier transform. Basically, all the program scripts are contained in the "work/ShapeThem" directory. Input data (such as long bone cross-sections) and output data are contained in the "work/morpho" directory. Set path to "work/naoki_function" (including the subdirectories). The detailed procedure is the following (matlab script files are shown in bold typeface):

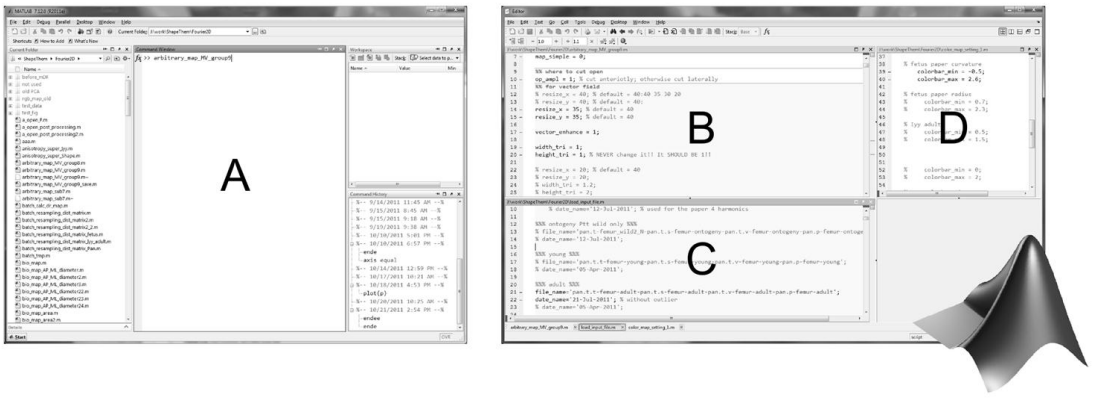

Fig. 1 Example of Matlab windows. A, command window. B-C, editor window. Programs can be run either by typing the name of the program in the command window (A) as in the console, or by clicking the "run program" button in the editor window. The command window is also used to show the results of calculations.

Image processing

1. Prepare diaphyseal axis-aligned binarized (bone-thresholded) image volumes (tiff-format) of long bone cross-sections using Amira or Avizo
    a. Create the surface of the bone of interest
        i. Compute -> Surface Gen
        ii. Display -> Surface View
    b. Align the surface along its principal axes
        i. Compute -> AlignPrincipalAxes
    c. Resample the original data set along principal axes
        i. Type "GetTransform *.surf" in console to get the transform matrix *T*
        ii. Type "SetTransform * *T*" in console
        iii. Compute -> ApplyTransform
2. Make new entries in the excel file ("work/morpho/slice_data/info.xls") which is referred to by the following matlab-codes.
    a. Here, each long bone is given a specimen number
3. Go to "work/ShapeThem/image_process"
4. Specify the specimen number(s) in "**batch_ImageProcessingAll_N.m**"
5. Run "**batch_ImageProcessingAll_N.m**"
    a. "**batch_ImageProcessingAll_N.m**" contains "**All_imageprocess.m**" that does dilation and erosion, contour-detection
    b. This calculates the coordinates of the contour points for each cross-section
    c. This also calculates the centroid coordinate for each cross-section

Elliptic Fourier analysis

1. Go to "work/ShapeThem/EllipticalFourier"
2. Specify the specimen number(s) in "**batch_AllFourier_N.m**"
3. Run "**batch_AllFourier_N.m**"
    a. This transforms contour coordinates into elliptic Fourier descriptors
4. Specify the specimen number(s) and the number of harmonics (i.e., level of detail) in "**batch_FourierMap_N.m**"
5. Run "**batch_FourierMap_N.m**"
6. Do the same (steps 4,5) for "**batch_FourierMap_diameter_N.m**" and "**batch_FourierMap_local_c_N.m**"

```
%% Pan subspecis
%%% ontogeny %%%
file_name='pan.t.t-femur-ontogeny-pan.t.s-femur-ontogeny-pan.t.v-femur-ontogeny-p
date_name='21-Jul-2011'; % data set 1
% date_name='20-Jul-2011'; % data set 2
```

Fig. 2 Example of specification in input file (a capture from an editor window). Here, *file_name* indicates names of taxa, bone, and data set (e.g., ontogenetic series versus adult individuals), and *date_name* indicates the date when the analysis was performed. Note that there are two datasets, but only one dataset is activated and the other one is commented out.

a. "**batch_FourierMap_N.m**", "**batch_FourierMap_diameter_N.m**" and "**batch_FourierMap_local_c_N.m**" calculate the cortical bone thickness, radius, and the surface curvature along and around the long bone diaphysis, respectively

Multi-dimensional Fourier transform

1. Go to "work/ShapeThem/Fourier2D"
2. Run "**Fourier2Dn_AP.m**"
    a. This transforms morphometric maps (MMs) into 2 (or higher) dimensional Fourier descriptors
    b. Each MM is normalized by its median value here
    c. A parameter to be specified is whether Fourier transform runs on entire MM, or separately on proximal, middle and distal part of each MM
3. Create text files that contain specimen numbers in "work/morpho/output_data/2D_Fourier/input_files"
    a. For example, files such as "homo-femur-fetus.txt", "pan-femur-fetus.txt", "gorilla-femur-fetus.txt" and "pongo-femur-fetus.txt" can be created
4. Specify which input files are used in the following analyses in "**input_file_link.m**"
    a. For example, make the lines of "homo-femur-fetus.txt" and "pan-femur-fetus.txt" active when comparing these two species.
5. Run "**rotate_Fourier7.m**"
    a. First, for each input file (i.e., typically for each species)
    b. And for all input file.
    c. This aligns MMs through rotation about their main axis (longitudinal axis) by minimizing the inter-MM distances in Fourier space
6. Run "**PCA_Fourier2D_fitting_map4_3.m**".
    a. Parameters to be specified are

i. number of harmonics (level of detail) for horizontal and longitudinal axes of MM matrix to be used for PCA (Principal Component Analysis). This parameters are critical to memory usage (if the value is too large, one gets an "out of memory" error), and

ii. map type (cortical thickness, radius, surface curvature, etc).

b. The results are saved in "work/morpho/output_data/2D_Fourier". For example, result of the analysis of the surface curvature of the femur of human and great ape fetuses is saved in the directory "work/morpho/output_data/2D_Fourier/curvature_n/homo-femur-fetus-pan.t-femur-fetus-gorilla.g-femur-fetus-pongo-femur-fetus_29-Jun-2011". The program saves the date automatically.

Post-processing of multi-dimensional Fourier analysis

1. Go to "work/ShapeThem/Fourier2D"
2. Specify which result of PCA is used for the post-processing calculations in "**load_input_file.m**" (Fig. 2)
    i. For example, make the line of "homo-femur-fetus-pan.t-femur-fetus-gorilla.g-femur-fetus-pongo-femur-fetus_29-Jun-2011" active, which corresponds to the directory containing the result of PCA on femora of human and great ape fetuses.
3. Run "**multivariate_regression7.m**" to calculate multivariate regression (e.g., PC scores versus diaphyseal length)
4. Run "**plot_vector_group5.m**" to plot (common) allometric ontogenetic vectors in shape space (Fig. 3)

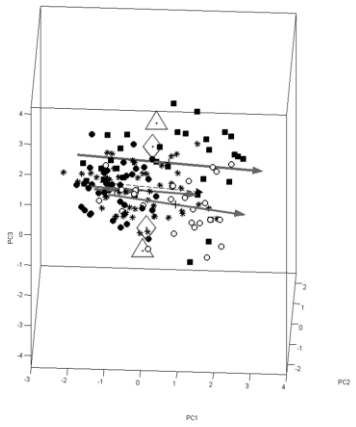

Fig. 3 Example of visualization of ontogenetic vectors in PC space. Taxon-specific ontogenetic trajectories are shown as gray arrows. Common allometric ontogenetic vector is shown by the dashed arrow.

5. Run "**resampling_dist_matrix5.m**" and "**bootstrap_species_expanded3.m**" (the former produces resampled distance matrices that can be used in Phylips for similarity analyses, and the latter calculates *p*-values) to perform resampling statistics on

    i. distance between taxon-specific means

    ii. divergence of taxon-specific allometric ontogenetic vectors

    iii. divergence of principal direction of taxon-specific distribution

    iv. difference between taxon-specific modes of distribution (distance between variance-covariance matrices; see Mitteroecker and Bookstein (2009))

6. Run "**arbitrary_map_MV_group9.m**" to generate MMs (Fig. 4) from the results of PCA (visualization in physical space)

    i. **color_map_setting_1.m**" contains the settings for the false-color mapping such as color scale

    ii. This visualizes the ontogenetic changes along allometric ontogenetic vectors

Calculate the mid-line of the diaphysis

1. Go to "work/ShapeThem/Axis3D"

2. Specify the specimen number and run "batch_Axis3D.m"

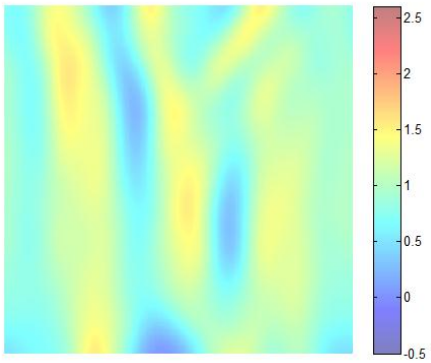

Fig. 4 Example of visualization of morphometric maps. Average femoral diaphyseal surface morphology is shown. It is possible to change the mode of false-color mapping and color scale in this window.

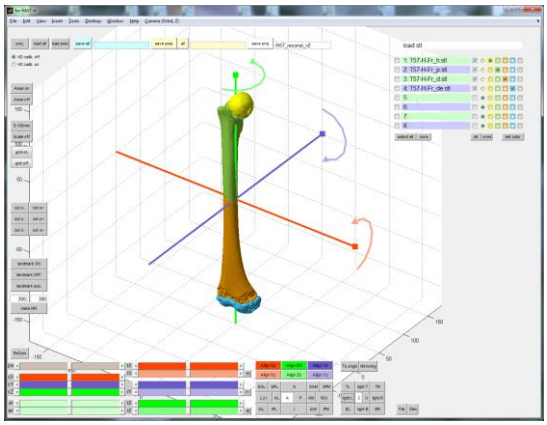

Fig. 5 Surface-data based morphometric mapping. Fragmented bone parts (indicated by different colors of the surface) can be assembled and then analyzed with the methods described above.

Surface-data based morphometric mapping

1. Prepare stl files
2. Go to “work/ShapeThem/ ForMATit”
3. Open “**forMATit_7_6.m**”, the window of the program appears (Fig. 5)
4. Align surface parts along z-axis
5. Click “make MM”

The script files are available on request.

Reference

Mitteroecker P, Bookstein F. 2009. The ontogenetic trajectory of the phenotypic covariance matrix, with examples from craniofacial shape in rats and humans. Evolution 63:727-737.

B. Database for morphometric maps

Each hominoid specimen typically has twelve long bones. During analyses using morphometric mapping methods, analysis of each bone results in various morphometric maps of different features. Comparative analyses of long bone morphologies using morphometric mapping methods thus result in literally thousands of images (Fig. 6). It is of particular importance to utilize a database system for effective data-mining.

There are various ways to build a database; here, a web-oriented approach is taken. One advantage of this approach is that the database functions independent of the underlying operation system. The database was implemented using the combination of Apache (http://www.apache.org/), PHP (Hypertext Preprocessor; http://php.net/index.php) and MySQL (http://www.mysql.com/). MySQL offers a database management system, Apache is the web server software, and PHP produces dynamic web pages (rather than static ones).

The process is the following. Morphometric maps are saved on the http server as image files. Each image has various "tags" such as taxon name, age and bone length. Using a function of MySQL, one can define a query that "picks up" the requested information (i.e., tag). For example, one can ask for "**male chimpanzees**", and a query lists up the specimens which have both tags of "male" and "chimpanzee" in the database. PHP then exports the page code that shows the information requested by the user.

The front page of the database gives the user various options to select data (Fig. 7). One can choose the type of morphometric map, species, sex, bone, side of the bone (left/right), etc. One can refine the resulting list by defining parameters such as the range of the bone length and specimen name. One can also reach the relevant data associated with specific morphometric maps of each specimen. For example, one can refer to the original cross-sectional images (Fig. 3; dicom files cannot be shown in the present version of the database). The php codes are available on request.

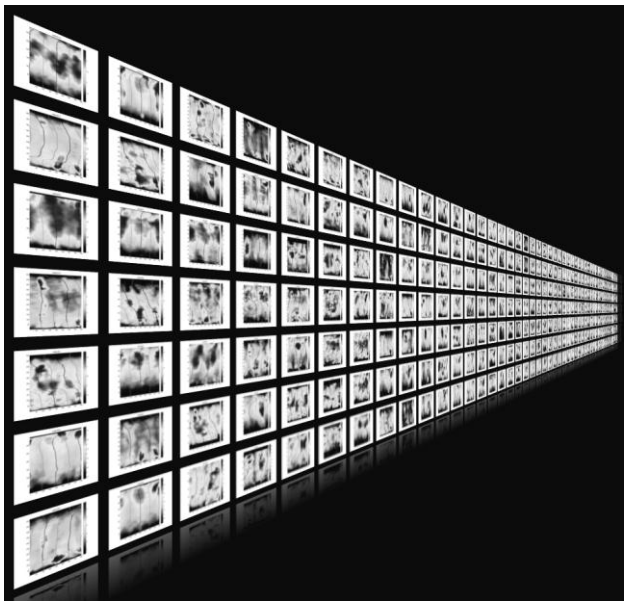

Fig. 6 Pile of morphometric maps. The aim is to retrieve biologically relevant information from this pile.

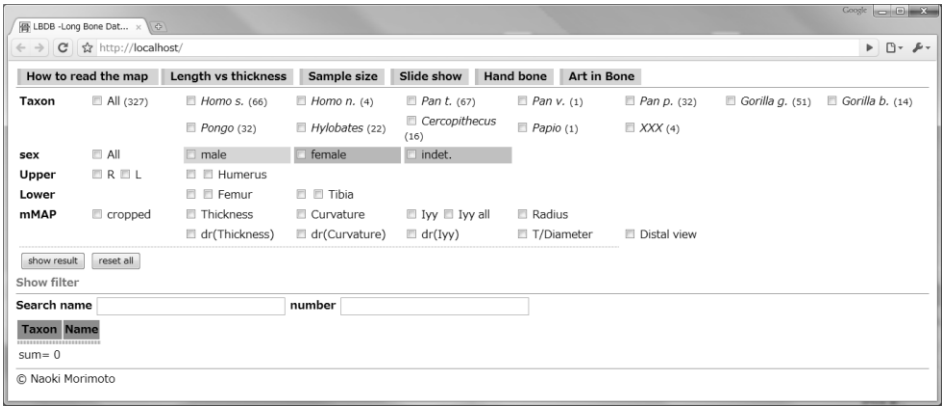

Fig. 7 User interface of the data base.

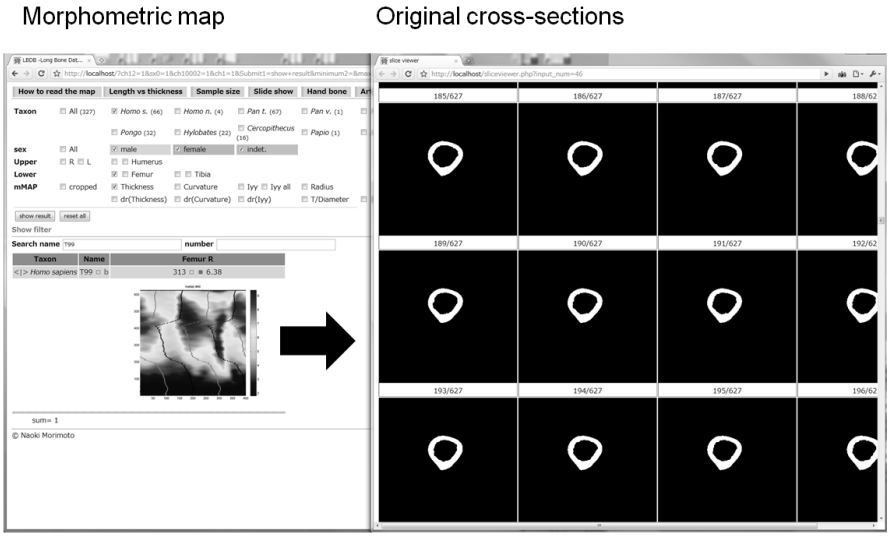

Fig. 8 Morphometric map and corresponding cross-sectional data. Relevant information can be "linked".

Acknowledgements

I express sincere “ARIGATO” to Prof. Dr. Christoph Zollikofer and Dr. Marcia Ponce de León for their generous support during the study. I am also grateful to Peter Jans, Dr. Emmanuel Gillissen, Walter Coudyzer, Dr. Wim Wendelen, Prof. Dr. Michael Walker, Prof. Dr. Clive Finlayson, Prof. Dr. Takeshi Nishimura, Prof. Dr. Jeremy DeSilva, Alik Huseynov, Andrea Lutz, Ani Margvelashvili, Fabian Hilti, Dr. Fernand Ventrice, Dr. Jody Weissmann, José Luis Alatorre Warren, Dr. Juanma Jimenez-Arenas, Dr. Marco Miella, Dr. Matthias Specht, Natalie Tkachenko, Peter Holdener, Dr. Renaud Lebrun, Dr. Ronan Ledevin, Dr. Simone Callegari, Susanne Suter, Dr. Tea Jashashvili, Dr. Walther Fuchs, Beno Schoch, Sabrina Beutler, Claudia Zebib, Ruth Haegi, Nicolas Goudemand, Séverine Urdy, and my family.

This study was financially supported by Swiss NSF grants #3100A0-109344/1.

CV

Name

MORIMOTO Naoki

Date of birth

16 Aug. 1982

Nationality

Japan

Education

March, 2001 Chiben Gakuen Wakayama High school
March, 2005 BSc in Biological science (Kyoto University, Japan)
March, 2007 MSc in Biological science (Kyoto University, Japan)
Master thesis: Three-dimensional ontogenetic shape changes in the human cranium during the fetal period
Employed as PhD student at the University of Zurich since April, 2007

Publication

Papers in refereed journals:

- **Naoki Morimoto**, Marcia S. Ponce de León, Takeshi Nishimura, Christoph P.E. Zollikofer (2012) Shared human-chimpanzee pattern of perinatal femoral shaft morphology and its implications for the evolution of hominin locomotor adaptations, PLoS ONE 7(7), e41980, doi:10.1371/journal.pone.0041980, doi:10.1371/journal.pone.0041980

- Dean Falk, Christoph P. E. Zollikofer, **Naoki Morimoto**, Marcia S. Ponce de León (2012) The metopic suture of Taung (*Australopithecus africanus*) and its implications for hominin brain evolution Proc. Natl. Acad. Sci. USA, doi: 10.1073/pnas.1119752109

- **Naoki Morimoto**, Marcia S. Ponce de León, Takeshi Nishimura, Christoph P.E. Zollikofer (2011) Femoral morphology and femoropelvic musculoskeletal anatomy of humans and great apes: a comparative virtopsy study, Anatomical Record 294, 1433-1445, doi:10.1002/ar.21424

- **Naoki Morimoto**, Marcia S. Ponce de León, Christoph P.E. Zollikofer (2011) Exploring femoral diaphyseal shape variation in wild and captive chimpanzees by means of morphometric mapping: a test of Wolff's Law, Anatomical Record 294, 589-609, doi: 10.1002/ar.21346

- **Naoki Morimoto**, Naomichi Ogihara, Kazumichi Katayama, Kohei Shiota (2008) Three-dimensional ontogenetic shape changes in the human cranium during the fetal period, Journal of Anatomy 212, 627-635, doi:10.1111/j.1469-7580.2008.00884.x

Papers in refereed conference proceedings volumes:

- **Naoki Morimoto**, Marcia S. Ponce de León, Christoph P.E. Zollikofer (2011) Visualization and quantitative analysis of human femoral diaphysis. BIOLOGICAL SHAPE ANALYSIS: Proceedings of the 1st International Symposium, 266-273, World Scientific Publishing of Singapore, June 2011, ISBN: 978-981-4355-23-0

Conference presentations:

- **Naoki Morimoto**, Marcia S. Ponce de León, Takeshi Nishimura, Christoph P.E. Zollikofer. Great ape virtopsy as a tool for musculoskeletal structure-function analysis. The 81st Annual meeting of the American Association of Physical Anthropologists (Portland, Oregon, US, April 2012)

- **Naoki Morimoto**, Marcia S. Ponce de León, Christoph P.E. Zollikofer. Ontogenetic patterns of long bone shape of humans and great apes. The 79th Annual meeting of the American Association of Physical Anthropologists (Albuquerque, New Mexico, US, April 2010)

- **Naoki Morimoto**, Marcia S. Ponce de León, Christoph P.E. Zollikofer. Visualization and quantitative analysis of morphological variation of long bone shape in human and great apes. The 1st International Symposium of Biological Shape Analysis. (Tsukuba, Japan, June 2009)

- **Naoki Morimoto**, Marcia S. Ponce de León, Christoph P.E. Zollikofer. Ontogenetic patterns of sexual dimorphism in long bone shape of gorillas. The 63rd Annual meeting of the anthropological society of Japan (Tokyo, Japan, October 2009)

- **Naoki Morimoto**, Marcia S. Ponce de León, Christoph P.E. Zollikofer. Visualization and quantitative analysis of morphological variation of long bone shape in human and great ape fetuses. The 62nd Annual meeting of the anthropological society of Japan (Nagoya, Japan, Nov 2008)

Teaching

2011, 2012	Teaching assistant, Evolutionary and functional morphology of primates (BIO202), University of Zurich
2009, 2010, 2011	Teaching assistant, Geometric morphometrics (BIO208), University of Zurich

Fellowships

2010 Schultz Foundation (University of Zurich)